

130
/TESTS ON A MICRO-CONCRETE MODEL
OF A LONG-SPAN FOLDED PLATE SHELL/

by

YOUSSEF NAGI AHMAD (Assaliny)
Diploma in Civil Engineering, Kiev Civil
Engineering Institute, Kiev, USSR, 1974
M.S., Kansas State University, 1981

A MASTER'S THESIS

Submitted in partial fulfillment of the
requirements for the degree

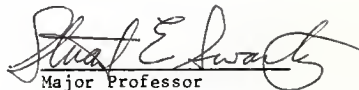
MASTER OF SCIENCE

Department of Civil Engineering

KANSAS STATE UNIVERSITY
Manhattan, Kansas

1985

Approved by:


Major Professor

LD
2668
.T4
1985
A35
C.2

TABLE OF CONTENTS

A11202 942089

	<u>Page</u>
LIST OF TABLES	iv
LIST OF FIGURES.	v
CHAPTER I. INTRODUCTION	1
CHAPTER II. REVIEW OF LITERATURE.	4
2.1 Review of Methods of Analysis.	4
2.1.1 Basic Assumptions	6
2.1.2 The Elasticity Method	7
2.1.3 The Ordinary Method Neglecting Relative Joint Displacements	8
2.1.4 The Ordinary Method Considering Relative Joint Displacements	8
2.1.5 The Beam Method	8
2.2 Review of Previous Experimental Work	8
2.2.1 Experimental Study of Moorman	9
2.2.2 Experimental Study of Dykes	10
2.2.3 Experimental Study of Chacos and Scalzi	11
2.2.4 Experimental Study of Aldridge.	11
2.2.5 Experimental Study of Scordelis and Gerasimenko	12
2.2.6 Experimental Study of Lee	14
2.2.7 Experimental Study of Sutton.	15
2.2.8 Experimental Study of Pudhaphongsiriporn. . .	16
2.2.9 Experimental Study of Resheidat	17
CHAPTER III. FOLDED PLATE ANALYSIS	19
3.1 General.	19
3.2 Elasticity Method.	19

TABLE OF CONTENTS (continued)

	<u>Page</u>
3.2.1 Joint Force-Displacement Equations for Edge Beam	24
3.2.2 Matrices	26
CHAPTER IV. CONSTRUCTION OF THE MODEL STRUCTURE AND INSTALLATION OF THE MEASUREMENT GAGES	31
4.1 General	31
4.2 Fabrication	31
4.2.1 Formwork	31
4.2.2 Formwork Erection	33
4.3 Reinforcement	34
4.4 Casting and Curing	34
4.5 Formwork Removal	35
4.6 Installation of MEasurement Instruments	35
CHAPTER V. LOADING SYSTEM AND TESTING PROCEDURE	46
5.1 Loading System	46
5.1.1 Description of the System	46
5.1.2 Whiffle Tree Loading System and Instrumentation	47
5.2 Testing Procedure	48
CHAPTER VI. TEST RESULTS AND DISCUSSION	56
6.1 Surface Thickness Values and Contours	56
6.2 Quality Control of Cylinders	56
6.3 Ram Calibration Tests	57
6.4 First Test	57
6.5 Second Test	57
6.6 Response of the Whiffle Tree	58
6.6.1 Strains	58

TABLE OF CONTENTS (continued)

	<u>Page</u>
6.7 Elastic Response of the Model.	59
6.7.1 Deflection.	59
6.7.2 Strains	59
6.8 Discussion of Edge Beam Results.	60
CHAPTER VII. SUMMARY AND CONCLUSIONS.	85
7.1 Summary.	85
7.2 Conclusions.	86
7.3 Recommendations.	86
REFERENCES	87
APPENDIX A: NOTATION.	90
APPENDIX B: EDGE BEAM ANALYSIS AND THE COMPUTER PROGRAM . . .	93
APPENDIX C: EXPERIMENTAL AND THEORETICAL LOAD CALCULATIONS AND STRAIN DATA	138

LIST OF TABLES

<u>Table</u>		<u>Page</u>
4.1	Properties of Micro-Concrete Sand.	37
4.2	Mix Quantities Per Cubic Foot.	37
6.1	Jack Calibrations.	62
6.2	3" x 6" Concrete Cylinders, Compression Test Results.	63
6.3	1" x 2" Concrete Cylinders, Compression Test Results.	64
6.4	Cylinder Stress-Strain Test Data	65

APPENDICES TABLES

B.1	Model Output Data.	126
C.1	Calculated Experimental vs. Theoretical Loads (Gages 31 and 32).	144
C.2	Calculated Experimental vs. Theoretical Loads (Gages 35 and 36).	144
C.3	Calculated Experimental vs. Theoretical Loads (Gages 37 and 38).	145
C.4	Calculated Experimental vs. Theoretical Loads (Gages 41 and 42).	145
C.5	Calculated Experimental vs. Theoretical Loads (Gages 43 and 44).	146
C.6	Calculated Experimental vs. Theoretical Loads (Gages 45 and 46).	146
C.7	Calculated Experimental vs. Theoretical Loads (Gages 47 and 48).	147
C.8	Calculated Experimental vs. Theoretical Loads (Gages 49 and 50).	147
C.9	Calculated Experimental vs. Theoretical Loads (Gages 57 and 58).	148
C.10	Calculated Experimental vs. Theoretical Loads (Gages 59 and 60).	148

LIST OF FIGURES

<u>Figure</u>		<u>Page</u>
1.1	Typical Folded Plate Structure.	3
3.1	Slab Coordinate System, Internal Forces and Displacements	28
3.2	Axes' Orientation for Folded Plate Structure With Edge Beams	29
3.3	Cross-Section of the Model with Edge Beams.	30
4.1	Cross-Section of the 216 in. (5.5m) Long Model.	38
4.2	Formwork Units.	39
4.3	Wood Frame.	40
4.4	View of the Reinforcing Mesh on the Model	41
4.5	Data Acquisition System.	42
4.6	Location of the Strain Gages on Whiffle Tree Bars	43
4.7	Dial Gage Map	44
4.8	Scales to Measure Creep Deflections	45
5.1	Loading Points on the Inclined Plate.	51
5.2	Schematic Drawing of the Whiffle Tree Loading System.	52
5.3	Layout of Loading System.	53
5.4	Strain Gage Layout on the Whiffle Tree.	54
5.5	Whiffle Tree Arrangement.	55
6.1	Contour Map of Plate Thickness.	66
6.2	Compressive Stress-Strain Curve for the Micro- Concrete - Cylinder 53.	67
6.3	Compressive Stress-Strain Curve for the Micro- Concrete - Cylinder 43.	68
6.4	Deflection Due to Cyclic Loading for Service Load at Centerline of Top Plate.	69
6.5	Midspan - Top Plate Transverse Deflection, Third Cycle	70

LIST OF FIGURES (continued)

<u>Figure</u>		<u>Page</u>
6.6	Stress-Strain Curve for a 1/2" x 1/2" Bar	71
6.7	Load Point Response Near End Support.	72
6.8	Load Point Response Near Midspan.	73
6.9	Load Point Response Near End Support.	74
6.10	Load Point Reponse Near Midspan	75
6.11	Inclined Load Point Response Near Edge Beam	76
6.12	Middle Load Point Response Near Midspan	77
6.13	Whiffle Tree Bar Response Near End Support.	78
6.14	Whiffle Tree Bar Response Near Midspan.	79
6.15	Load Point Response at Midspan of the Top Plate	80
6.16	Whiffle Tree Bar Response Near Midspan of the Top Plate	81
6.17	Deflection Profiles Along Center of Top Plate	82
6.18	Deflection Profiles Transverse to Top Plate at Midspan	83
6.19	Longitudinal Strain in the Center of the Top Plate, Test Two	84

APPENDICES FIGURES

B.1	Cross-Section of the Model with Edge Beams.	100
B.2	Resolution of Forces on Folded Plate and on Edge Beams	101
B.3	Shear Diagram	132
B.4	Edge Beam Bending Moment About y-axis	133
B.5	Edge Beam Torsion	133
B.6	Edge Beam Axial Force	134
B.7	Edge Beam Bending Moment About z-axis	134

LIST OF FIGURES (continued)

<u>Figure</u>		<u>Page</u>
B.8	Shear Diagram	135
B.9	Edge Beam Bending Moment About y-axis	136
B.10	Edge Beam Torsion	136
B.11	Edge Beam Axial Force	137
B.12	Edge Beam Bending Moment About z-axis	137
C.1	Layout of Whiffle Tree Load Points	142
C.2	Load Distribution on Whiffle Tree	143

I. INTRODUCTION

Folded plate shells may be defined as structures constructed from individual plane surfaces, or plates, joined together to form a surface. The lines of intersection between the individual plates are usually termed fold lines.

The structural behavior of folded plates is characterized by "slab" and "plate" actions. The loads acting normal to each plate cause it to bend transversely between the ridges as a continuous "slab". The plates supported at their ends on end-diaphragms, bend due to the in-plane "plate" loads. This behavior of the folded plate gives rise to longitudinal ridge stresses and transverse bending moments at ridges.

Several kinds of structural materials can be used to construct folded plate structures, but reinforced concrete has been the most commonly used.

Reinforced concrete folded plates provide a useful and economical method of construction for roof and floor systems in a wide variety of structures. This has proven exceptionally economical where relatively large spans are needed as for auditoriums, industrial buildings, hangars, department stores and parking garages. They have a striking appearance. The materials required are usually much less than needed for flat slab, beam and slab, or other conventional systems. A typical, simply supported folded plate structure is shown in Fig. 1.1.

Knowledge of the structural behavior of reinforced concrete folded plate structures due to applied loads is limited. Only a few tests of reinforced concrete folded plate structures have been reported in literature sources.

This thesis is a report of analytical and experimental results from a study of a direct model of a simply supported, prismatic, reinforced

concrete folded plate structure, with an inverted-U type cross section stiffened by edge beams along the free edges. The study's focal point is to determine the actual performance of the whiffle tree loading system and the distribution of loads, the response of the model at service load level, and the effect of edge beams on the structural response.

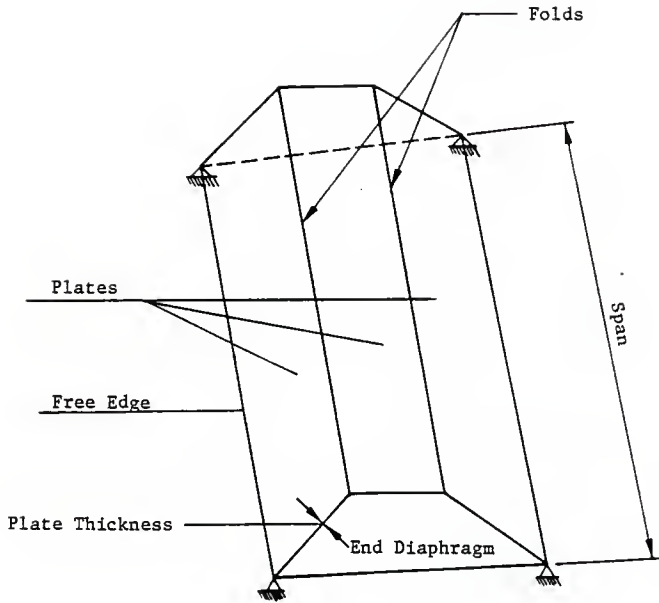


Fig. 1.1 Typical Folded Plate Structure

II. REVIEW OF LITERATURE

2.1 Review of Methods of Analysis

Folded plate roof structures have become widely used in recent years and several acceptable methods for analyzing such structures have been developed. Within recent years there have been numerous papers published, presenting various techniques for the analysis of the folded plate structure (4,5,8,9,11,12,13-19,21,23,25,31-34). An extensive review of the literature concerning the folded plate has been presented recently by Sutton (30). This interest has arisen because the concrete folded plate is attractive for long spans, and also the folded plate may be used as a mathematical model to approximate simply supported and continuous barrel-vault shells (5).

The methods of analysis of folded plate structures may be considered to fall within four principal categories. The categories are designated herein on the basis of the overall distinguishing characteristic of the method proposed as (i) beam method, (ii) folded plate theory neglecting relative joint displacements, (iii) folded plate theory considering relative joint displacements and (iv) elasticity method.

Since Craemer (8) and Ehlers (11) published their papers in 1930, various similar and increasingly more advanced linear-elastic methods have been proposed by numerous authors. Theoretical interest has focused primarily on methods of analysis which apply to folded plates exhibiting linear-elastic behavior. Two basic classes of analytical approach are applicable to linear elastic folded plate systems: the so-called "simplified, approximate methods," sometimes called the "Ordinary Folded Plate Theories," and the "exact," or "elasticity" methods. The "exact" method was presented by Goldberg and Leve (17). An excellent summary of the various methods of analysis was presented by the ASCE Task Committee on

Folded-Plate Construction in its Phase I Report (25) and also by Sutton (30). In this report the Task Committee recommended that Gaffar's method (16), a theory of the "ordinary" type, be used for design purposes with correction for relative joint displacements. For the complete procedure of analysis the reader is referred to the bibliography listed at the end of Ref. (25), to the text by Billington (5) and also the very extensive bibliography by Sutton (30).

In recent years, developments in structural analysis through utilization of high-speed digital computers have made complex analytical approaches practical and feasible.

In conjunction with the general implementation of ultimate strength design concepts for designing reinforced concrete members, analytical approaches which allow the assessment of the actual load-carrying capacity and the true structural response of folded plates have been developed. Limit design (13, 15) and yield line analysis (14) are of this general type.

Several simplified methods of analysis of continuous folded plate structures based on a one-dimensional approach are available. Of these, Yitzhaki's (34) and Gruber's (19) can be used without resorting to digital computation. Yitzhaki's treats the problem by considering each span individually, the end conditions being then idealized as fixed, free, or simply supported. Hence, his method is applicable only when there is longitudinal symmetry of geometry and loading. Gruber shows that if the deformations due to transverse forces are neglected, the different plates can be dealt with separately as continuous beams. Such an approach is not restricted by considerations of longitudinal symmetry.

Under similar assumptions, i.e., in bending normal to its plane the plate behaves as a one-way slab and neglecting the stresses induced by longitudinal slab action and twisting of the plate, Beaufait (4) presented

an analysis that requires the use of a digital computer. Swartz (32) presented a method of analysis of folded plates with transverse stiffeners limited to symmetrical loading and cross section with interior, rigid, diaphragm stiffeners. The method requires a computer implementation, though the concept is simple. In all these studies the interior supports are limited to rigid diaphragms. A more rigorous solution makes use of the formulation advanced by Goldberg and Leve (17) for single span simply-supported folded plates.

Traum (12) presented an analysis of prismatic folded plates in which the ridges are first considered as unyielding supports for the calculation of all transverse moments in the slab. Then the ridges are subjected to unknown loads which constitute the true slab reactions, taking into account the settlement of the ridges. The concept presented here is quite similar to work done by Gaafar (16). The only difference appears to be that Traum (12) has chosen the loads on the ridges as the desired unknowns, while Gaafar (16) chose the relative displacements .

The available methods of linear-elastic analysis may be classified as follows:

1. The Elasticity "Exact" Method (17);
2. The Ordinary "Approximate" Methods (16, 33);
3. The Beam Method.

2.1.1 Basic Assumptions

The following basic assumptions are made in all of the linear methods applicable to simply supported, prismatic folded plate structures:

- 1) The material is homogeneous and linearly elastic.

2) The actual deflections are minor relative to plate width and length. Consequently, equilibrium conditions for a given plate may be developed using the configuration of the undeflected plate.

3) The principle of superposition holds.

4) The structure is monolithic and joints are rigid.

5) The length of each plate is more than twice its width.

6) In all plates, plane sections remain plane after deformation. (It is, however, to be carefully noted that a plane cross section of the entire structure does not necessarily remain plane after deformation.)

7) Each supporting end diaphragm is infinitely stiff parallel to its own plane, but perfectly flexible, normal to its plane.

2.1.2 The Elasticity Method

The classical theory for simply supported prismatic folded plate structures was presented by J. E. Goldberg and H. L. Leve (17) in 1957. The elasticity or so-called "Exact" method involves separate analysis of the slab and plate actions of each individual plate, and requires satisfying equilibrium and compatibility equations at each joint when the plates are assembled to form the complete structure. The plate action is analyzed by the application of two-dimensional elasticity principles and the slab action is analyzed by the plate bending theory. The solution procedure involves the use of Fourier half-range series and the application of a semi-inverse technique.

Its application becomes practical with the use of a digital computer. DeFries-Skene and Scordelis (9) reported their programming of the original elasticity method, using the equations presented by Goldberg and Leve (17) in 1957.

2.1.3 The Ordinary Method Neglecting Relative Joint Displacements (33)

This method is based on the assumption that the additional transverse moments due to relative joint displacements are negligible in comparison with those set up in the transverse direction by the external loads. The solution is initiated by analyzing the transverse slab system, assuming rigidly supported joints, under the external loads, and then subsequently analyzing the longitudinal plate system as loaded by the slab reactions. The calculations involved are relatively simple.

2.1.4 The Ordinary Method Considering Relative Joint Displacements (16)

In this method, the additional moments created by the relative joint displacements are considered in the analysis; additional slab reactions due to joint displacement are taken into account. The method is suitable for hand calculations—less computational effort than the elasticity method.

2.1.5 The Beam Method

This method is based on the assumption that the behavior of a folded plate structure is similar to that of a thin-walled beam spanning between the end supports. The application of this method is simple but yields only approximate solutions.

2.2 Review of Previous Experimental Work

A brief review of the literature indicates that there have been a large number of experimental studies of folded plate structures conducted in various research programs.

In general, there are two types of folded plate model tests: tests of linear-elastic models, and full loading range (including ultimate strength) tests of reinforced concrete or micro-concrete models. Small elastic models have frequently been used by workers to verify analytical solutions (18). The reasons for using elastic models are numerous. The most important ones are: simple similitude requirements, a wide choice of materials, and ease of fabrication and testing.

2.2.1 Experimental Study of Moorman (24)

A large-scale model (single quarter scale model) of a reinforced concrete folded plate structure was built and tested at Syracuse University by a group under the direction of R. B. Moorman (24) in 1956. The cross section of the model was an inverted-U shape with two vertical edge plates, one horizontal top plate and two plates which were inclined thirty degrees to the horizontal.

The design thickness of all plate elements was 1 1/2 in. (38.1 mm). Difficulty was experienced in controlling the plate thicknesses during the placement of concrete. These were found to vary between 1.52 in. to 2.01 in. (38.61 mm to 51.1 mm). The simply supported model had: end diaphragm thickness 3 in. (76.2 mm), span length 26 ft. 3 in. (8001 mm), and plate width 13 ft. 9 1/2 in. (4203.7 mm). Reinforcement was designed to resist transverse bending moments and longitudinal middle-surface tractions obtained from "ordinary" (elastic) theory considering relative joint displacements. Strains were measured by electrical resistance strain gages attached on both longitudinal and transverse reinforcing steel, as well as on the concrete surfaces. Vertical and horizontal deflections at selected locations were measured. Uniformly distributed load was applied to the

test structure by means of sand bags placed over the surface of the plates. Sand bags were added in increments of 25 psf. (1.20 KPa). Cracks were recorded. Hairline cracks were first noticed in the edge plates at the design live load of 50 psf. (2.39 KPa). The failure load was between 200 psf. (9.58 KPa) and 225 psf. (10.77 KPa). The failure mode was shear at the joint between the inclined plate and the end diaphragm. The author found the vertical deflections and steel stresses were closely predicted by the ordinary reinforced concrete cracked-section theory. He also concluded that the relative importance of considering relative joint displacements in the ordinary folded plate theory could not be determined from this test. Further tests of large-scale models were strongly recommended.

2.2.2 Experimental Study of Dykes (10)

In 1960, Dykes presented the results from tests of six reinforced mortar folded plate models with the inverted-U cross section. The basic dimensions of the models were: span 29.5 in. (749.3 mm); width 20.5 in. (520.7 mm); rise 6.8 in. (172.72 mm); and plate thickness 0.5 in. (12.7 mm). A lever system was used in the load testing of the models to distribute discrete point loads located on four inch centers longitudinally and transversely. The structures had these different supporting conditions: only longitudinal edges supported and no end diaphragms; free longitudinal edges and simply supported end diaphragms; and simply supported on both the edges and end diaphragms. The author applied the yield line theory by Johansen (20) to predict collapse modes and ultimate loads of all models. The predicted values were in close agreement with those obtained from the model tests.

2.2.3 Experimental Study of Chacos and Scalzi (6)

The report of a single test of a simply supported reinforced concrete folded plate model was made by Chacos and Scalzi. The inverted-U shape was selected as the cross section for this model. The basic dimensions of the model were: span 60 in. (1524 mm); rise 5.07 in. (128.78 mm); width 43.72 in. (1110.49 mm); and plate thickness 0.5 in. (12.7 mm).

The unit tested was supplied with end diaphragms and was simply supported. The model was loaded to collapse by placing bricks over a three inch sand cushion. Only the top plate was loaded in this manner. The longitudinal (tensile) steel of the side plates was proportioned in accordance with strength design principles by beam theory using the Whitney stress block. In order to prevent a plate-bending type of failure, the structure was well reinforced for transverse bending moment and diagonal tension of the plates. The authors concluded that failure occurred when the tensile reinforcement ruptured. The predicted ultimate load using the Whitney stress block and simple beam theory agreed with that observed from the test.

2.2.4 Experimental Study of Aldridge (3)

The author reported a study of three models having a butterfly-type cross section. All models were alike in every respect except for the reinforcing systems. Overall plan dimensions were: span 96 in. (2438.4 mm); width 48.75 in. (1238.25 mm); span to height ratio 8.35 in. (212.5 mm); plate elements were 0.5 in. (12.7 mm) thick; and the end diaphragms were 1.375 in. (34.93 mm) thick. The first model was designed by using the results of ordinary folded plate theory neglecting relative joint displacements; for the other two models the

effects of these displacements were included in the analysis. The third model was prestressed in the longitudinal direction. The models exhibited flexural beam-type failures accompanied by extensive cracking. The second model required about 50 percent more reinforcement than the first model. Model tests were conducted by the application of load over the entire horizontal projection of the plate surfaces by means of a tension-type whiffle tree loading system. Static load was increased monotonically in increments from dead load of the model to collapse. Both vertical and horizontal deflections were recorded at each load increment along each ridge line at the end diaphragms, quarter points and centerline point. Deflection readings were taken using dial gages mounted on fixed and portable frames.

The load deflection responses of the test structures were presented and compared with theoretical values predicted by the folded plate theory, considering relative joint displacements and a nonlinear theory based on beam theory. Cracking was observed only on the upper surfaces of the models.

Aldridge found that predictions of deflection response were not satisfactory, even at the service load level. He concluded that the ultimate load-carrying capacity may be predicted quite closely by ordinary ultimate strength procedures for flexural members.

2.2.5 Experimental Study of Scordelis and Gerasimenko (29)

The authors reported an experimental and analytical study of two simply supported, prismatic, reinforced concrete folded plate structures. The two models had free longitudinal edges. The two models, identical in all respects except for the quantity and arrangement of reinforcement, were tested. Plan dimensions were: 30 in. (762 mm)

width by 70 in. (1778 mm) length; plates .5 in. (12.7 mm) thick; and end diaphragms 1.5 in. (38.1 mm) thick. One model was proportioned in accordance with the results of the elasticity method, the other by elementary beam theory.

The former model had generally more reinforcement, particularly in the transverse direction. The steel was placed in two layers adjacent to the middle surface for both models, with the transverse steel being on the top in each case. The loading used for the test consisted of uniform line loads acting at the folds applied by means of a whiffle tree system. "These design line loads were equal to joint reactions produced by a uniform design load acting on a continuous transverse slab strip rigidly supported at the folds." Two distinct loading phases were considered for each model: seven loading cycles from zero to applied design load and a single loading to failure. The instrumentation was designed to measure vertical and horizontal deflections of each joint at the midspan cross section and also to monitor strain in certain longitudinal reinforcement bars at the same cross section. Crack formation was noted and marked directly on the models.

For loading to the design service load, both models "generally behaved as predicted by folded plate theory in terms of deflection and strain." No cracking was observed for this loading level. Failure of both models was "caused by diagonal cracking near the support and cracking in the supporting diaphragms" that was produced by warping of these elements. The structure exhibited amazing ductility, sustaining maximum deflection of nearly 3 in. (76.2 mm) before failure. The failure load occurred at 4.5 times the design service load for both models.

The authors concluded that folded plate theory can be used to predict the behavior in the working load range for structures similar to the model tested in cross section with similar ratios of span to height, and type of loading. Either the folded plate theory or elementary beam theory will yield a satisfactory design in terms of deflections at the service load, ultimate strength and overall behavior. The need for further experimental study of reinforced concrete folded plate models having different types of cross section, span to height ratio and type of loading was also stressed.

2.2.6 Experimental Study of Lee, D. W. (22)

The author tested four reinforced micro-concrete models of a simple span folded plate structure with free longitudinal edges. Three models had a double inverted trough-type cross section; the other model had a single inverted trough-type cross section. The models had span to height ratios of 13.5 and 20.2 and were considered to be long span folded plate structures. The plate elements and the end diaphragms were 0.5 in. (12.7 mm) and 1.5 in. (38.1 mm) thick, respectively. Tests of the models were conducted by applying load as a monotonically increasing static load from the dead load of the specimens to collapse. Service live load patterns were simulated by a pull-type whiffle tree loading system. In analyzing the structures, the ordinary method neglecting the relative joint displacement was used. A nonlinear solution based on the observed structural response was developed. The author proposed that load factors of 1.5 and 4.0 for dead and live load, respectively, be used for intermediate and long-type structures. He recommended that the ultimate strength design procedure for beams

can be used to design the longitudinal steel in folded plate structures by using his recommended load factors.

2.2.7 Experimental Study of Sutton (30)

The author reported an experimental and analytical study of three simply supported prismatic reinforced concrete folded plate structures with an inverted-U cross section. Key dimensions were: span length 184 in. (4673.6 mm); element plate width 45 in. (1143 mm); element plate thickness 1.5 in. (38.1 mm); and end diaphragms thickness 4 in. (101.6 mm). The plate inclination was 30 degrees with respect to the horizontal. The major variable was the system of reinforcement. The first model was designed in accordance with minimal reinforcement for ductility and had a reinforcement system consisting of an orthogonal mesh, spaced equally in both directions and placed in the middle surface of the concrete. The other two models were designed using the elasticity, or "exact", method.

The second model was reinforced by a system designed in accordance with contemporary practice, while the third model had a reinforcement system with features which reflected inferences drawn from the complete results of an exact of linear-elastic analysis. Loading was applied monotonically to the structure in increments by means of a system of nine hydraulic cylinders delivering nominally identical vertical loads.

The arrangement of applied loads consisted of groups of three hydraulic cylinders which were mounted on each of three transverse beams located at each quarter span section and at the midspan section. The results were presented through an extensive documentation including tables and photographs, as well as complete crack records. The first model exhibited excessive cracking, strains, and deflections at the

service load level and large deflection as it approached collapse. The model sustained a load equal to 4.1 times the service load. The second model exhibited cracking, deflections and strains at the service load level which were acceptable. The third model was generally superior to the other two. No cracking was observed for this model through the service load level; deflections and strain data agreed very well with analytical predictions. The mode of failure was a localized collapse under one of the off-ridge concentrated loads in the midspan cross section under a load of 9.14 times the service load level. The author pointed out that the cracking pattern observed from the tested structures showed good agreement between crack orientations and the directions of normals to the maximum principal strains predicted by the exact-elastic analytical method. He also concluded that the character of the reinforcement system significantly influenced the nature of structural response throughout the entire range of loading.

2.2.8 Experimental Study of Pudhaphongsiriporn (26)

The author reported an experimental study of five reinforced micro-concrete folded plate models with inverted-U cross sections. Each model had span 96 in. (2438.4 mm) and 68 in. (1727.2 mm) width. The major variable was the system of reinforcement. Loads were applied through a "whiffle tree" (pull-type) loading system of a simple beam interconnected by bolts and threaded rods to the load points on the model. The instrumentation was designed to measure the deflection and strains on the steel reinforcement and the concrete plate surfaces. Visible crack development was observed and recorded. The five systems of reinforcement were: (1) model 1 had a single longitudinal steel bar at each free longitudinal edge; (2) model 2 was reinforced with a light

orthogonal membrane grid; (3) model 3 had a system designed according to contemporary practice; (4) model 4 had a system designed in accordance with the complete results of the elastic analysis by an "exact" method; and (5) model 5 had a more optimum system based on the same analytical results. The author presented his results through an extensive documentation and demonstrated the validity of the exact method for predicting the response at the service load level. Load factors at failure for the last three models were very high. He concluded that the character of the reinforcement system significantly influences the nature of structural response.

2.2.9 Experimental Study of Resheidat (27)

The author reported an experimental study of two reinforced micro-concrete folded plate models with edge beams. The structure was simply supported and the cross section configuration was of an inverted-U type. The ratio of span to height was equal to 8. The structure was subjected to one cycle of uniform static loading. The models were tested by applying simulated uniform load by means of a "whiffle tree" loading system. Plan dimensions were span length 144 in. (3657.6 mm); element plate width 24 in. (609.6 mm); element plate thickness 1 in. (25.4 mm); and edge beam depth and width 6 in. (152.4 mm) and 2 in. (50.8 mm), respectively. The two models had the same characteristics except for differences in the reinforcement system.

The author concluded that the exact method of analysis yielded a safe design and accurate predictions of structural response for loads in the service load range. He also pointed out that by including edge beams, the amount of inclined diagonal reinforcement and transverse reinforcement was reduced and the stiffness of the structure, and its

ultimate capacity significantly increased. The author stated that both models failed in a longitudinal flexural mode and they exhibited considerably higher load-carrying capacities than that predicted by conventional strength design criteria.

III. FOLDED PLATE ANALYSIS

3.1 General

Folded plate structures are usually designed to include edge beams attached along their longitudinal free edges. It is to be expected that the behavior of folded plates with longitudinal edge beams will differ from that of folded plates with free longitudinal edges.

The elasticity method is the method used to analyze the edge beams. The complete general version of the mathematical development of the exact method of analysis is presented by Goldberg and Leve (17). The method developed herein is an adaption of this method to the specific problems of direct interest for this study.

3.2 Elasticity Method

The assumptions stated in Chapter II are valid here to obtain an "elasticity solution" which relates the internal forces and deformations to the applied loads and deformations at the joint lines. Figure 3.1 shows a typical plate element with an x, y, z coordinate system.

External loads and internal tractions which act on the element in their positive senses are shown in separate groups.

The loads, forces and deformations are expressed as trigonometric series in the x -direction. All relations between loads, displacements and forces are given by Goldberg and Leve (17).

The plate equations are briefly presented in this chapter, whereas the beam equations are given in Appendix B. For the case of a simply supported structure having a cross section consisting of (n) plates, the number of longitudinal joints is equal to $(n + 1)$. The key joint deformations include a joint rotation (θ) and three displacements $(u, v, \text{ and } w)$ in the $x, y, \text{ and } z$ directions, respectively.

The orientation of axes for folded plate structures with edge beams is shown in Fig. 3.2.

The internal tractions at the joints can be expressed in terms of these unknowns. Once the joint forces and the joint displacements are expressed as Fourier Series, it is then only necessary to solve 4 (n + 1) equilibrium equations for each Fourier harmonic considered in the analysis.

For the beam, the equations are expressed in terms of the unknown joint displacements of the connecting joint between the beam and adjacent plate.

- a. The normal displacement w_i for the i^{th} plate may be expanded into the Fourier Series:

$$w_i = \sum_{m=1}^{\infty} \bar{w}_m (y_i) \sin \frac{m\pi x}{a} \quad (\text{III.1})$$

where,

m is the odd term of a Fourier Series. Note that a bar over the symbol indicates the maximum value for a particular harmonic of any force or displacement.

If we admit only the m^{th} term, then the deflection must satisfy the homogeneous differential equation

$$\nabla^4 w_i = 0 \quad (\text{III.2})$$

The solution of (III.2) is

$$\begin{aligned} \bar{w}_m (y_i) = & A_{1m} \sinh \frac{m\pi y_i}{a} + A_{2m} \cosh \frac{m\pi y_i}{a} \\ & + A_{3m} \frac{m\pi y_i}{a} \sinh \frac{m\pi y_i}{a} + A_{4m} \frac{m\pi y_i}{a} \cosh \frac{m\pi y_i}{a} \end{aligned} \quad (\text{III.3})$$

The coefficients $A_{1m} - A_{4m}$ are determined from the boundary conditions for each mode m at the edges j, k of the i^{th} plate in terms of edge displacements.

The boundary conditions are

$$\left(\frac{\partial \bar{w}_m}{\partial y}\right)_i y_i = \frac{b_i}{2} = \bar{\theta}_j$$

$$\left(\frac{\partial \bar{w}_m}{\partial y}\right)_i y_i = -\frac{b_i}{2} = \bar{\theta}_k$$

(III.4)

$$(\bar{w}_m)_i y_i = \frac{b_i}{2} = \bar{w}_{jk}$$

$$(\bar{w}_m)_i y_i = -\frac{b_i}{2} = \bar{w}_{kj}$$

where $\bar{\theta}_j, \bar{\theta}_k$ are the edge rotations and $\bar{w}_{jk}, \bar{w}_{kj}$ are the edge displacements of the i^{th} plate. The differential plate equation of bending including load effect is given as

$$\nabla^4 w_i = \frac{P_{ni}}{D} \quad \text{(III.2a)}$$

By substituting into the general plate bending equations (III.2a) the internal forces and moments are determined in terms of the rotations and displacements.

The fixed end moments and forces due to a normal load on the i^{th} plates, p_{ni} , are determined by assuming a deflection function w_{Fi} .

Assuming a sine distribution for the normal loading the deflection function must satisfy the boundary conditions of zero edge displacements and rotations and the following equation.

$$\nabla^4 w_{Fi} = \frac{P_{ni}}{D_i} = \frac{\bar{p}_i}{D_i} \sin \frac{m\pi x}{a} \quad \text{(III.5)}$$

The final result is obtained by adding each fixed end moment and force to its corresponding moment and force due to edge displacements.

b. In-plane displacement in the i^{th} plate:

The displacements in the direction of x and y , u_i and v_i , respectively, are given as

$$u_i = \sum_{m=1}^{\infty} \bar{u}_m(y_i) \cos \frac{m\pi x}{a} \quad (\text{III.6})$$

$$v_i = \sum_{m=1}^{\infty} \bar{v}_m(y_i) \sin \frac{m\pi x}{a} \quad (\text{III.7})$$

The associated two dimensional stresses are

$$\sigma_{xi} = \frac{E_i}{1-\mu_i} \left(\frac{\partial u_i}{\partial x} + \mu_i \frac{\partial v_i}{\partial y} \right) \quad (\text{III.8})$$

$$\sigma_{yi} = \frac{E_i}{1-\mu_i} \left(\frac{\partial v_i}{\partial y} + \mu_i \frac{\partial u_i}{\partial x} \right) \quad (\text{III.9})$$

$$\tau_{xyi} = \frac{E_i}{2(1+\mu_i)} \left(\frac{\partial u_i}{\partial y} + \frac{\partial v_i}{\partial x} \right) \quad (\text{III.10})$$

From equilibrium equations for the homogeneous solution, the stresses must satisfy

$$\frac{\partial \sigma_{xi}}{\partial x} + \frac{\partial \tau_{xyi}}{\partial y} = 0 \quad (\text{III.11})$$

$$\frac{\partial \tau_{xyi}}{\partial x} + \frac{\partial \sigma_{yi}}{\partial y} = 0 \quad (\text{III.12})$$

From this the total displacements for the m^{th} mode are obtained by substituting for u_i and v_i for mode m into equations (III.8) through (III.10)

which yields the solution. The coefficients are determined from the boundary conditions for the m^{th} mode at the edges j, k of the i^{th} plate.

Finally the longitudinal force, the transverse force, and the in-plane shearing force are determined in terms of edge displacements.

In order to determine the fixed end forces due to a load in the $+y_i$ direction of the i^{th} plate, p_{ti} , the associated deflections u_{Fi} and v_{Fi} must first be calculated from the equilibrium equations (III.11) and (III.12). However, Equation (III.12) becomes

$$\frac{\partial \sigma_{yi}}{\partial y_i} + \frac{\partial \tau_{xyi}}{\partial x_i} + \frac{p_{ti}}{h_i} = 0$$

where

$$p_{ti} = \sum_{m=1}^{\infty} \bar{p}_{ti} \sin \frac{m\pi x}{a} \quad (\text{III.13})$$

Fixed edge boundary conditions must also be satisfied. The longitudinal, transverse, and the shearing forces determined from the above cases are added to those corresponding to the edge displacement.

A number of simultaneous equations are determined in terms of edge displacements. These equations may be written in matrix form and the forces and the displacements transformed to a global coordinate system. The equilibrium and compatibility equations at the ridges are applied along with the boundary conditions at the edges which results in the matrix equation,

$$K\Delta = F_F \quad (\text{III.14})$$

where $K = HCH^T$, a $4(n+1) \times 4(n+1)$ stiffness matrix;

C = the plate stiffness matrix

and H = transformation matrix, $4(n+1) \times 8n$.

Δ is a $4(n + 1)$ displacement matrix and can be obtained by transforming each joint displacement for each plate to a global displacement. The fixed end forces matrix, F_F , a $4(n + 1)$ must also be transformed. Finally, n is the total number of plates.

The plate stiffness matrix can be arranged accordingly. Premultiplying both sides of Eqn. (III.14) by K^{-1} , yields

$$\Delta = K^{-1} F_F \quad (\text{III.15})$$

from which the unknown edge displacements and rotations can be determined. The coefficients for each plate can be determined too, and by substituting into the appropriate equations, the state of stress for mode m is determined.

3.2.1 Joint Force-Displacement Equations for Edge Beam

The beam to be considered is of rectangular cross-section and attached along the joint j . The ends $x = 0$ and $x = a$ are simply supported with respect to bending and completely restrained from twisting because of the assumed behavior of the end diaphragms of the folded plate structures. Fig. 3.3 shows a cross-section of the model with edge beams.

In a previous analysis of this model the edge beam was considered as a plate and the stresses were determined according to this. This method was used in Ref. (35). Herein an attempt is made to analyze the edge beams by determining the stiffness matrix and internal forces of the edge beam. Two subroutines were added to the main program for this purpose. The details of the analysis and the computer program are presented in Appendix B. The results of this analysis are more

accurate than the one considering the edge beams as end plates in the analysis. The data are shown in Appendix B.

The equations for a beam are written in a similar manner to those for the plate. For the m^{th} term of a Fourier expansion the four tractions at joint j , are written as follows (17):

$$M_{j0} = \frac{Et^3 d}{48k_1} k^2 \left\{ \left[16 \frac{G}{E} (1-0.63 \frac{t}{d}) k_1 + k^2 d \right] \bar{\theta}_j + 2dk^2 \bar{w}_{j0} \right\} \sin kx,$$

$$V_{j0} = -\frac{Et^3 d}{24k_1} k^4 [d \theta_j + 2 \bar{w}_{j0}] \sin kx,$$

(III.16)

$$N_{j0} = \frac{Etd^2}{6k^2} k^3 [-2dk\bar{v}_{j0} + 3\bar{u}_j] \sin kx,$$

$$S_{j0} = \frac{Etd}{2k^2} k^2 [dk\bar{v}_{j0} - 2k_3\bar{u}_j] \cos kx$$

where

$$k_1 = \left(1 + \frac{Et^2 k^2}{10G} \right), \quad k_2 = \left(1 + \frac{2Et^2 k^2}{5G} \right), \quad k_3 = \left(1 + \frac{Ed^2 k^2}{10G} \right)$$

$$k = \frac{m\pi}{a}, \quad d = \text{depth of edge beam, } t = \text{width of edge beam,}$$

$$G = \frac{E}{2(1+\mu)}$$

If edge $n+1$ is the contacting edge, then

$$M_{n+1,n+2} = \frac{Et^3 d}{48k_1} k^2 \left\{ \left[16 \frac{G}{E} (1-0.630 \frac{t}{d}) k_1 + k^2 d^2 \right] \bar{\theta}_{n+1} - 2d d^2 \bar{w}_{n+1,n+2} \right\} \sin kx$$

$$V_{n+1,n+2} = \frac{Et^3 d}{24k_1} k^4 [d \bar{\theta}_{n+1} - 2\bar{w}_{n+1,n+2}] \sin kx,$$

(III.17)

$$N_{n+1,n+2} = \frac{Etd^2}{6k^2} k^3 [2dk\bar{v}_{n+1,n+2} + 3\bar{u}_{n+1}] \sin kx,$$

$$S_{n+1,n+2} = \frac{Etd}{2k^2} k^2 [dk\bar{v}_{n+1,n+2} + 2k_3\bar{u}_{n+1}] \cos kx$$

If we call the connection of the left edge beam and first plate joint j , and the following joint k , with the free edge designated 0 , then the equilibrium equations for joint j are (in global coordinates)

$$\begin{aligned}
 \bar{M}_{j0} + \bar{M}_{jk} &= 0 \\
 \bar{N}\eta_{j0} + \bar{N}\eta_{jk} &= 0 \\
 \bar{N}\xi_{j0} + \bar{N}\xi_{jk} &= 0 \\
 \bar{S}_{j0} + \bar{S}_{jk} &= 0
 \end{aligned}
 \tag{III.18}$$

A similar system of equations occurs for the right edge beam and is given in Appendix B. These equations replace the usual free edge equations for the first and last plate of the structure.

3.2.2 Matrices

The local transformation matrix H_i for any plate i is

$$H_i = \begin{bmatrix} 1 & 0 & 0 & 0 \\ 0 & \cos\phi_i & -\sin\phi_i & 0 \\ 0 & -\sin\phi_i & -\cos\phi_i & 0 \\ 0 & 0 & 0 & 1 \end{bmatrix}
 \tag{III.19}$$

The edge displacements in the local coordinates for plate i can be written as follows:

$$\delta_i = \begin{bmatrix} \delta_i^j \\ - \\ \delta_i^k \end{bmatrix} = \begin{bmatrix} \bar{\theta}_j \\ \bar{w}_{jk} \\ \bar{v}_{jk} \\ \bar{u}_j \\ - \\ \bar{\theta}_k \\ \bar{w}_{kj} \\ \bar{v}_{kj} \\ \bar{u}_k \end{bmatrix} \text{ for the } i^{\text{th}} \text{ plate}
 \tag{III.20}$$

The global displacement column vector, δ_i^* for plate i is

$$\delta_i^* = \begin{bmatrix} \delta_i^{j*} \\ \delta_i^{k*} \end{bmatrix} = \begin{bmatrix} \bar{\delta}_j \\ \bar{\eta}_j \\ \bar{F}_j \\ \bar{u}_j \\ \bar{\delta}_k \\ \bar{\eta}_k \\ \bar{F}_k \\ \bar{u}_k \end{bmatrix} \quad (\text{III.21})$$

The local displacement vectors are related to the global displacement vectors as follows:

$$\{\delta_i^j\} = [H_i]^{-1} \{\delta_i^{j*}\}, \quad \{\delta_i^k\} = [H_i]^{-1} \{\delta_i^{k*}\}$$

- = maximum value function in span for mode m of series.

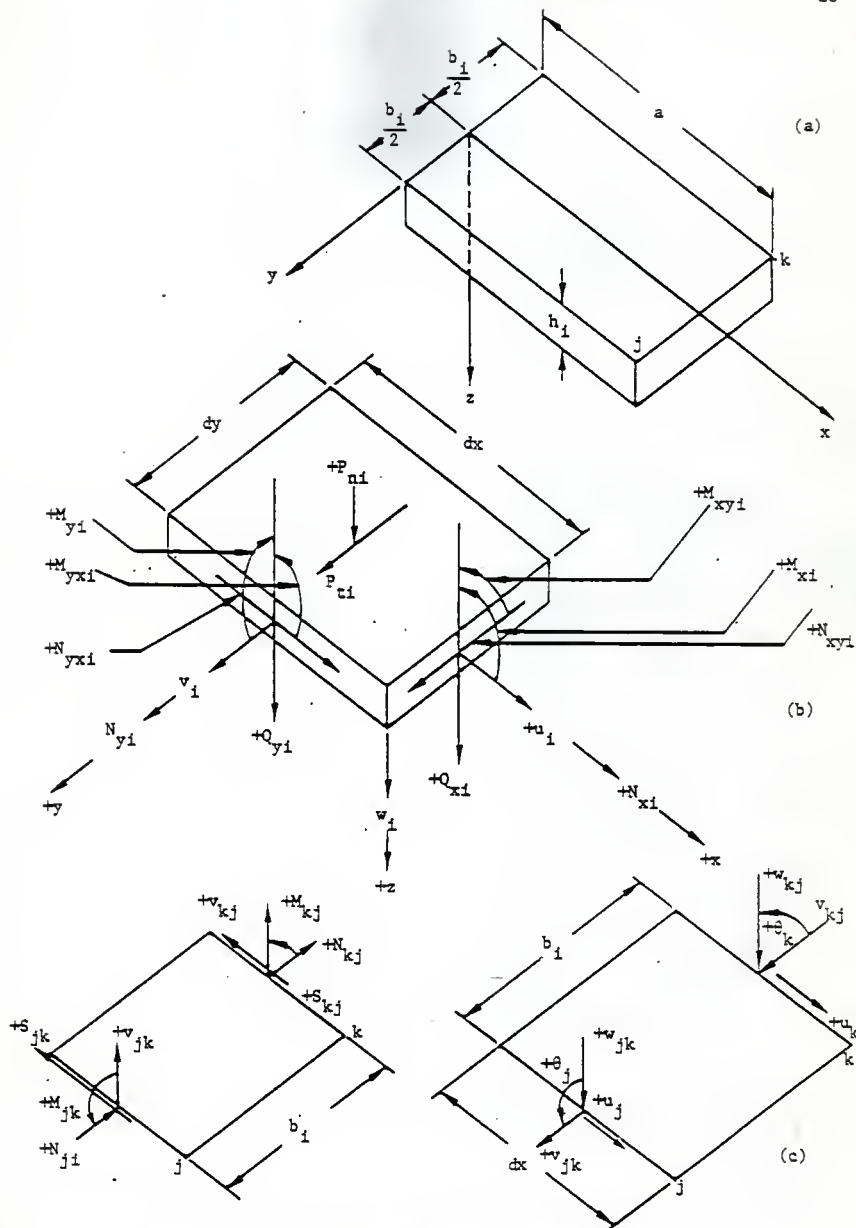


Fig. 3.1 Slab Coordinate System, Internal Forces, and Displacements

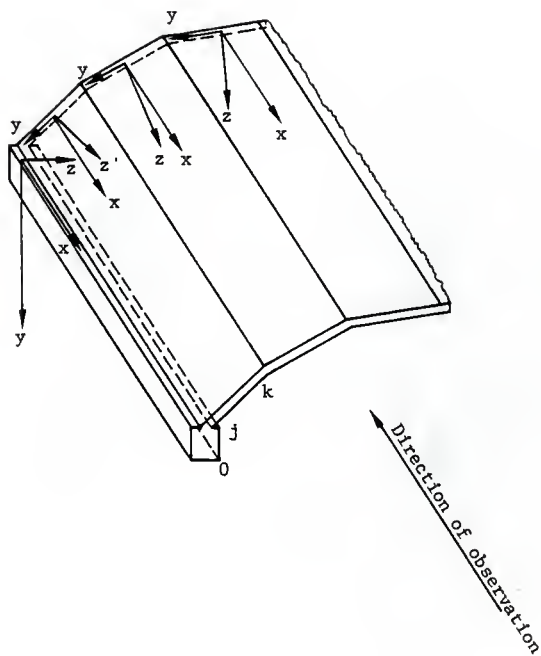


Fig. 3.2 Axes' Orientation for Folded Plate Structure with Edge Beams

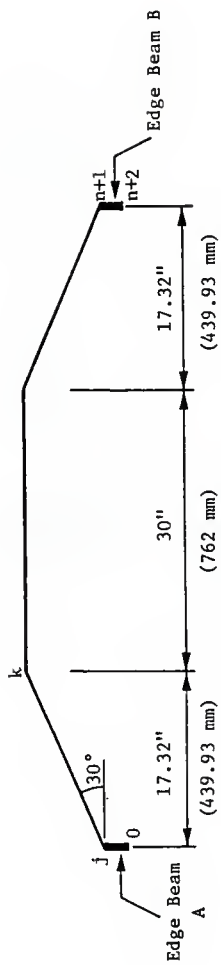


Fig. 3.3 Cross-section of the Model with Edge Beams

IV. CONSTRUCTION OF THE MODEL STRUCTURE AND INSTALLATION OF THE MEASUREMENT GAGES

4.1 General

A model of an inverted-U type cross section folded plate structure with end diaphragms, and edge beams along the free longitudinal edges was built. A brief description of the model construction and material will be introduced here. For full details of the construction procedures and design the reader is referred to Ref. (35). The cross section consists of three plates and two edge beams. The two edge beams are identical. One plate is horizontal and two are inclined 30 degrees with respect to the horizontal. The key dimensions of each plate are: inclined plate thickness 0.75 in. (19.05 mm); horizontal plate thickness 0.6 in. (15.24 mm); span length 216 in. (5486.4 mm); plate width 64.6 in. (1641.86 mm); and diaphragm thickness 4 in. (101.6 mm). The beam width is 2 in. (50.8 mm), the beam depth is 3 in. (76.2 mm), and its span is that of the plates. The cross section of the model is shown in Fig. 4.1. The supports were designed and constructed as described in Ref. (35). The micro-concrete mix used was a sand-cement-water mortar with a W/C ratio of 0.5. This mix was designed and used in previous work (7). The sieve analysis of the sand and the quantities per cubic foot are shown in Table 4.1 and Table 4.2, respectively.

4.2 Fabrication

4.2.1 Formwork

The model formwork consisted of two major parts, the wood supporting frame and the basic form elements. The function of the wood supporting frame was to facilitate both erection and removal of the various elements of the forms. The basic form elements consisted of steel, plywood and plexiglass. Six units of formwork were constructed,

along with two end bulkheads and four unit formworks. The end bulkheads were made of one-quarter inch thick steel plate. They were cut and dimensionally shaped into the designed cross sections and used to form the outer faces of the structural end diaphragms. The four unit formworks were cut from one-quarter inch thick plates, were machined into the desired inverted-U cross-section shape and functioned as end supports for each unit formwork. The steel supports were held rigidly in place. Longitudinal braces consisting of eleven 1" x 1" x 1/8" steel angles were cut 35.5" (901.7 mm) long and were fastened along the top and inclined edges of the steel supports for each unit formwork. One-eighth inch holes were drilled in each angle, for wood screws to hold 3/4" (19.05 mm) plywood. Plywood of 3/4" (19.05 mm) thickness was cut for the inner form of the model. The pieces were assembled together and leak-free joints were produced.

Plexiglass of 3/8" (9.53 mm) thickness was employed as the interior form surface for the top and inclined plates and was used as an exterior form only for the inclined plates and the edge beams. The individual plexiglass pieces were cut and machined so that leak-free joints were achieved.

The plexiglass was used to allow visual confirmation of consolidation of the mix during placement from the outside edge beam and the top of the inclined plates.

Holes were drilled in the individual form plates at specific locations to allow the application of spacers, spreaders and load points. These were used to maintain uniform thickness between the exterior and interior forms when connecting these two pieces together. Size 5/16 in. (7.94 mm) brass tubing was cut in 2 in. (50.8 mm) lengths for the edge beams, and 0.87 in. (22.1 mm) for the inclined plates to

get 3/4 in. (19.05 mm) thickness. Size 7/16 in. (11.11 mm) brass tubing spacers were used for the end diaphragm to give 4 in. (101.6 mm) thickness.

Load points for the top plates were made from 5/16 in. (7.94 mm) brass tubes of length 0.6 in. (15.24 mm).

The forms served as a mold for casting the micro-concrete. They were supported by three wood frames. Pieces were cut and connected by straps of 1/4 in. (6.35 mm) thick steel.

4.2.2 Formwork Erection

Erection was begun by fixing the end supports for the model. At each corner two concrete blocks were placed one on top of the other. The reinforced concrete beams rested on the blocks. The concrete blocks, in turn, rested on the laboratory floor. The wood frames were raised by manual jacks at each corner of each wood frame. Then the unit forms were placed on the top of the frames. The six forms were aligned and adjusted. The plywood was attached to the units using wood screws. Positioning of the unit formworks to obtain flush joints between adjacent units was a tedious, time consuming job. The units were connected together at their adjacent bulkheads which had four holes flush to the other four holes of the other bulkhead. Threaded rods were inserted in the holes and tightened with nuts from both sides. The joints were sealed by silicon to prevent leakage during casting. The forms' surfaces were then cleaned and greased to facilitate form removal. Spreader-load points were installed in their proper locations. The fabrication process is shown in Figs. 4.2 and 4.3.

4.3 Reinforcement

Assembly of the reinforcement was performed on the form surface after the formwork system was completely arranged and aligned in its proper position. The longitudinal and transverse reinforcements on the inclined plates were connected to form a grid. The ends of both wires were bent inside the end diaphragms. The top plate reinforcement was fabricated aside, then moved on to the top plate. The steel cages for the beams were then assembled aside and placed in the forms. The cage assembly was made sufficiently rigid by using fine wire ties at selected joints. The reinforcements for the end diaphragms were assembled.

All reinforcement was reassembled in place again, and chairs were provided for the cover. The thicknesses were controlled by the brass tubing. The plexiglass was greased and placed in its corresponding location. Figure 4.4 shows the reinforcement assembled on the model. The formwork system thus assembled met the requirements of rigidity and watertightness.

4.4 Casting and Curing

The micro-concrete was mixed in a laboratory concrete mixer of three cu. ft. capacity. After the sand was placed in the oven to dry it was sieved to pass a #16 sieve. Eight batches were required for the model and its quality control cylinders. Each batch consisted of one 94 lbs. (418.11 N) sack of cement, 47 lbs. (209.05 N) of water, and 188 lbs. (836.22 N) of sand. A set retarder also was used of 61.1 m per batch. The mixing procedure used for each batch was: sand and cement were placed into the drum mixer and mixed for thirty seconds, then water was poured gradually over a period of thirty seconds while the mixer was running.

Mixing continued for four minutes; the set retarder was added after the first two minutes. The mix was placed in pans, and poured on the model. A sander was used for vibration to help the mix flow easier. The quality control cylinders, six 3 in. x 6 in. (76.2 mm x 152.4 mm) and six 1 in. x 2 in. (25.4 mm x 50.8 mm) were taken according to ACI 318.83 (1, 2). The cylinders were covered with plastic. The model was covered with a plastic sheet to cure the concrete. Water was sprayed on the model twice a day to keep the model wet for the period of curing.

4.5 Formwork Removal

The steel tubing of the edge beams, the side form, and the outside form of the end diaphragms were removed on the fourth week after casting. The rest of the formworks were removed thirty-three days after casting. The bottom plywood forms were unscrewed. The north wood frame was lowered by the jacks under the corners. All shims were removed. The middle wood frame was lowered and moved away as the first one. Both middle form units were removed. The south wood frame and the fourth unit form were removed in the same sequence. The end unit formwork was stuck in the concrete beams and the diaphragms, and was therefore difficult to remove. Both ends were removed by employing a chisel and a hammer to chip off the concrete under the bulkhead.

4.6 Installation of Measurement Instruments

Locations for strain gages and dial gages for measuring deflection were preselected (See Figs. 4.5 and 4.7).

Eleven small vertical scales were placed on the top plate to be used as measurement reference for short term deflection due to self-weight. The locations are shown in Fig. 4.8. A total of fourteen conventional dial

gages with ranges of two inches were used. The gages were mounted on a separate rigid frame.

Strain gages selected for the experiment consisted of single elements, two element rosettes and three element rosettes. Sixty strain gages were employed. Thirty gages were mounted on the model and the rest were mounted on fifteen 1/2 in. x 1/2 in. (12.7 mm x 12.7 mm) bars of the whiffle tree, to determine the load in the whiffle tree delivered to the model. Three different kinds of strain gages were used. The first kind was a single element type strain gage, gage type EA-06-120LZ -120, which has a 120 Ohms $\pm 0.3\%$ resistance, gage length of 0.24 in. (6 mm) and a gage factor of $2.05 \pm 0.5\%$. The second kind was a two element gage and the third was a three element gage. They were of gage type EA-06-125TF-120 and EA-06-125YA-120, respectively. Each has 120 Ohms $\pm 0.2\%$ resistance, gage length of 0.125 in. (3.2 mm) and gage factor of $2.015 \pm 0.5\%$. The first kind of these strain gages was used for the whiffle tree.

Gages 31 through 38 were mounted on the whiffle tree bars connected directly to the load points in the angle plates near the end support. Gages 39 through 46 were mounted to whiffle tree bars which connected directly to the load points in the angle plate near mid-span. Gages 53, 54 and gages 57 through 60 were on the whiffle tree bars at mid-span (See Fig. 5.4).

Other strain gages were attached to the top and bottom surfaces of the plates. The lead wires from the strain gages were then hooked in to the data acquisition system with the help of pin connectors prepared for the purpose. For the measurement of the strains, an automatic data acquisition system (Optilog) coupled with an Apple micro-computer was used. The installation of strain gages and the Optilog is pictured in Figs. 4.5 and 4.6.

Table 4.1 Properties of Micro-Concrete Sand

Sieve Analysis of Sand	
<u>Sieve Size</u>	<u>Cumulative Percent</u>
No. 16	0
No. 30	17
No. 50	78
No. 100	98
No. 200	<u>99</u>
	292
fineness modulus = 2.92	

Table 4.2 Mix Quantities per Cubic Foot

<u>Material</u>	<u>Quantities</u>
Cement Type I	38.46 lb. (171.1 N)
Sand	76.92 lb. (342.3 N)
Water	19.23 lb. (85.6 N)
Set Retarder	25 ml
Air	2 percent

unit weight = 135 lb/cu. ft., (21.2 KN/m)

- a. ϕ .105 in @ 1 in c.-c. (ϕ 2.7 mm @ 25 mm)
- b. ϕ .105 in @ 4 in c.-c. (ϕ 2.7 mm @ 102 mm)
- c. ϕ .105 in @ 3 in c.-c. (ϕ 2.7 mm @ 76 mm)
- d. ϕ .125 in @ 1.25 in c.-c. (ϕ 3.2 mm @ 32 mm)
- e. 8 No. 3 (8 ϕ 10 mm)

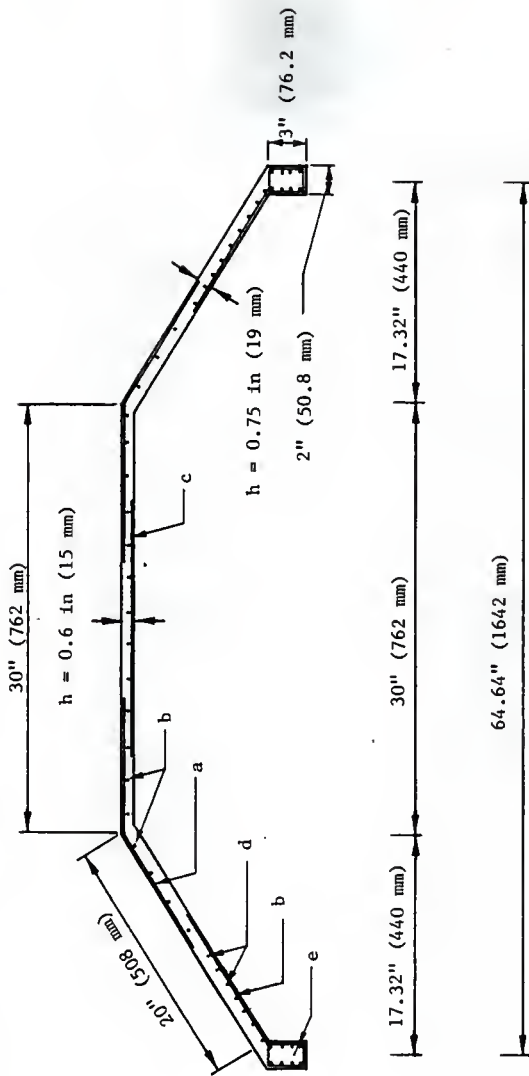


Fig. 4.1 Cross-section of the 216 in (5.5 m) Long Model

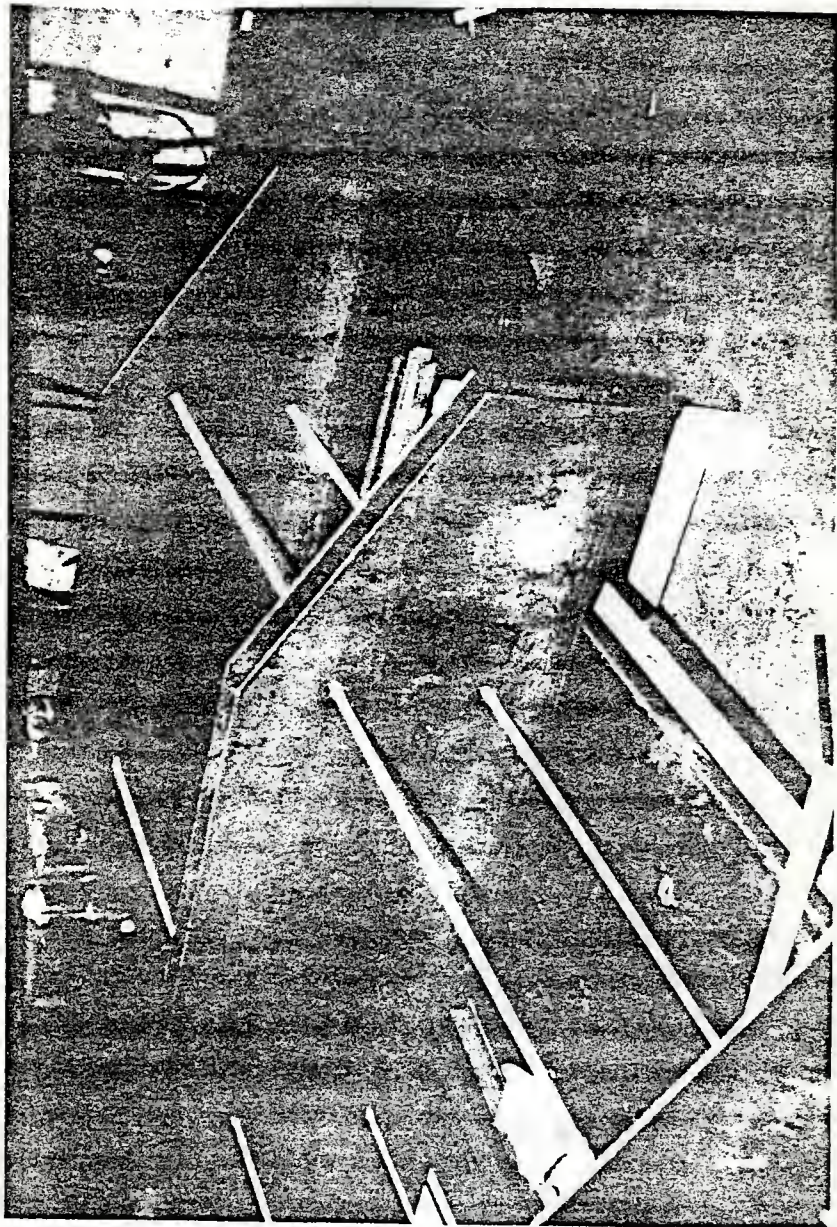


Fig. 4.2 Formwork Units

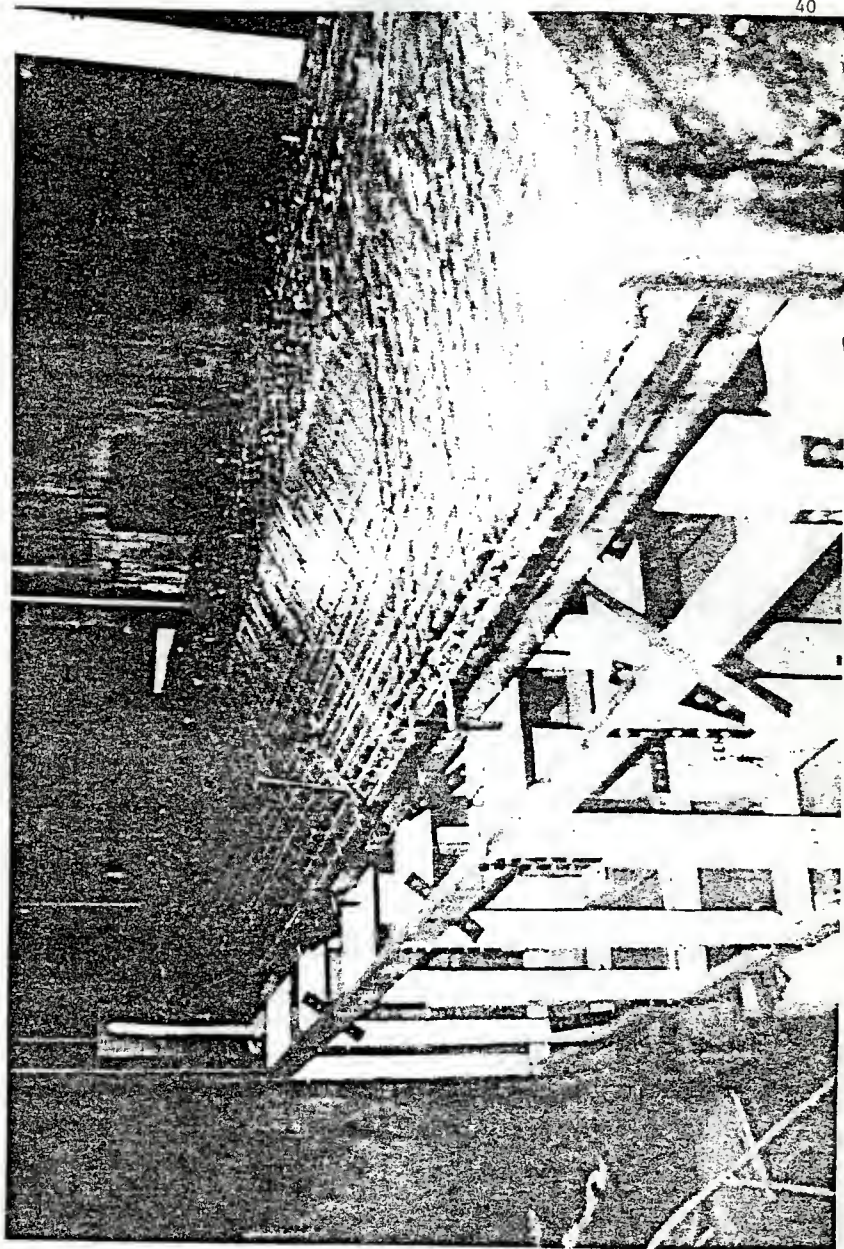


Fig. 4.3 Wood Frame

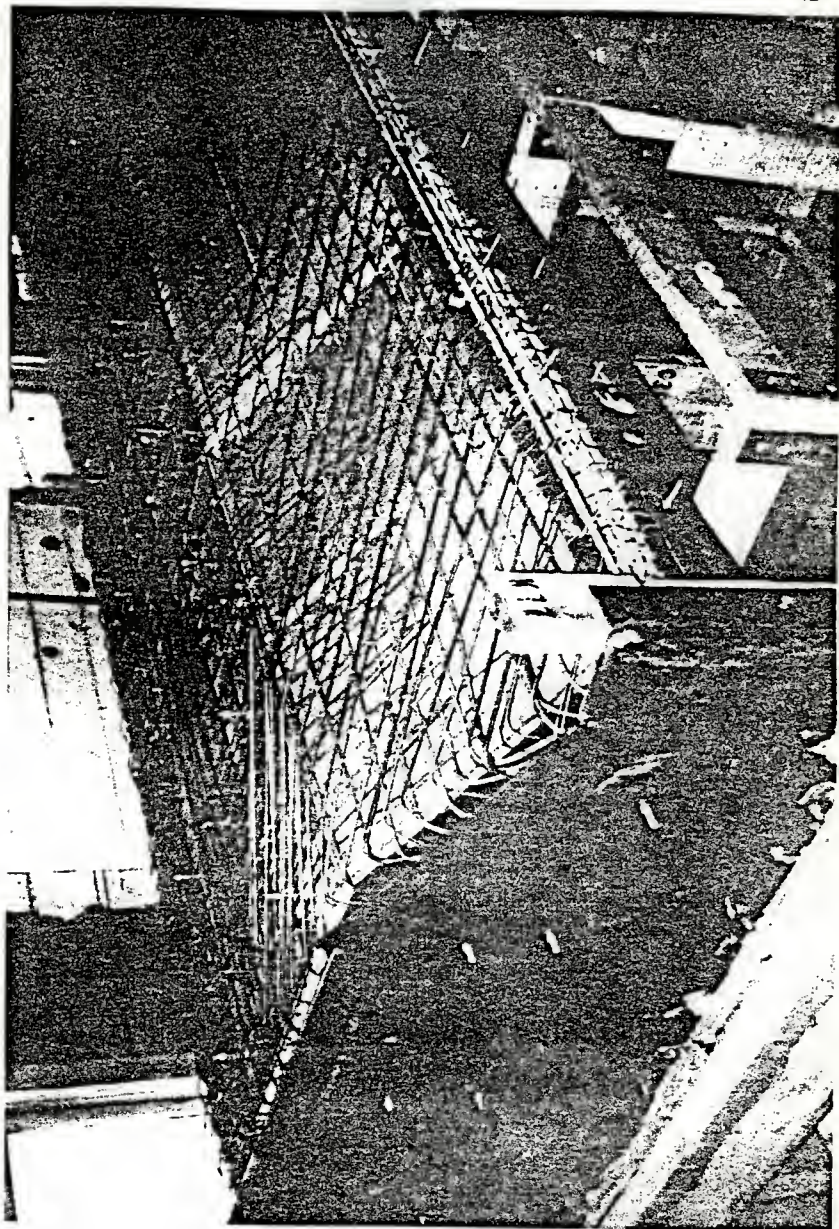


Fig. 4.4 View of the Reinforcing Mesh on the Model

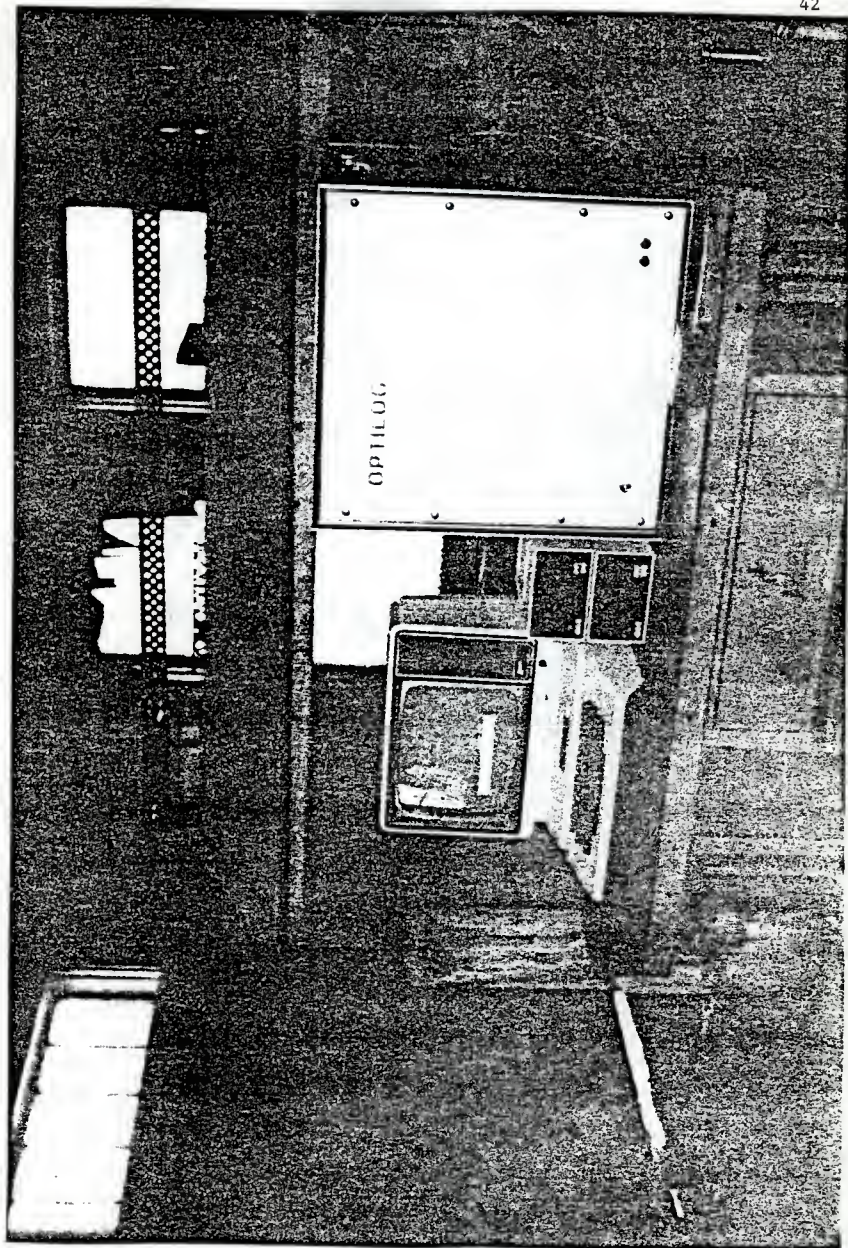


Fig. 4.5 Data Acquisition System

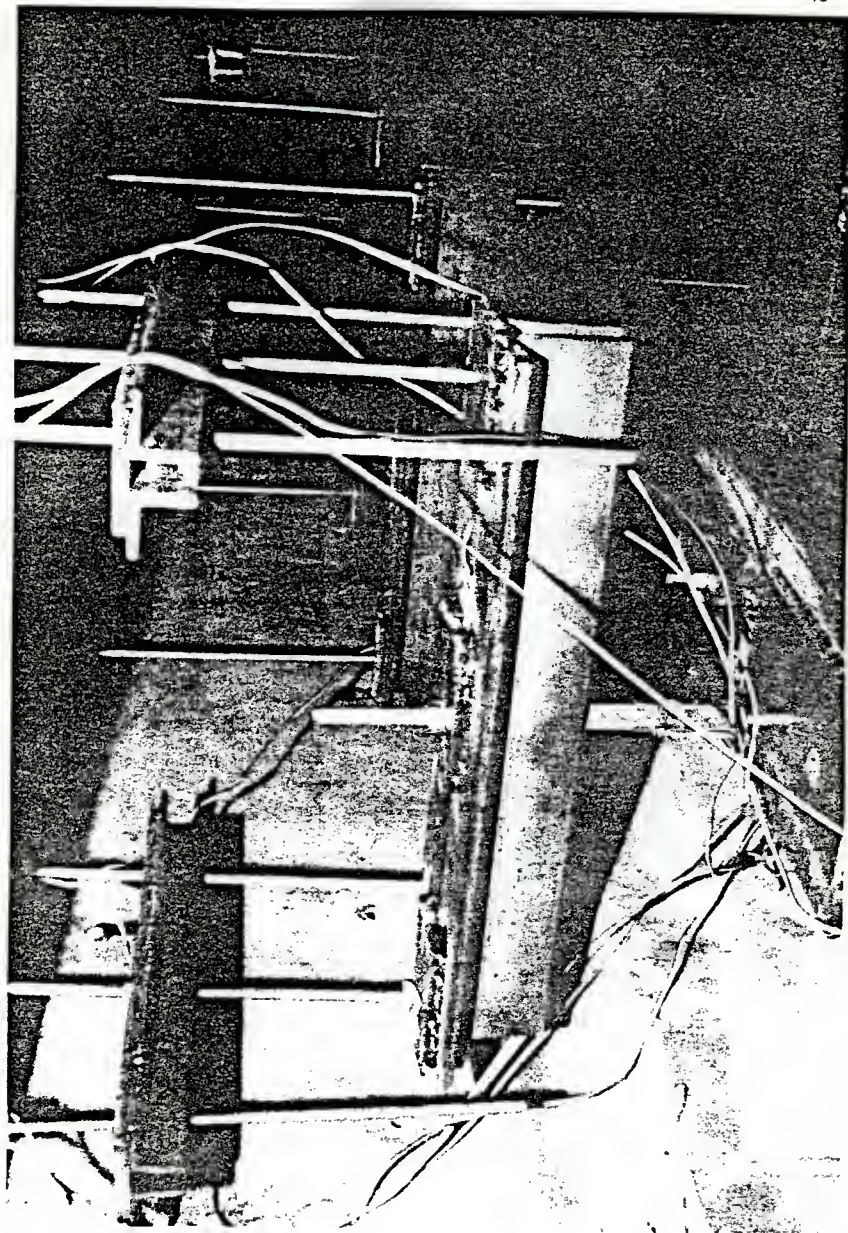


FIG. 4.6 Location of Strain Gages on Whiffle Tree Bars

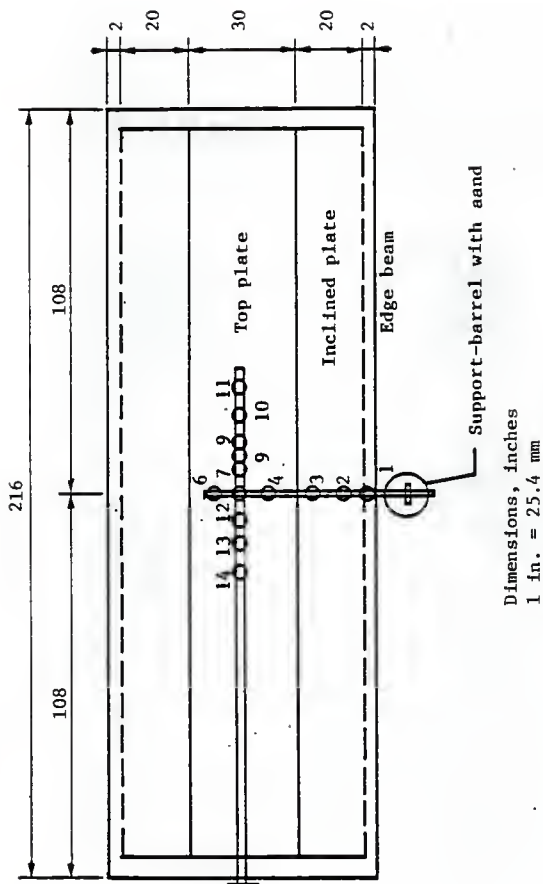


Fig. 4.7 Dial Gage Map

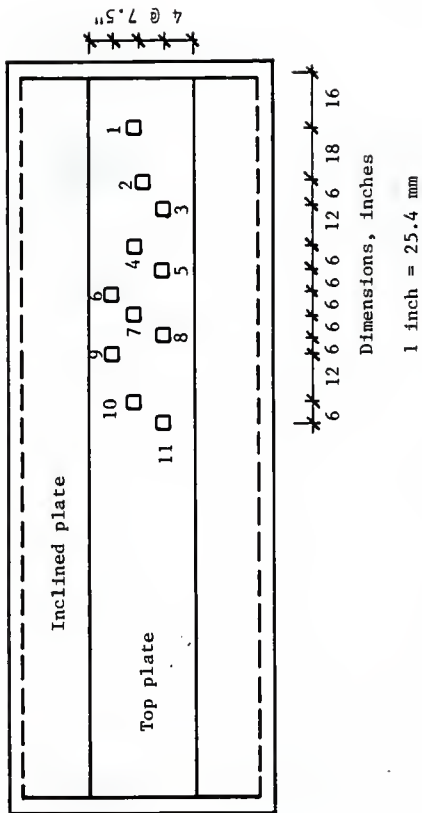


Fig. 4.8 Scales to Measure Creep Deflections

V. LOADING SYSTEM AND TESTING PROCEDURE

5.1 Loading System

Selection of the loading method is one of the most important parts of an experimental model study. The success of any such study depends upon the precision with which the desired loading can be produced.

Various methods have been employed in experimental structural research to simulate uniform loading. The most commonly used methods are: dead weight loading system, vacuum air pressure system, and discrete point load systems. The most popular type is the discrete point loading system, which is commonly used to simulate the effect of uniform loading.

Hydraulic cylinders are widely employed to deliver load to discrete load points. Hydraulic cylinders can be used to transmit load directly to load points or indirectly by means of a so called "whiffle tree" lever system. A discrete point loading system, a whiffle tree system was employed in this study.

5.1.1 Description of the System

The loading system designed to apply load to the model consisted of whiffle trees, hydraulic rams, a pump equipped with a pressure gage, pressure hoses and loading frame. The loading frame consisted of a steel girder and the concrete end beams (35). The whiffle tree consisted of channels and angles, that added up to one hundred eighty-four bars which were cut to the desired length. Each two bars were welded back to back with a gap provided in between for the threaded rods to pass through (see Fig. 4.6). Three small steel plates with a hole in each were welded in predetermined locations to the two pieces. Ninety-two simple beams were manufactured in five

different cross sections, thirty-two pieces of the first and the second type, sixteen pieces of the third, eight pieces of the fourth and four pieces of the fifth type were made. These ninety-two pieces are the main simple beams of the whiffle-tree which will pull at ninety-six discrete points on the shell.

The whiffle-tree bars were installed in a way to assure the loading was evenly distributed, i.e., layer by layer. At first the loading points were installed, then the first layer, second layer and third layer. The pressure hoses were connected to each other and then to the pump. The rams were attached to the girder at their location. Finally the fourth and fifth layers of the whiffle-tree were installed and the rams were hooked to the hoses as shown in Fig. 5.3. The whiffle-tree connected to the hydraulic rams. These four hydraulic rams were connected to the pump.

The whiffle tree bars were connected to the shell with threaded rods at ninety-six discrete load points. At each point a bearing plate and rubber bearing pad were used to assure the distribution of the loads to the shell surface as described in Ref. (28) and shown in Fig. 5.1. The four hydraulic rams were attached to a girder which was bolted to the end reinforced concrete beams. All hydraulic rams and the pump had an allowable pressure of 10,000 psi (68,950 KPa). Each ram had a 30 ton (27,216 Kg) capacity and a 6 in. (152.4 mm) stroke.

5.1.2 Whiffle Tree Loading System and Instrumentation

The whiffle tree loading system was made up of several layers of simple beams interconnected by bolts and threaded rods. The top layer of the system was connected by threaded rods to the load points on the model surface at ninety-six discrete load points. The schematic

drawing of the whiffle-tree system is shown in Fig. 5.2. Each group of twenty-four point loads was connected to whiffle-tree bars and one hydraulic ram. The single load was created by a hydraulic ram placed between the lowest level of the whiffle-tree system and the girder. The hydraulic fluid in the ram was supplied through high pressure hoses connecting the rams to the pump. Figure 5.3 shows the layout of the loading system. Thirty channels of electrical resistance strain gages were mounted on various whiffle tree bars to convert these into load cells. All channels were connected to an Optilog data acquisition system, which was used to monitor strain. The strain gage layout is shown in Fig. 5.4 and the whiffle-tree arrangement is pictured in Fig. 5.5.

5.2 Testing Procedure

The cylinder compressive strength test was conducted for four sets of cylinders. Eight 3 in. x 6 in. (76.2 mm x 152.4 mm) cylinders were tested, averaging 3850 psi (26.55 MPa), 4390 psi (30.27 MPa), 5180 psi (35.72 MPa) and 6080 psi (41.922 MPa). The intervals of testing corresponding to these were seven days, 15 days, 28 days, and 62 days. Another 36 small cylinders 1 in. x 2 in. (25.4 mm x 50.8 mm) were tested with an average of 5000 psi (34.47 MPa).

A split-cylinder test was performed on four cylinders with an average result of 430 psi (2.97 MPa). For more information on these tests and the reinforcement tests, the reader is referred to Ref. (35).

It was mentioned earlier that four jacks were connected to one pump equipped with a pressure gage. It was necessary for the pressure vs. load to be determined for each hydraulic ram. For the jack calibration, each one was connected to the pump along with a pressure gage. The jack was

placed in a compression machine to measure direct force. The jack was raised by the pump until the ram touched the compression machine head. Then the indicators of the load gage on the machine and the pressure gage on the pump started to move. The reading was taken in intervals from the pressure gage and the corresponding reading on the machine. From these data the load to be delivered to the model structure was determined. The data can be found in the next chapter. Tension tests were performed on a typical 1/2 in. x 1/2 in. (12.7 mm x 12.7 mm) bar that was used for the strain gages on the whiffle tree system. Stress-strain curves to failure were plotted using the Riehle tension machine. The modulus of elasticity, yield point and ultimate strength were calculated and are shown in Fig. 6.6.

Three separate tests were conducted on the model. In the first test the model was loaded in increments up to the service load level. This test was done three times with data on strain and deflection recorded. The main reason for this test was to stabilize the strain gages and loading system. The maximum live load reached was 88.9 psf (4.3 KPa). There were no cracks observed during this test.

Before the second test was performed a visual inspection for cracking was done, and none were found. This test was intended to be conducted until the model failed. The load was applied to the model by the hydraulic jacks. The jacks were activated by the pump on increments of 100 psi (0.69 KPa) as in the previous test; at each load level, the load was held constant until the corresponding data were collected. The data consisted of deflections, strains, and crack records. Deflections measured by dial gages were recorded manually. The strains were taken by the Optilog and were printed. Cracking was recorded at each level and marked by ink to show their locations and extent. The loading continued to a load beyond that which caused the top plate to buckle, but less than the failure load. A connection of

the whiffle tree which was not correctly made failed, then the test was stopped.

The third test was conducted, but for this test it was noticed that cracks and permanent deformation were present from the start of the test. The test was performed without whiffle tree rods which contained strain gages.

The same steps were followed as in the second test. This time only one increment more was achieved than in the second test to reach 228 psf (10.92 KPa) total load. When pumping for the next increment, the model failed to take any more load and the pressure at the pump dropped suddenly. Descriptions of the failure modes are presented with other detailed data in Ref. (35).

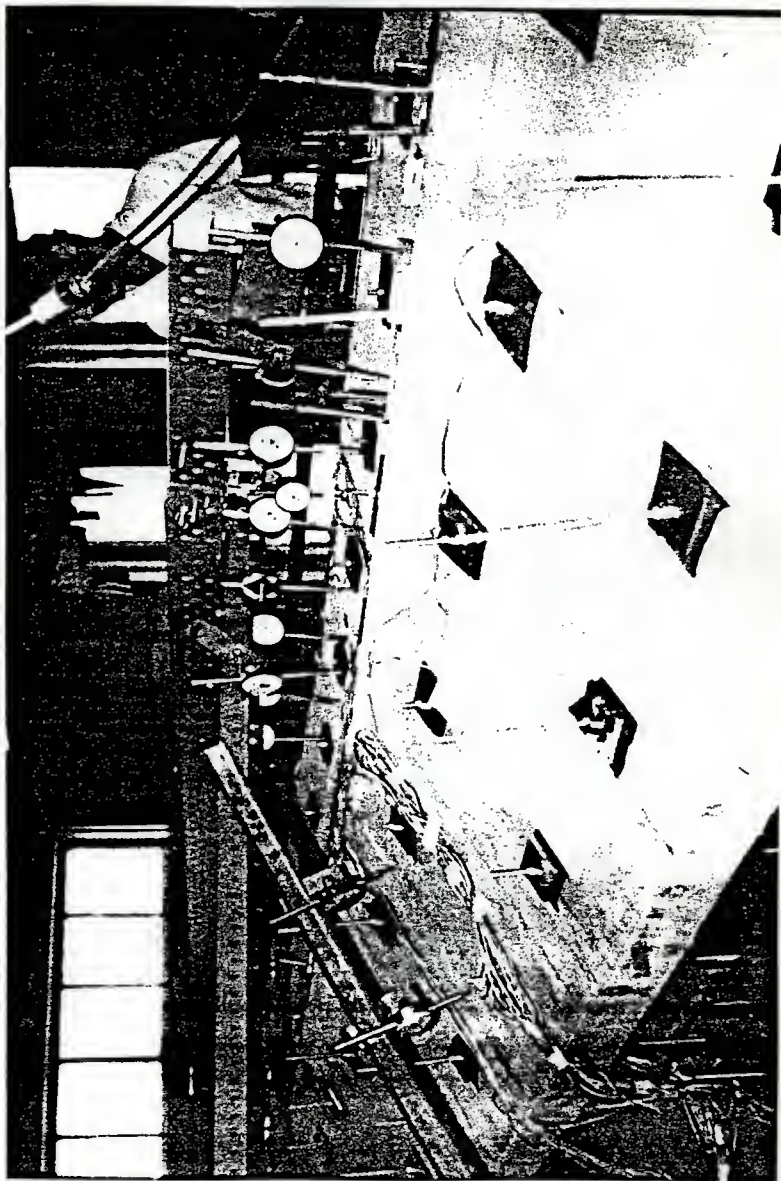
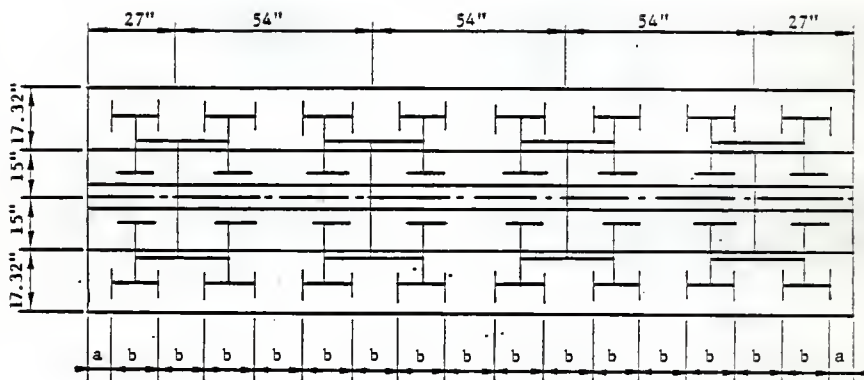


Fig. 5.1 Loading Points on the Inclined Plate



1 inch = 25.4 mm
 a = 6.75 in. (171.45 mm)
 b = 13.5 in. (342.9 mm)

Fig. 5.2 Schematic Drawing of the Whiffle Tree Loading System

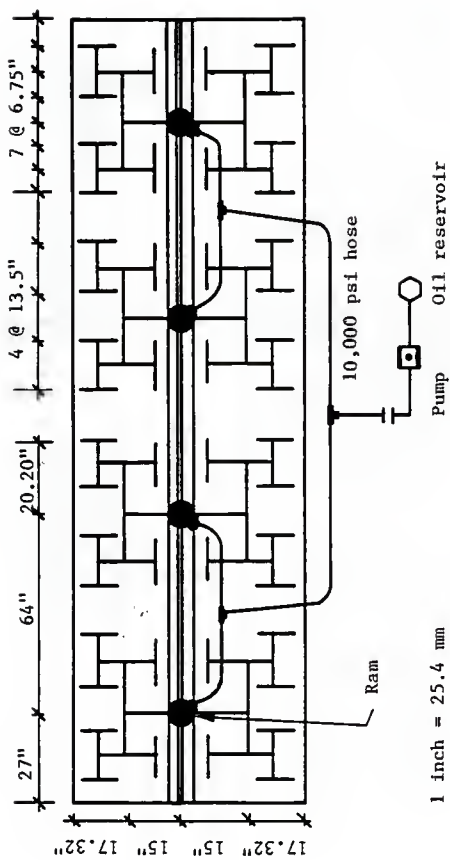


Fig. 5.3 Layout of Loading System

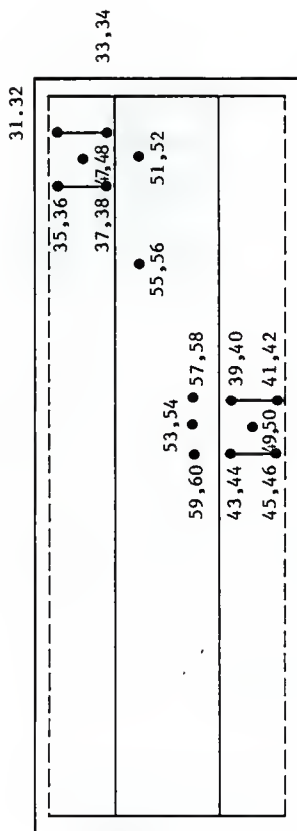


Fig. 5.4 Strain Gage Layout on the Whiffle Tree

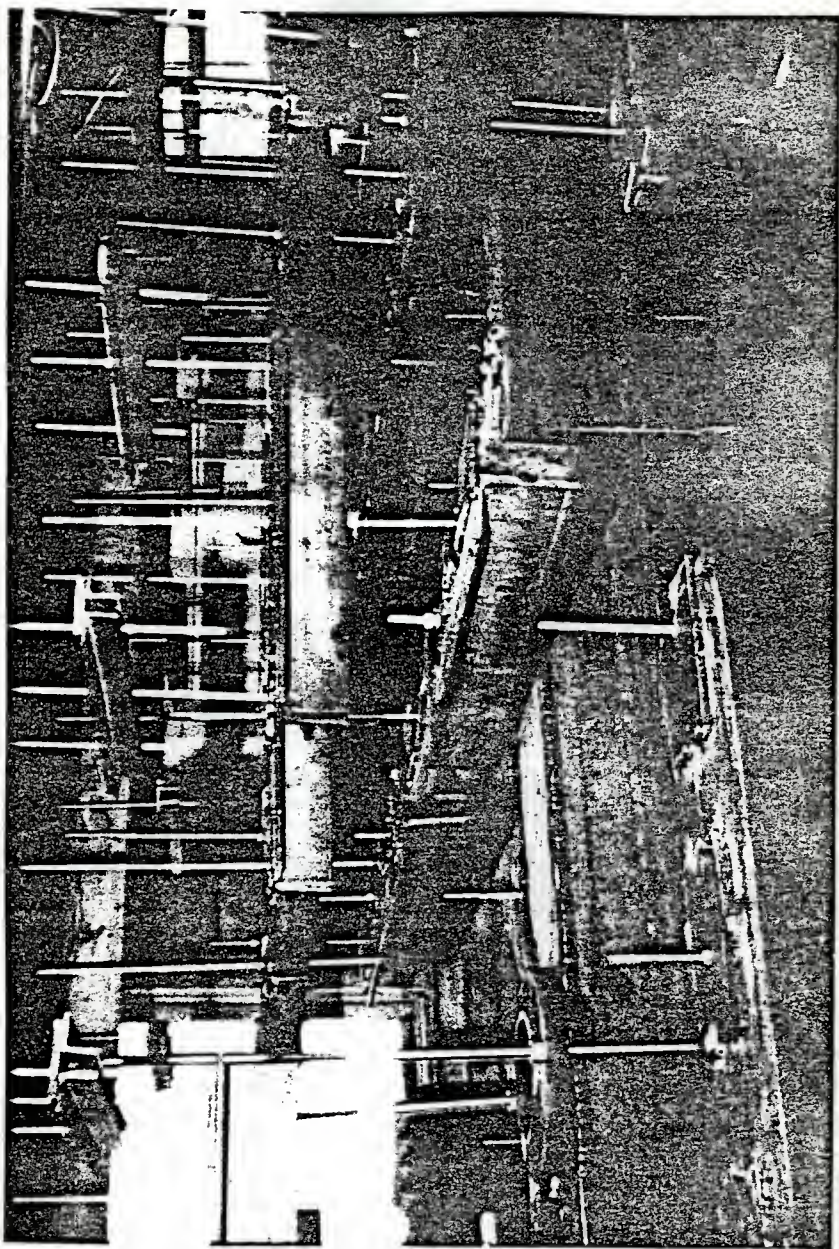


Fig. 5.5 Whiffle Tree Arrangement

VI. TEST RESULTS AND DISCUSSION

6.1 Surface Thickness Values and Contours

Contour lines of thickness for each plate are given in Fig. 6.1 in which it is seen that for the major portion of each plate the thickness did not deviate by more than 0.03 in. (0.76 mm) in the side plates, or 4 percent and by 0.01 in. (0.25 mm) in the top plate or 1.7 percent.

In the top plate, local deviations occurred at the load points due to the problem with the screed around the tubes through the plate. However, these were quite localized and should not affect the structural response any more than the local load bearing would.

6.2 Quality Control of Cylinders

The 1 in. x 2 in. (25.4 mm x 50.8 mm) cylinders are about the smallest that can be tested. Cylinders that are 3 in. x 6 in. (76.2 mm x 152.4 mm) in diameter can be successfully tested. Plexiglass tubes were used for the 1 in. x 2 in. (25.4 mm x 50.8 mm) cylinders and cardboard molds were used for the 3 in. x 6 in. (76.2 mm x 152.4 mm) cylinders. The average strength at sixty-two days, using all data for 3 in. x 6 in. (76.2 mm x 152.4 mm) cylinders, was found to be 6294 psi (43.39 MPa).

Tables 6.2 and 6.3 show the test results for the cylinders. Figures 6.2 and 6.3 show the compressive stress-strain curves for the micro-concrete tested at sixty-two days. The average Young's modulus is 3.38×10^6 psi (23.31 GPa) and the average ultimate strain ϵ_o is 0.0031 in./in. (mm). The data are shown in Table 6.4.

6.3 Ram Calibration Tests

The jacking forces corresponding to readings of the pressure gage are shown in Table 6.1. These relations were used to calculate the force applied on the model during testing, i.e., to interpret the reading on the pressure gage on the pump as force per each ram. Every increment of loading was conducted based on the force shown in the table for all rams.

6.4 First Test

The first test conducted on the model consisted of three cycles of loading. This was done to monitor and record the behavior of the model up to the service load. The deflection and the strain were recorded. However, the objective of this test, as was mentioned before, was to exercise the strain gages and the loading system. The deflection response of the model in the first cycle and the second cycle revealed an inconsistent pattern. Figure 6.4 shows the deflection response of the model along a longitudinal line at the midspan due to cycling loading. It can be seen from this figure in the third cycle that the deflection due to this loading has stabilized. Figure 6.5 shows the transverse deflections of the midspan cross section of the top plate. These deflections show an elastic behavior. Deflection response of the edge beam at midspan showed very good agreement with the elastic theory during the three cycles, as documented in Ref. (35).

6.5 Second Test

The loading was conducted in 100 psi (0.69 KPa) increments until 700 psi (4.83 MPa) was read on the gage at the pump. The corresponding uniformly distributed load was interpreted from the jack calibration table and the area of the horizontal projection of the model which has approximately 98 sq. ft. (9.1 sq. m). The corresponding incremental surface loadings were

25.78 lb./sq. ft. (1.23 KPa) as the first increment and the last was 199 lb./sq. ft. (9.53 KPa).

6.6 Response of the Whiffle Tree

The whiffle tree loading system was made up of several layers of simple beams interconnected by threaded rods and bolts. This loading system was used to simulate a uniform live load on the model, as mentioned earlier.

6.6.1 Strains

Strain gages were mounted on a 1/2 in. x 1/2 in. (12.7 mm x 12.7 mm) bar which is interconnected to the whiffle tree bars. The stress-strain curve for this bar and the physical properties are shown in Fig. 6.6.

Strains on 15 whiffle tree bars were recorded. Their locations are given in Fig. 5.4. Strain gages 31 to 38 were placed on rods going directly through the plate surface close to the support. Strain gages 39 to 46 were placed near midspan in the same manner. Figures 6.7 through 6.12 show the measured load versus theoretical load for rods on the whiffle tree going directly through the inclined plate surface near the support and near the midspan.

Calculations of P_{exp} , P_{Theo} , and average readings of the gages are tabulated in Appendix C.

These figures clearly illustrate that the average readings agree well with theory. From the graph it is seen that the effect of deformation influenced the mid-span rod greatly, giving it fairly large bending moment. This can be seen in Figs. 6.8, 6.10 and 6.12. Figures 6.13 and 6.14 show theoretical load versus experimental load for rods not going directly through the angle plate surfaces. For the gages near the support (gages 47 and 48) the average readings

agree well with theoretical. But for the gages near the mid-span (gages 49 and 50), the average readings deviate from theoretical. This may be due to eccentricity of the middle rod on the whiffle tree's bar which gave a big jump in the strain. Figures 6.15 and 6.16 show the agreement of the average experimental readings with theoretical for rods at mid-span, not going directly through the top plate surface (gages 59 and 60).

6.7 Elastic Response of the Model

It is assumed that under the service load the structural behavior is linearly elastic. The response of the model is discussed.

6.7.1 Deflections

At each level of load, deflections were recorded from which the deflection profiles along the center of top plate and transverse to the top plate at midspan were obtained. The deflection patterns, as shown in Figs. 6.17 and 6.18 display stability and consistency of response up to 110 lb./sq. ft. (5.27 KPa). The model exhibited linear response up to this point. After that, a sudden increase in deflection can be seen at dial gage numbers, keeping the same wave form that appeared from the previous load increment. For more details on buckling the reader is referred to Ref. (35).

6.7.2 Strains

Longitudinal strain gage response at mid-span of the top plate is shown in Fig. 6.19. This figure shows a linear relationship of stress versus load up to 75 lb./sq. ft. (3.59 KPa), then both strains deviated. As it was shown in Ref. (35), all strains are approximately linear up to a certain loading level, then they start to deviate.

Thus, it is concluded that elastic analysis is adequate up to these load levels, which are within the service load range.

6.8 Discussion of Edge Beam Results

The forces transferred from the plates to the edge beams are shown in Appendix B, in the section of development of equations for left edge beam and Fig. B.2.

The equations for beam internal tractions were developed using the trapezoidal rule. The loading is expressed as a trigonometric series in the longitudinal direction. Using this approach the internal forces on the edge beam were determined in terms of equations. A subroutine was written to perform this calculation. The shear, moment, axial forces and torsion for edge beams were calculated and the printout of the computer is listed in Appendix B. The results are plotted and they show the same numerical values for both edge beams as it is expected. The graphs of the results are shown in Appendix B.

An output from the computer showing the results of the model including the effect of the edge beam in the analysis is listed in Appendix B. From this output we can see that the effect of the edge beam in the analysis reduces the moment capacity in the transverse direction compared to the analysis that did not include the effect of the edge beam. This comparison is tabulated in Table B.1. The table reflects the symmetrical effect in the plates and influence of edge beam stiffness on traction distribution.

From Table B.1 it is seen that the transverse moment, M_y is decreased by including the edge beam in the analysis. The stresses at midspan of the top plate are reduced too. Moreover, it is noticed that all tractions are uniformly distributed. However, M_x stays almost the same in both analyses.

The computer output for edge beams is listed in Appendix B. The results of edge beam analyses are plotted in Figs. B.3-B.12. It is seen

from Figs. B.3 and B.8 the shear forces are equal for left and right edge beams as it was expected, due to symmetrical shape of the model and uniform load. The edge beam bending moment, M_y has the same numerical values with opposite sign according to the coordinate system established in Fig. B.2. The torsion for both edge beams as shown in Figs. B.5 and B.10 display equality with opposite sign due to the rotations of both edge beams toward each other.

The edge beam axial forces N_x are equal for both edge beams and they are in tension as expected. They have maximum value at midspan and zero at end diaphragms. The results are shown in Figs. B.6 and B.11. The bending moments, M_z for left and right edge beams exhibit the same magnitudes and sign as shown in Figs. B.7 and B.12.

Table 6.1 Jack Calibrations

No.	Pressure psi	Ram #1, lb.* 2151	Ram #2, lb.* 2576	Ram #3, lb.* 2328	Ram #4, lb.* 2346	Average lb.
1	100	600	700	600	600	625
2	200	1400	1200	1500	1500	1400
3	300	2100	1900	2100	2100	2050
4	400	2700	2600	2800	2600	2675
5	500	3500	300	3400	3200	3275
6	600	4200	4400	4100	4100	4200
7	700	4900	4900	4700	4800	4825

1 psi = 6.89 kPa

1 lb = 4.45 N

* Serial number of the ram.

Table 6.2 3" x 6" (76.2 mm x 152.4 mm) Concrete Cylinders,
Compression Test Results

Cylinder No.	Age, days	Compression force lb.	Stress, f'_c psi
11	7	34,800	4923
21	7	20,000	2829
31	7	29,000	4102
41	7	31,000	4386
51	7	24,200	3424
61	7	24,100	3409
71	7	24,200	3424
81	7	30,600	4329

12	15	35,000	4952
22	15	25,000	3537
32	15	32,000	4527
42	15	32,000	4527
52	15	29,000	4102
62	15	35,000	4952
72	15	26,000	3678
82	15	34,200	4838

14	28	39,000	5517
24	28	45,000	6366
34	28	35,000	4951
44	28	36,000	5093
54	28	34,000	4810
64	28	35,000	4951
74	28	34,000	4810
84	28	35,200	4980

13	62	40,300	5701
23	62	50,700	7173
33	62	41,000	5800
43	62	42,000	5942
53	62	45,000	6366
63	62	47,000	6649
73	62	36,500	5164
83	62	41,400	5857

15	62	49,000	6932
25	62	53,000	7498
65	62	44,000	6225
85	62	44,000	6225

1 lb = 4.448 N
1 psi = 6.895 kPa

Average = 6294 psi (43.39 MPa)
at 62 days

Table 6.3 1" x 2" (25.4 mm x 50.8 mm) Concrete
Cylinders, Compressive Test Results

No. of Tests	Compressive Force (lb.)	No. of Tests	Compressive Force (lb.)
1	3620	18	3340
2	4620	19	4920
3	4600	20	3430
4	3000	21	3070
5	3200	22	3110
6	4000	23	2880
7	3900	24	4080
8	3450	25	3390
9	2850	26	4280
10	2900	27	2650
11	2600	28	3670
12	3820	29	5100
13	3280	30	4270
14	3490	31	3600
15	3790	32	5300
16	4250	33	3920
17	3170		

Average strength, 4689 psi
Testing age, 62 days

1 psi = 6.895 kPa
1 lb. = 4.448 N

Table 6.4 Cylinder Stress-Strain Test Data

Load (lb)	Stress (psi)	Long. Strain (Micro in./in.)		Average	Trans. Strain (Micro in./in.)		Average
		Gage 1	Gage 2		Gage 3	Gage 4	
3000	424	15	3	9	0	15	7
6000	449	23	39	31	2	14	8
9000	1273	86	67	76	10	5	7
12000	1697	156	111	134	0	14	7
15000	2122	241	154	197	0	12	6
18000	2546	339	199	269	4	15	9
21000	2970	443	239	341	0	1	.4

1 psi = 6.895 kPa;

1 lb. = 4.45 N

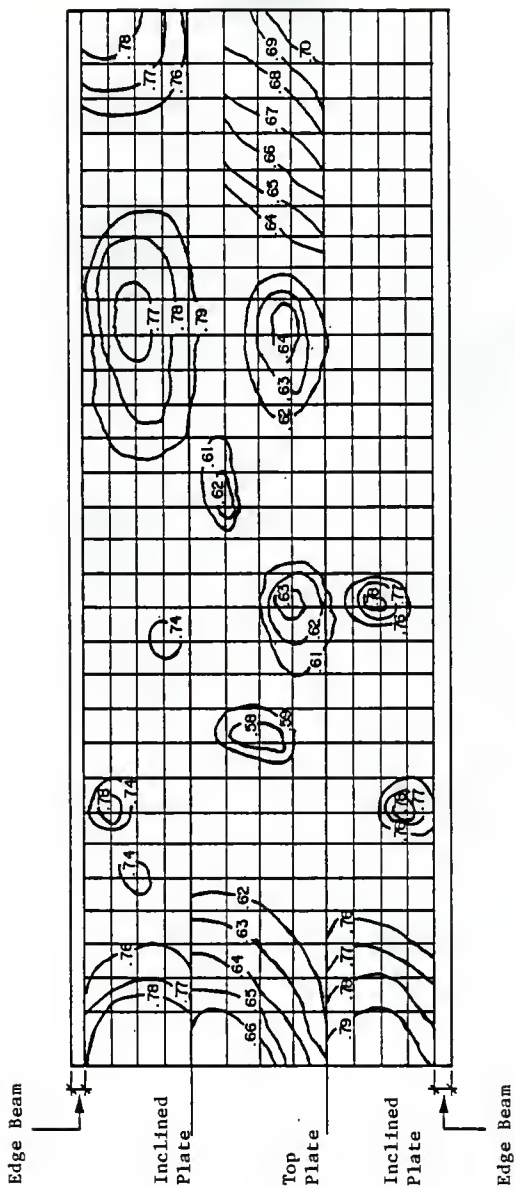


Fig. 6.1 Contour Map of Plate Thickness

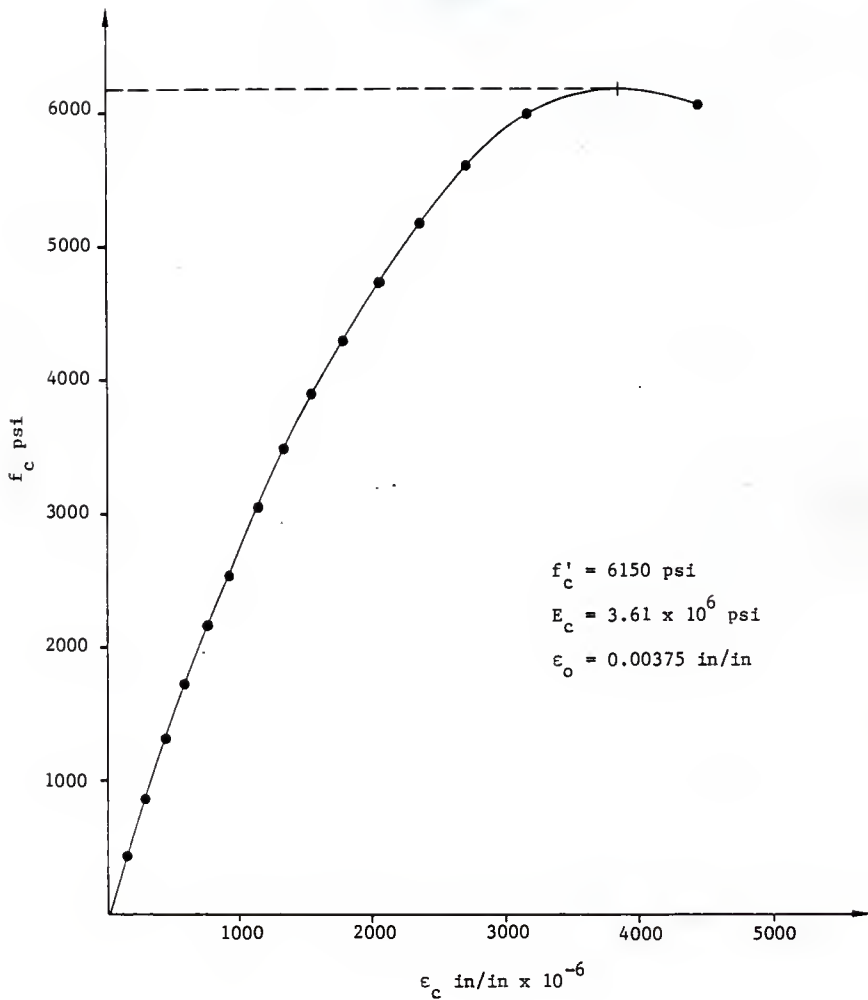


Fig. 6.2 Compressive Stress-Strain Curve for .
the Micro-Concrete - Cylinder 53
1 psi = 6.895 KPa

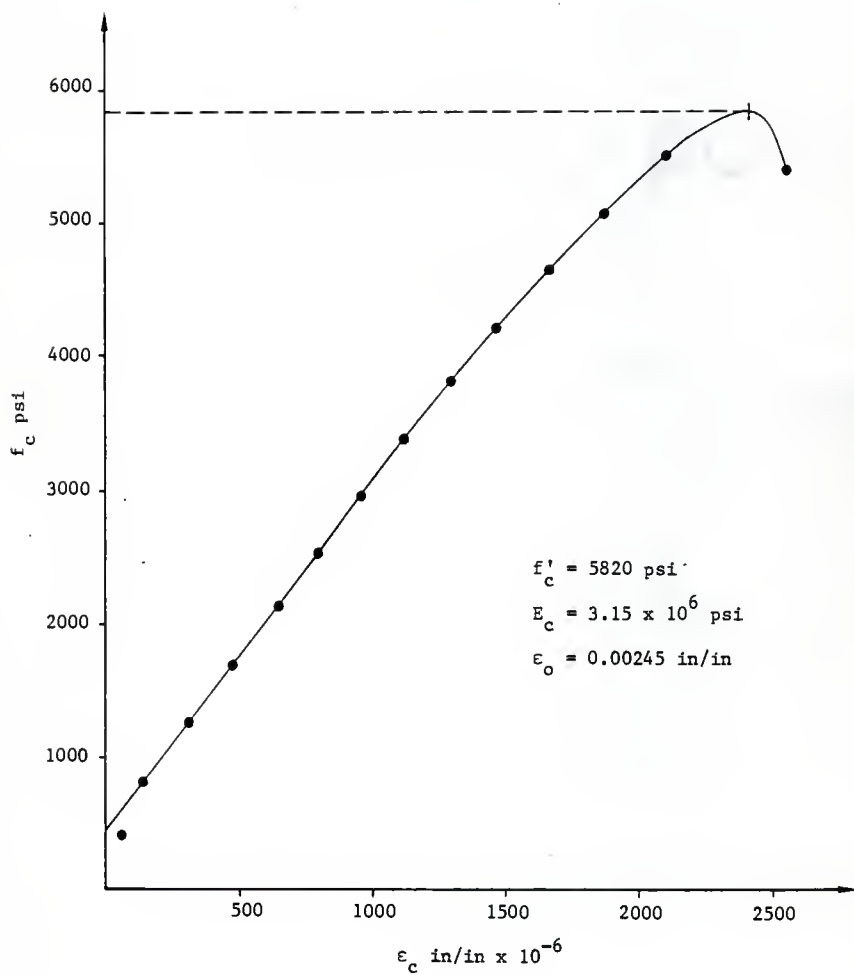


Fig. 6.3 Compressive Stress-Strain Curve for the Micro-Concrete - Cylinder 43
1 psi = 6.895 KPa

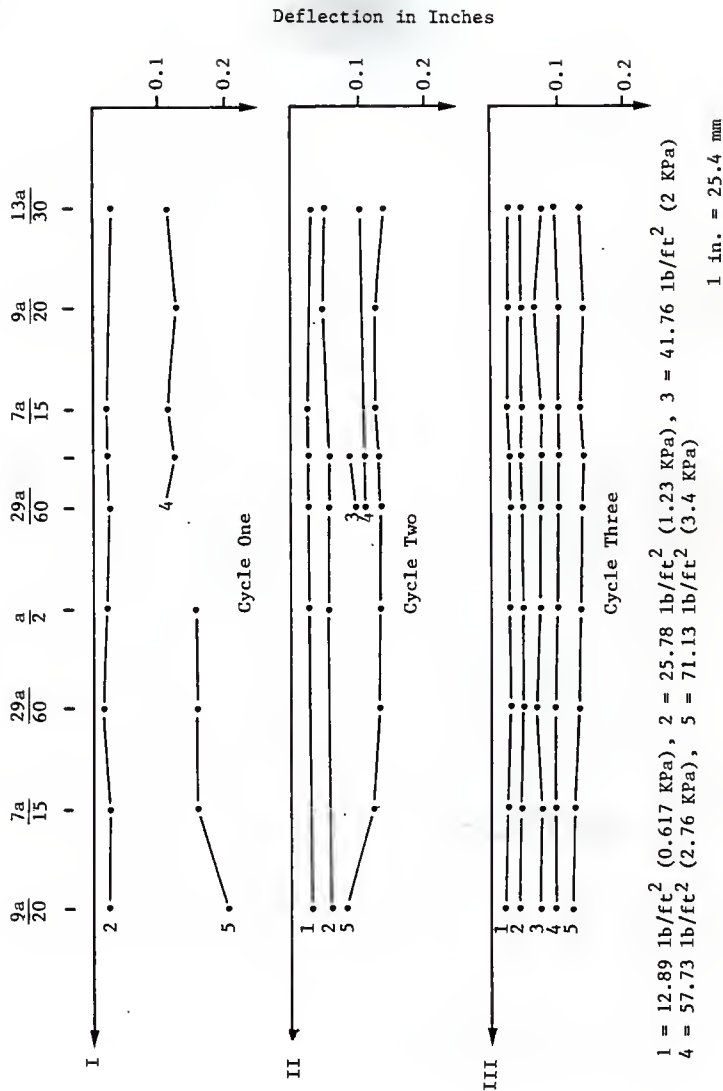


Fig. 6.4 Deflection Due to Cyclic Loading for Service Load at Centerline of Top Plate

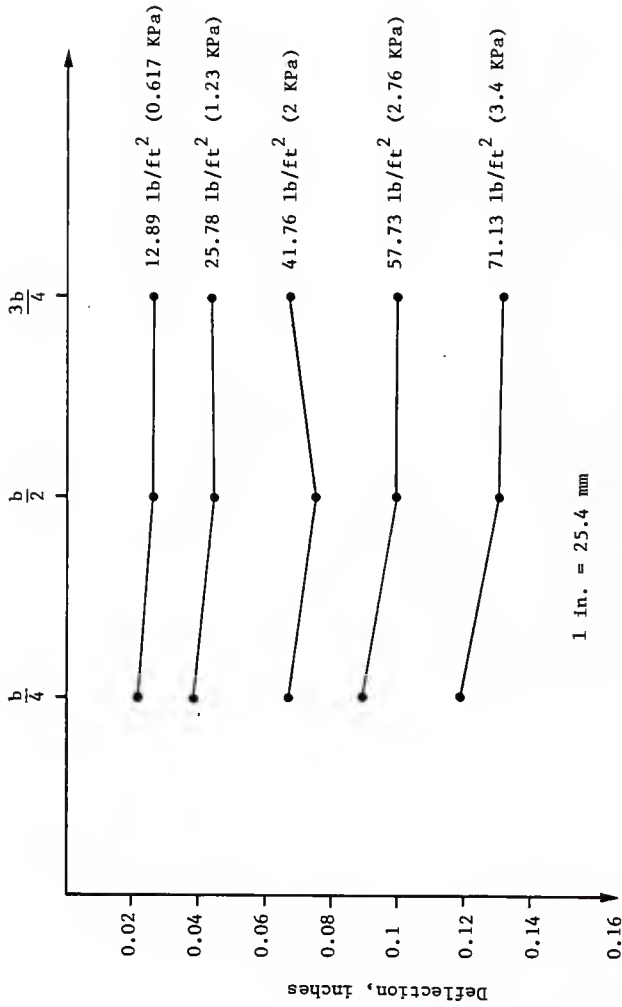


Fig. 6.5 Mid-span - Top Plate Transverse Deflection
Third Cycle

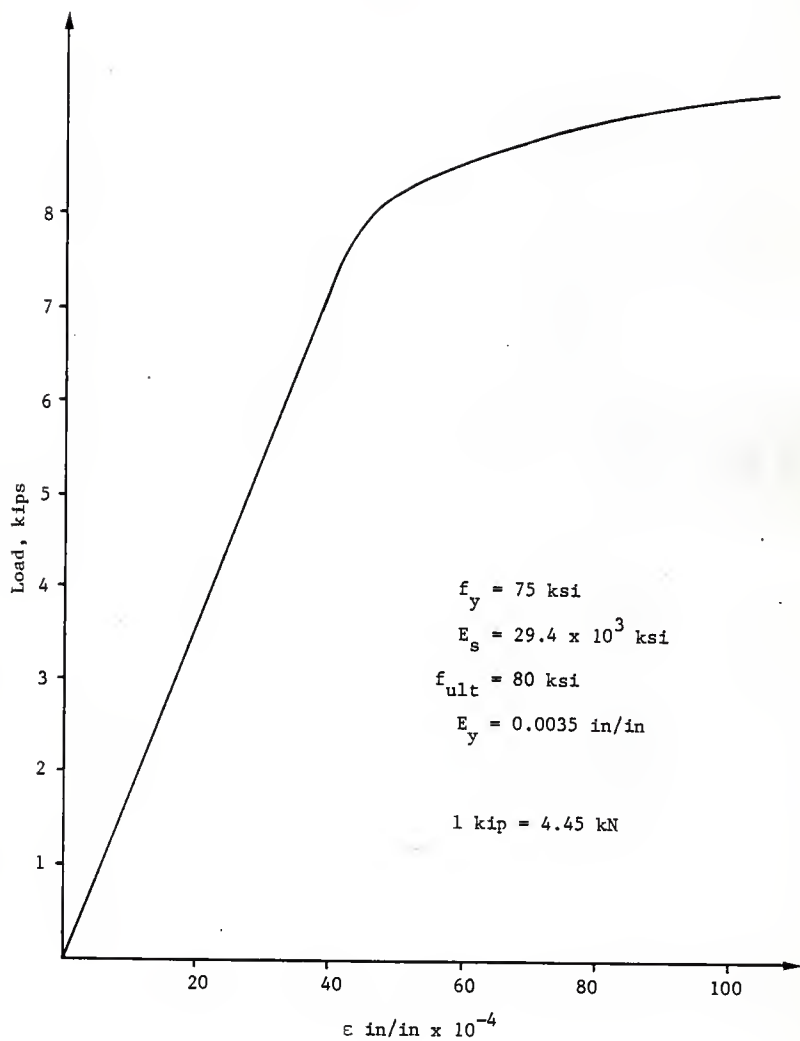
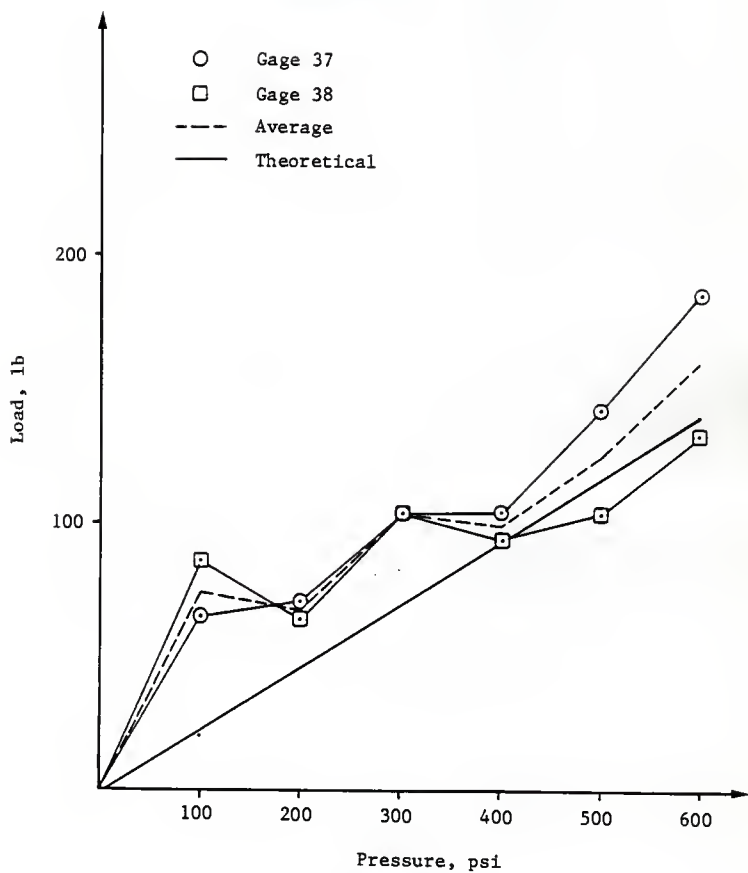
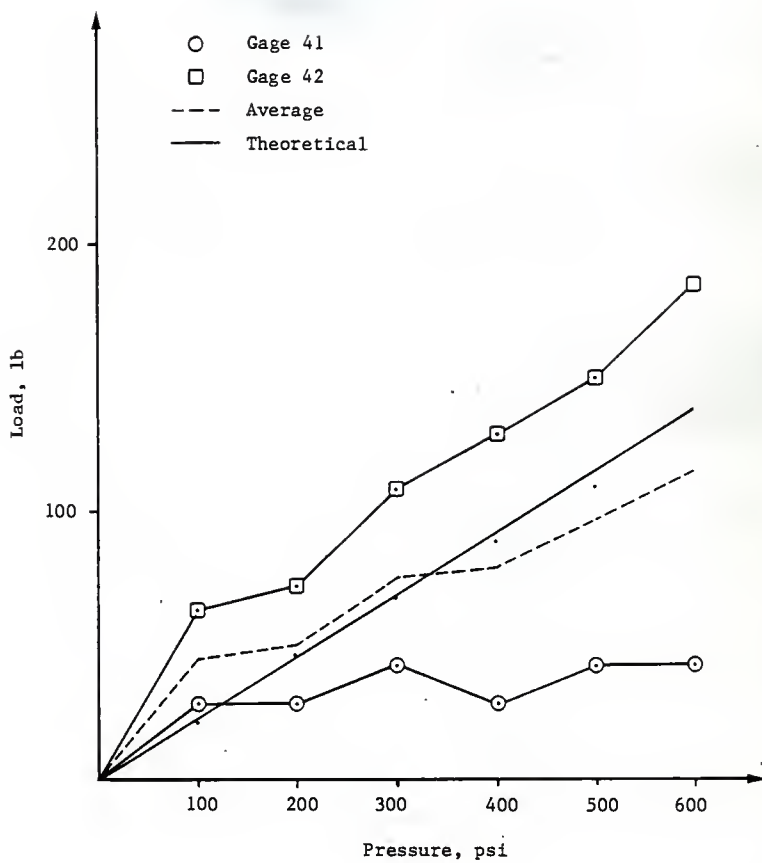


Fig. 6.6 Stress-Strain Curve for a $\frac{1}{2} \times \frac{1}{2}$ Bar



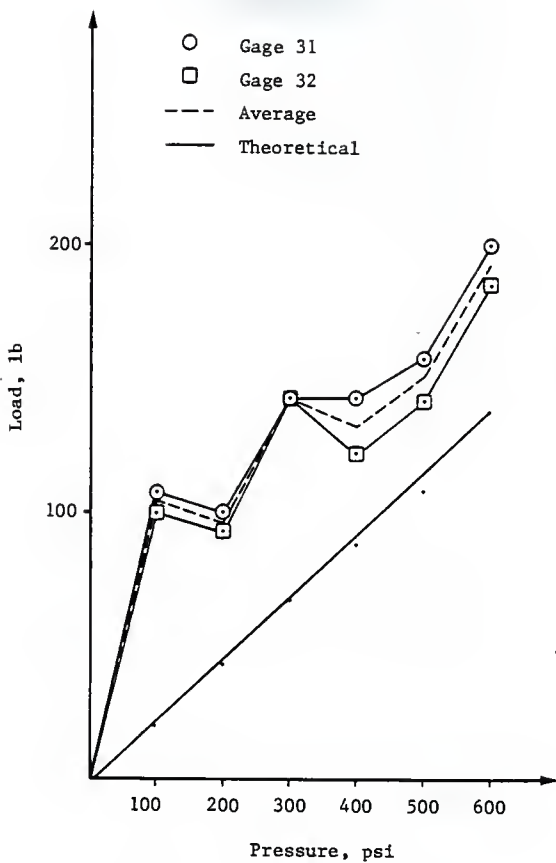
1 lb = 4.45 N, 1 psi = 6.89 kPa

Fig. 6.7 Load Point Response Near End Support



1 lb = 4.45 N, 1 psi = 6.89 kPa

Fig. 6.8 Load Point Response Near Mid-span



1 lb = 4.45 N, 1 psi = 6.89 kPa

Fig. 6.9 Load Point Response Near End Support

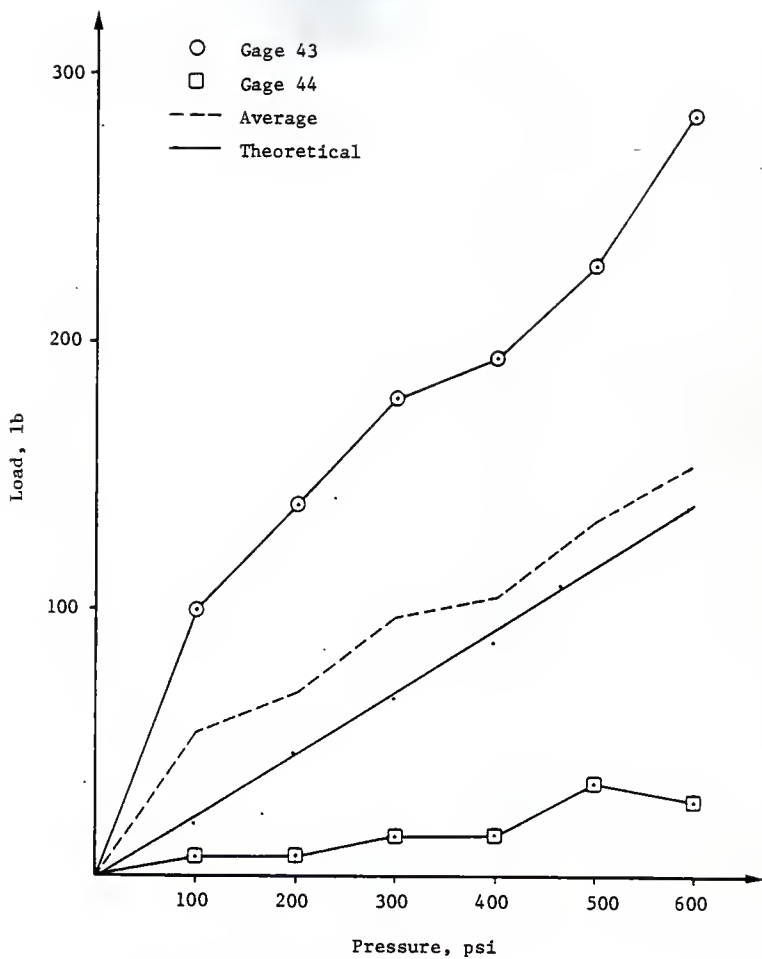
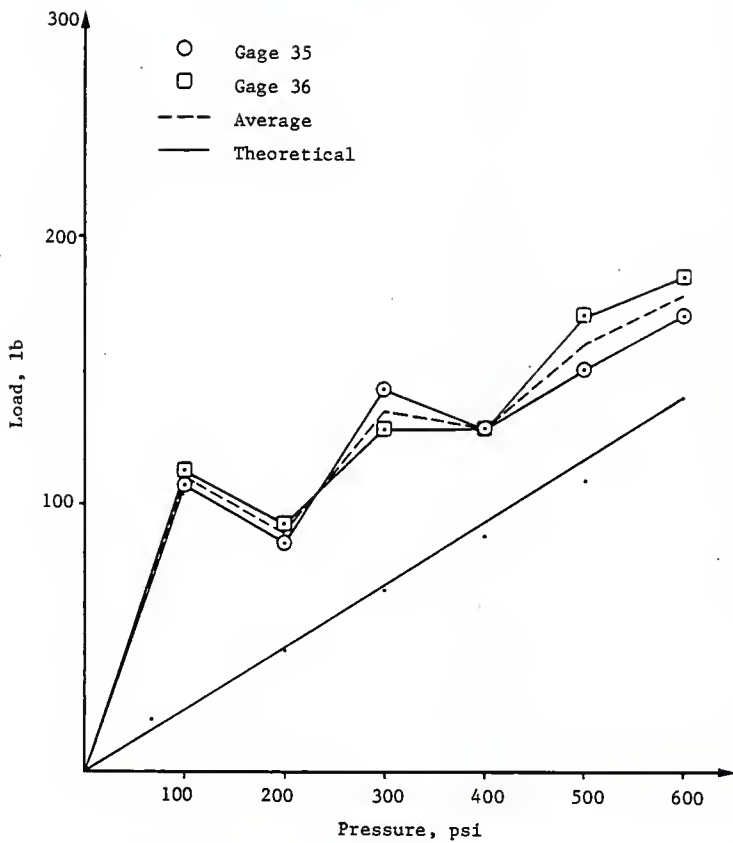
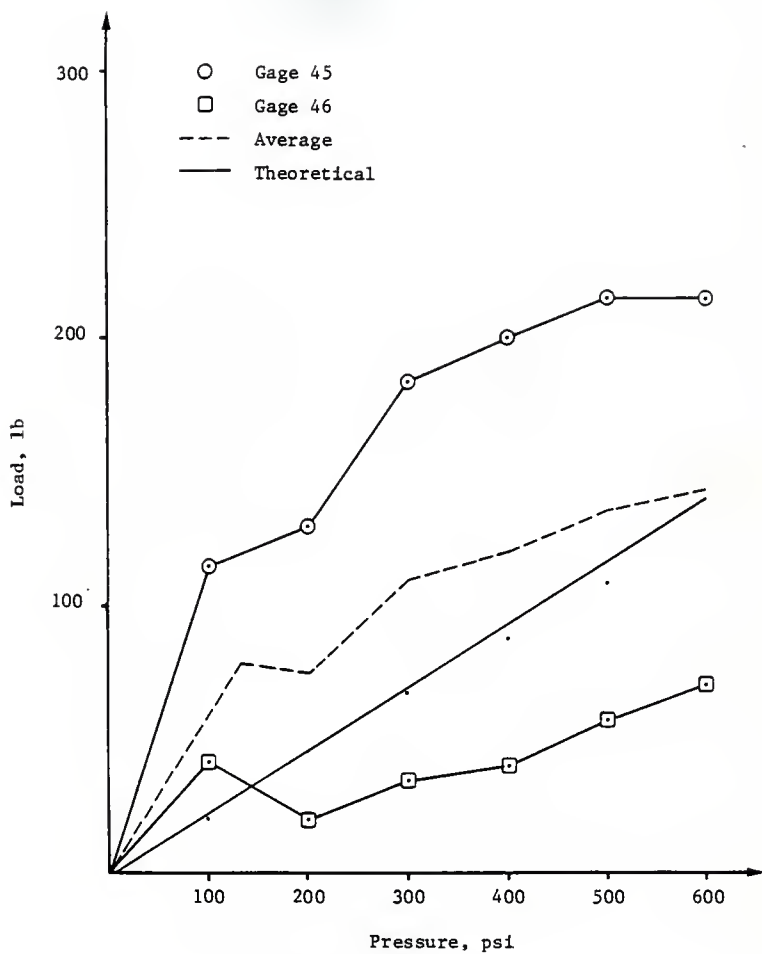


Fig. 6.10 Load Point Response Near Mid-span



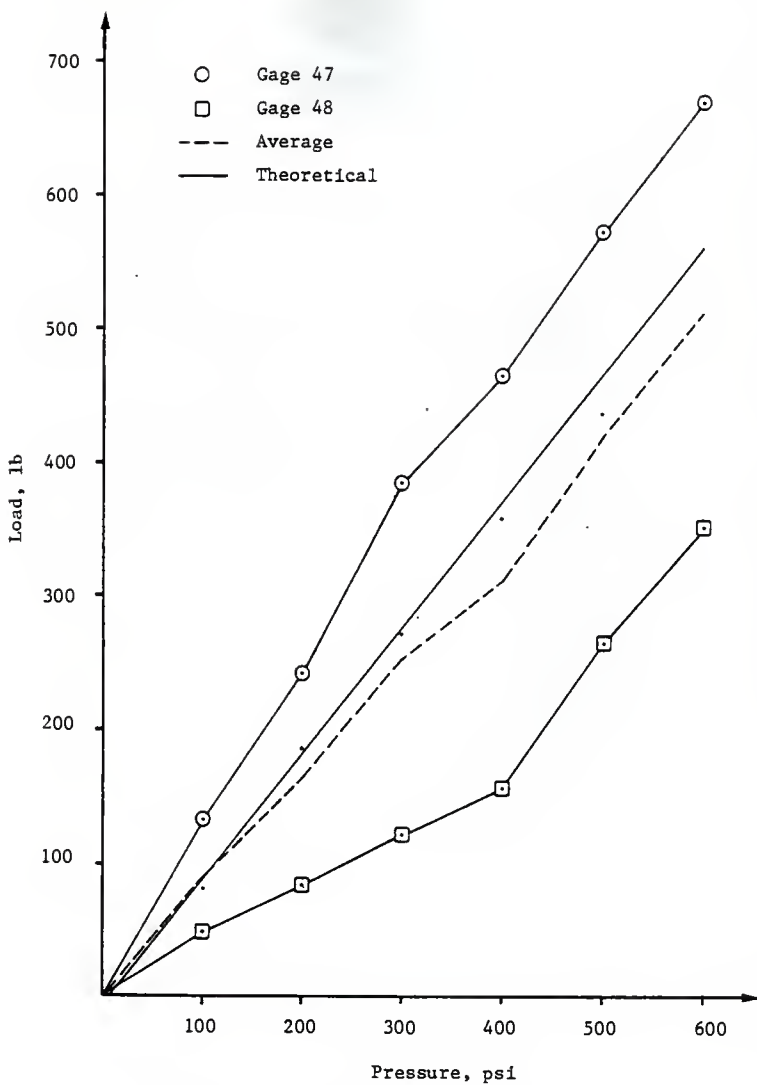
1 lb = 4.45 N, 1 psi = 6.89 kPa

Fig. 6.11 Inclined Load Point Response Near Edge Beam



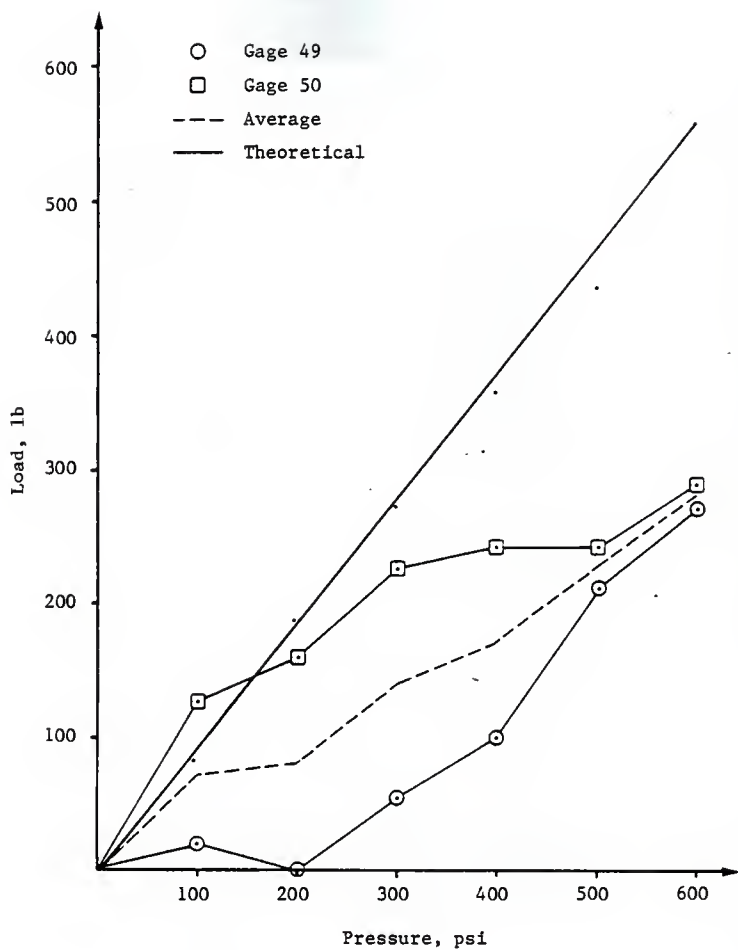
1 lb = 4.45 N, 1 psi = 6.89 kPa

Fig. 6.12 Middle Load Point Response Near Mid-span



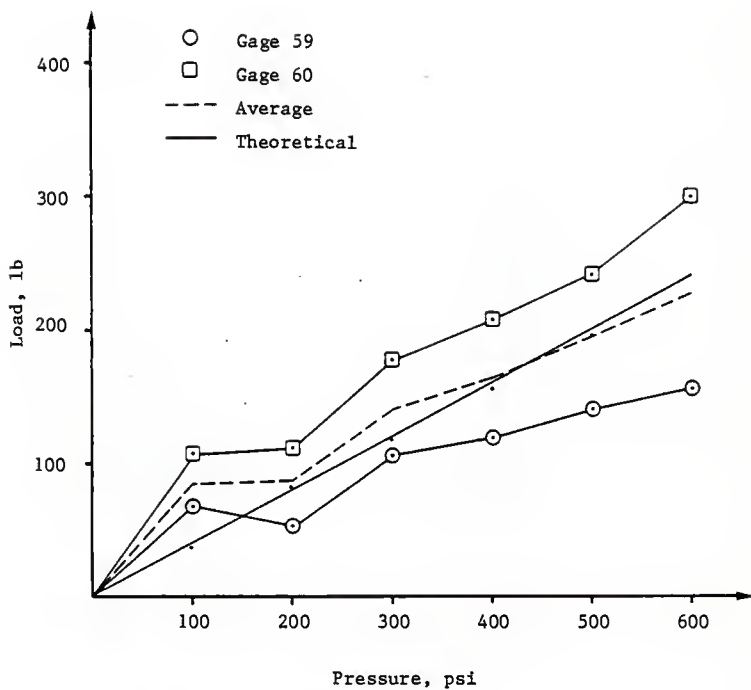
1 lb = 4.45 N, 1 psi = 6.89 kPa

Fig. 6.13 Whiffle Tree Bar Response Near End Support



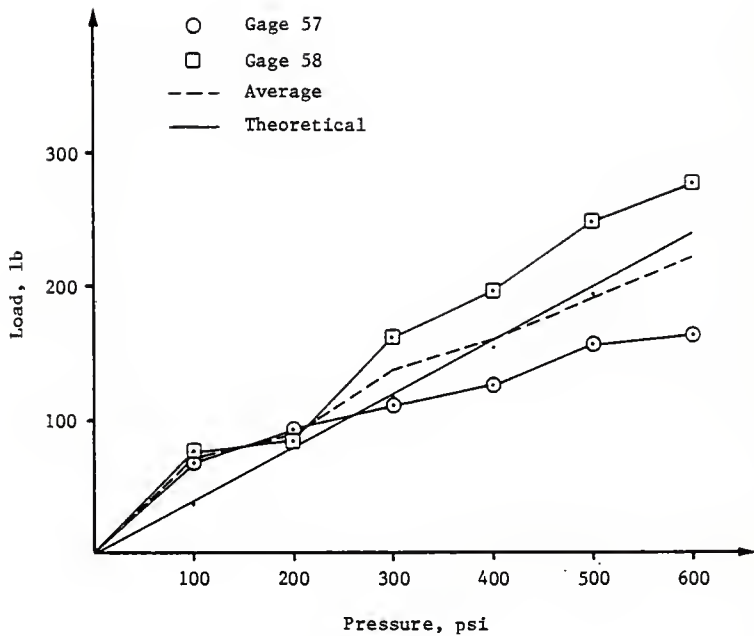
1 lb = 4.45 N, 1 psi = 6.89 kPa

Fig. 6.14 Whiffle Tree Bar Response Near Mid-span



1 lb = 4.45 N, 1 psi = 6.89 kPa

Fig. 6.15 Load Point Response at Mid-span of the Top Plate



1 lb = 4.45 N, 1 psi = 6.89 kPa

Fig. 6.16 Whiffle Tree Bar Response Near Mid-span of the Top Plate

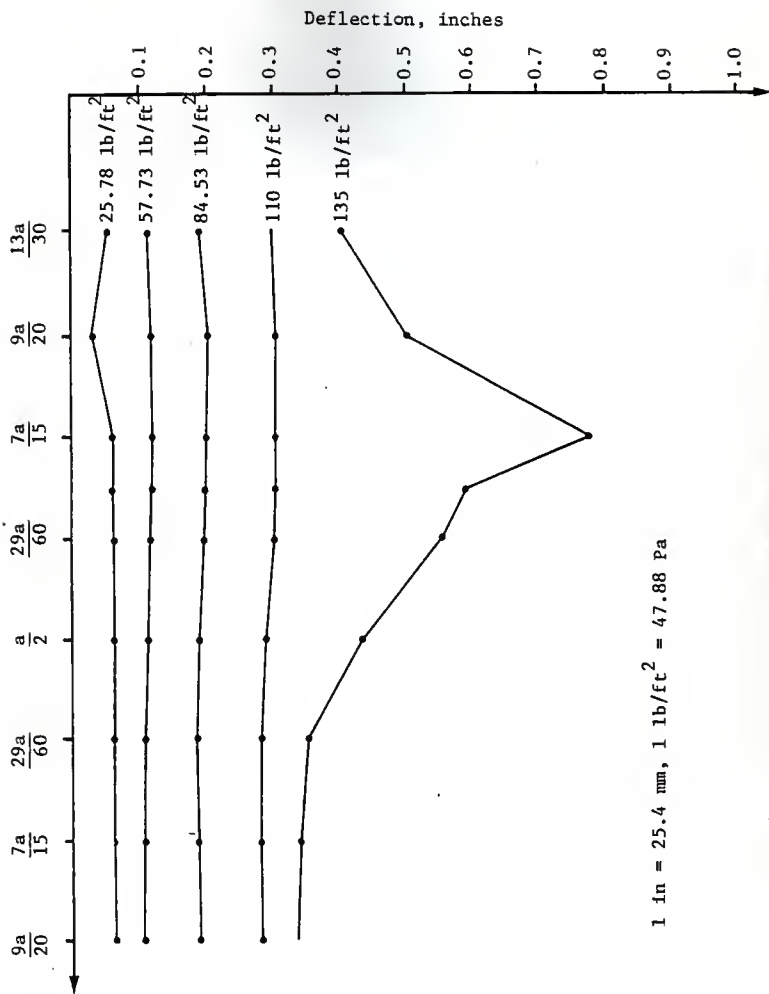


Fig. 6.17 Deflection Profiles Along Center of Top Plate

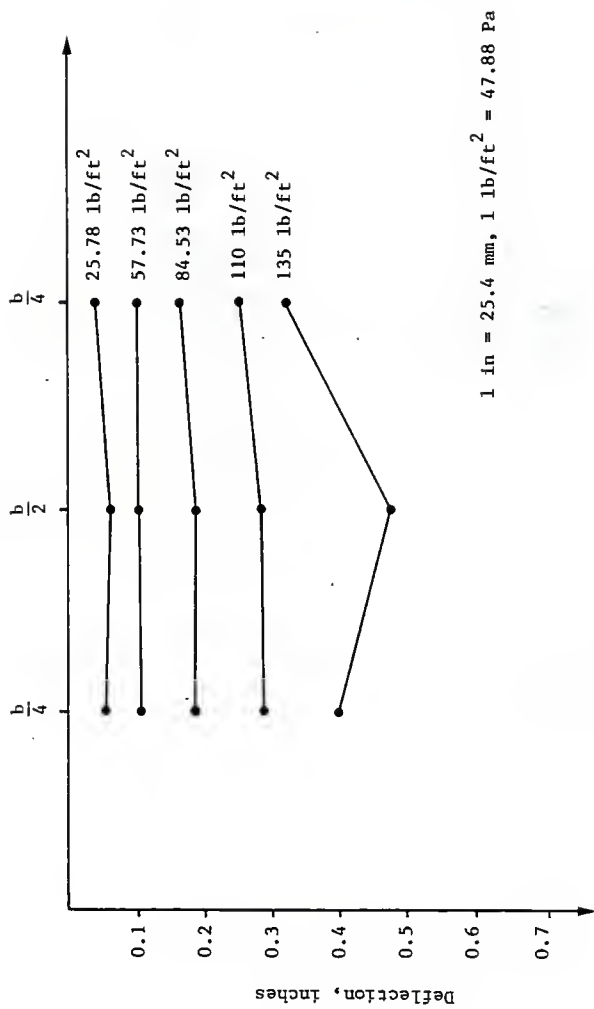


Fig. 6.18 Deflection Profiles Transverse to Top Plate at Mid-span

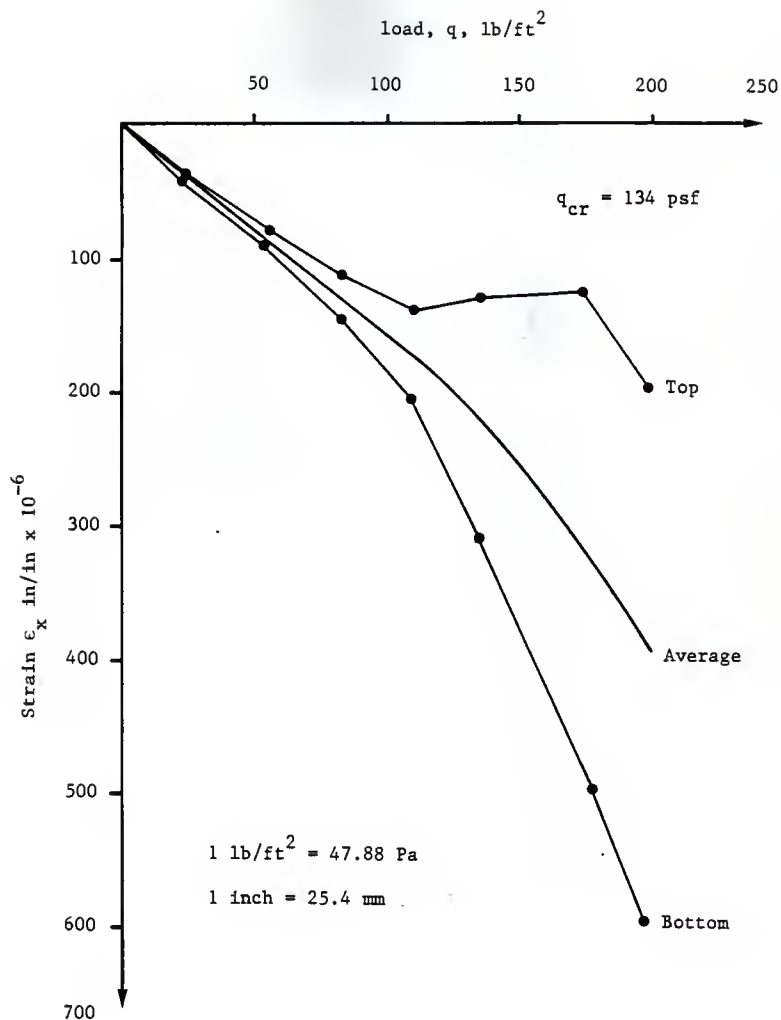


Fig. 6.19 Longitudinal Strain in the Center of the Top Plate, Test Two (Based on Reference 35)

VII. SUMMARY AND CONCLUSIONS

7.1 Summary

The objective of this study was to investigate analytically and experimentally the structural behavior of a reinforced concrete folded plate model with edge beams. An "exact" elastic method was selected as the method of analysis for use in this research. A brief review of the "exact" theory has been presented. The analytical solutions were obtained through the use of a computer program developed by Swartz (32) to handle the mathematical formulation of the "exact" elastic method of analysis. Two subroutines were added to the main program to account for analysis of edge beams. The coefficients for edge beams stiffness and stresses on edge beams were calculated. The focal point of this study was to determine the actual performance of the whiffle tree loading system and expected distribution of loads to the model.

The model was tested three times and the performance of the model under the service load was as expected by the analysis.

Loads were applied through a whiffle tree loading system of simple beams interconnected by bolts and threaded rods to load points on the model. Strain gages were mounted on the whiffle tree bars, which were used to calculate forces in the whiffle tree delivered to the model. High accuracy was achieved in controlling the geometry of the model.

Measured deflections and strains were presented.

7.2 Conclusions

The following conclusions were derived from this study:

1. The whiffle tree system distributed the loads to the shell in the predicted manner.
2. By including edge beams in the analysis the capacity of M_y is reduced in the range of 1.2 percent to 31 percent lower than in the method of analysis considered in Ref. (35).
3. The displacements remained the same in both analyses.
4. The membrane forces remained almost the same in both analyses.
5. Reliable results are obtained by including edge beams in the analysis.

7.3 Recommendations

1. There is a need for further experimental studies of reinforced concrete folded plate models having different span to height ratios.
2. Unsymmetrical loading should be performed to study the behavior of these structures.
3. Structural models should be well reinforced for transverse bending effects to prevent failure in this direction.
4. It was noticed that the girder of the loading system was deflected due to applied loads, so it is recommended to increase its moment of inertia for future use.

REFERENCES

1. ACI Committee 318, "ACI Standard Building Code Requirements for Reinforced Concrete (ACI 318-83)," American Concrete Institute, Detroit, 1983.
2. ACI Committee 318, "Commentary on Building Code Requirements for Reinforced Concrete (ACI 318-83)," American Concrete Institute, Detroit, 1983.
3. Aldrige, W. W., "Ultimate Strength Tests of Model Reinforced Concrete Folded Plate Structures," Ph.D. Thesis, The University of Texas, Austin, January 1966.
4. Beaufait, F. W., "Analysis of Continuous Folded Plate Surface," Journal of the Structural Division, ASCE, Vol. 91, No. ST6, Proc. Paper 4555, Dec. 1965.
5. Billington, D. P., Thin Shell Concrete Structures, McGraw-Hill Book Company, New York, 1982.
6. Chacos, G. P. and Scalzi, J. B., "Ultimate Strength of a Folded Plate Structure," Journal of the American Concrete Institute, Vol. 32, No. 8, February 1961.
7. Chien, K. Chia-Chang, "Construction and Testing of Reinforced Concrete Hyperbolic Cooling Tower Model," M. S. Thesis, Kansas State University, 1983.
8. Craemer, H., "Design of Prismatic Shells," Journal of the American Concrete Institute, February 1953.
9. DeFries-Skene, A. and Scordelis, A. C., "Direct Stiffness Solution for Folded Plates," Journal of the Structural Division, ASCE, Vol. 90, No. ST4, August, 1964.
10. Dykes, A. R., "Folded Plate Construction: An Investigation of Collapse Conditions," The Structural Engineer, Vol. 38, No. 2, London, February 1960.
11. Ehlers, G., "Ein Neues Konstruktionsprinzip," Bauingenieur, Vol. 9, 1930.
12. Eliahu Traum, "Prismatic Folded Plates - A Simplified Procedure of Analysis," Journal of the American Concrete Institute, Proceedings, Vol. 61, No. 10, October, 1964, pp. 1285.
13. Fialkow, M. N., "Safe Limit Loading of Folded Plate Structures," Journal of the Structural Division, ASCE, Proc., ST10, October 1972.
14. Fialkow, M. N., "Yield Line Analysis of Folded Plate Structures," Journal of the Structural Division, ASCE, Vol. 94, ST12, Proc. Paper 6306, Dec. 1968, pp. 2935-2962.

15. Fialkow, M. N., "Limit Design of Folded Plate Structures," Proceedings, ASCE National Structural Engineering Conference on Methods of Structural Analysis, Madison, Wisconsin, August 1976.
16. Gaafar, I., "Hipped Plate Analysis Considering Joint Displacements," Transactions, ASCE, Vol. 119, 1954.
17. Goldberg, J. E. and Leve, H. L., "Theory of Prismatic Folded Plate Structures," International Association of Bridges and Structural Engineering Publications, Vol. 17, Zurich, 1957.
18. Goldberg, J. E., Gutzwiller, M. J., and Lee, R. H., "Analytical and Experimental Study of Continuous Folded Plates," Engineering Bulletin of Purdue University, Research Bulletin 156, Vol. 49, No. 6, November 1965.
19. Gruber, E., "Die Durchlaufenden Prismatischen faltwerke," Memoires, International Association for Bridge and Structural Engineering, Zurich, Vol. 12, 1952.
20. Johnsen, J. W., "Yield Line Theory," Cement and Concrete Association, London, 1963.
21. Kaveti Seetharamulu and Mangesh G. Kulkarni, "Analysis of Short Span Folded Plates," Journal of the Structural Division, ASCE, Vol. 90, No. ST3, June 1964.
22. Lee, D. W., "Nonlinear Behavior of Reinforced Concrete Folded Plate Structures," Ph.D. Thesis, The University of Texas, Austin, 1969.
23. Meek, J. L., "Matrix Derivation of the Folded Plate Equations," Journal of the Structural Division, ASCE, Vol. 89, No. ST3, Proc. Paper 3549, June 1963.
24. Moorman, R. B., "Test of a Reinforced Concrete Folded Plate Structure," Report No. CE335-5910F, Syracuse University Research Institute, Syracuse, New York, October 1959.
25. "Phase I Report on Folded Plate Construction," by the Task Committee on Folded Plate Construction, Journal of the Structural Division, ASCE, Vol. 89, No. ST6, Proc. Paper 3741, Dec. 1963, pp. 365-406.
26. Pudhaphongsiriporn, P., "An Experimental Study of a Reinforced Concrete Folded Plate Structure," Ph.D. Thesis, Purdue University, December 1978.
27. Resheidat, M. R., "An Experimental Study of a Reinforced Concrete Folded Plate Structure with Edge Beams," Ph.D. Thesis, Purdue University, May 1981.
28. Sabnis, G. M., Harris, H. G., White, R. N. and Mirza, M. S., Structural Modeling and Experimental Techniques, Prentice-Hall, Inc., Englewood Cliffs, N.J., 1983.

29. Scordelis, A. and Gerasimenko, P., "Strength of Reinforced Concrete Folded Plate Models," Journal of the Structural Division, ASCE, Vol. 92, ST1, February 1966.
30. Sutton, C. D., "An Experimental and Analytical Study of a Reinforced Concrete Folded-Plate Structure," Ph.D. Thesis, Purdue University, August 1972.
31. Swartz, S. E., Mikhail, M. L., and Guralnick, S. A., "Buckling of Folded Plate Structures," Experimental Mechanics, Vol. 9, No. 6, June 1969.
32. Swartz, S. E., "Stress Analysis of Folded Plates with Transverse Stiffeners," Kansas State University Bulletin, Special Report No. 99, April 1971.
33. Winter, G. and Pei, M., "Hipped Plate Construction," Journal of the American Concrete Institute, Vol. 43, January 1947.
34. Yitzhaki, D. and Reiss, M., "Analysis of Folded Plates," Journal of the Structural Division, ASCE, Vol. 88, No. ST5, Proc. Paper 3303, Oct. 1962.
35. Zregh, A., "Local Instability Behavior and Collapse of a Long-Span, Concrete Folded Plate Model," Ph.D. Thesis, Kansas State University, June 1984.

APPENDIX A

NOTATION

A	= Cross-sectional area of a beam
a	= Span length of the model
b	= Plate width
d	= Depth of edge beam
E_c	= Modulus of elasticity for concrete
E_s	= Modulus of elasticity for steel
F_F	= Fixed end forces
f'_c	= Ultimate compressive stress in concrete
f_{ult}	= Ultimate strength of steel
f_y	= Yield stress of steel
G	= Shearing modulus of elasticity
h	= Plate thickness
i	= Subscript referring to a variable number
j	= Subscript referring to a variable number or joint j
K	= Stiffness matrix
m	= Mode number in Fourier Series
M_x, M_y	= Bending moment per unit length in the x- and y-directions, respectively
N_x, N_y, N_{xy}	= Internal in-plane, normal and shear forces
P_{ni}	= Load normal to the plate
P_{ti}	= Load tangential to the plate
T	= Torque or torsional moment
t	= Beam width
u_i	= Displacement in the x-direction of the i^{th} plate
v_i	= Displacement in the y-direction of the i^{th} plate
w_i	= Normal displacement in the i^{th} plate
Δ	= Edge displacement
ϵ, η	= Global displacements in the plane of cross-section

- μ = Poisson's ratio
- ϵ_o = Ultimate strain in concrete
- θ = Rotational displacement
- ϵ_y = Yield strain
- ϕ_i = Angle of inclination from vertical of i^{th} plate
- $\{ \}$ = Describes a vector
- $[]$ = Describes a matrix

APPENDIX B

EDGE BEAM ANALYSIS AND THE COMPUTER PROGRAM

EDGE BEAM ANALYSIS

The beam to be considered is of rectangular cross section and attached along the joint j . The ends $x = 0$ and $x = a$ are simply supported with respect to bending and restrained from twisting. The required joint force - joint displacement equations can be obtained by taking consistent Fourier series developments for the edge displacements and edge forces (17). If we first consider edge "j" to be the contacting edge, as shown in Fig. B.1, then the expressions for the forces may be written as follows (17):

$$\begin{aligned}
 M_{j0} &= \frac{Et^3d}{48k_1} k^2 \left\{ \left[16 \frac{G}{E} \left(1 - 0.630 \frac{t}{d} \right) k_1 + k^2 d^2 \right] \theta_j + 2dk^2 w_j \right\} \sin kx \\
 V_{j0} &= - \frac{Et^3d}{24k_1} k^4 [d\theta_j + 2w_j] \sin kx \\
 N_{j0} &= \frac{Etd^3}{6k_2} k^3 [-2dkv_j + 3u_j] \sin kx \\
 S_{j0} &= \frac{Etd}{2k_2} k^2 [dkv_j - 2k_3u] \cos kx
 \end{aligned} \tag{B.1}$$

If edge "n+1" is the contacting edge, then

$$\begin{aligned}
 M_{n+1,n+2} &= \frac{Et^3d}{48k_1} k^2 \left\{ \left[16 \frac{G}{E} \left(1 - 0.630 \frac{t}{d} \right) k_1 + k^2 d^2 \right] \bar{\theta}_{n+1} - 2dk^2 \bar{w}_{n+1} \right\} \sin kx \\
 V_{n+1,n+2} &= \frac{Et^3d}{24k_1} k^4 [d\bar{\theta}_{n+1} - 2\bar{w}_{n+1}] \sin kx \\
 N_{n+1,n+2} &= - \frac{Etd^2}{6k_2} k^3 [2dk\bar{v}_{n+1} + 3\bar{u}_{n+1}] \sin kx \\
 S_{n+1,n+2} &= - \frac{Etd}{2k_2} k^2 [dk\bar{v}_{n+1} + 2k_3\bar{u}_{n+1}] \cos kx
 \end{aligned} \tag{B.2}$$

where

$$k = \frac{m}{a}$$

$$k_1 = 1 + \frac{Et^2 k^2}{10G}$$

$$k_2 = 1 + \frac{2Et^2 k^2}{5G}$$

$$k_3 = 1 + \frac{Ed^2 k^2}{10G}$$

$$G = \frac{E}{2(1+\mu)}$$

The equilibrium equations for joint j are (in global coordinates):

$$\bar{M}_{j0} + \bar{M}_{jk} = 0$$

$$\bar{N}_{n_{j0}} + \bar{N}_{n_{jk}} = 0$$

$$\bar{N}_{\xi_{j0}} + \bar{N}_{\xi_{jk}} = 0$$

$$\bar{S}_{j0} + \bar{S}_{jk} = 0$$

(B.3)

Equilibrium equations for edge $n+1$:

$$\bar{M}_{n+1,n+2} + \bar{M}_{n+1,n} = 0$$

$$\bar{N}_{n_{n+1,n+2}} + \bar{N}_{n_{n+1,n}} = 0$$

$$\bar{N}_{\xi_{n+1,n+2}} + \bar{N}_{\xi_{n+1,n}} = 0$$

$$\bar{S}_{n+1,n+2} + \bar{S}_{n+1,n} = 0$$

(B.4)

These equations modify the first four and last four equations of the shell stiffness matrix by superimposing to them the matrix equations B.7b and B.8b.

Beam A

The coefficients for edge beam (A) stiffness can be determined

as:

$$k_{11} = \frac{Et^3d}{48k_1} k^2 \left[16 \frac{G}{E} \left(1 - 0.630 \frac{t}{d} \right) k_1 + k^2 d^2 \right]$$

$$k_{12} = 2 \cdot \frac{Et^3d^2}{48k_1} k^4$$

$$k_{21} = - \frac{Et^3d^2}{24k_1} k^4$$

$$k_{22} = -2 \frac{Et^3d}{24k_1} \cdot k^4$$

(B.5)

$$k_{33} = -2k^4 \cdot \frac{Etd^3}{6k_2}$$

$$k_{34} = 3k^3 \cdot \frac{Etd^2}{6k_2}$$

$$k_{43} = k^3 \cdot \frac{Etd^2}{2k_2}$$

$$k_{44} = -2k^3 \cdot \frac{Etd}{2k_2} k^2$$

Beam B

In the same manner we can write the coefficients for edge beam (B) stiffness as:

$$k_{N-3,N-3} = \frac{Et^3d}{48k_1} k^2 \left[16 \frac{G}{E} \left(1 - .630 \frac{t}{d} \right) k_1 + k^2 d^2 \right]$$

$$k_{N-3,N-2} = -2 \cdot \frac{Et^3d^2}{48k_1} k^4$$

$$k_{N-2,N-3} = k^4 \cdot \frac{Et^3d^2}{24k_1}$$

$$k_{N-2,N-2} = -2 \cdot \frac{Et^3d}{24k_1} k^4$$

(B.6)

$$k_{N-1,N-1} = -2 \cdot \frac{Etd^3}{6k_2} k^4$$

$$k_{N-1,N} = -3 \cdot \frac{Etd^2}{6k_2} k^3$$

$$k_{N,N-1} = -\frac{Etd^2}{2k_2} k^3$$

$$k_{N,N} = -2k_3 \cdot \frac{Etd}{2k_2} k^2$$

where k , k_1 , k_2 and k_3 are the same as defined in (B.2) and $N = 4 (n+1)$.

Beam A

$$\begin{Bmatrix} \bar{M}_{j0} \\ \bar{V}_{j0} \\ \bar{N}_{j0} \\ \bar{S}_{j0} \end{Bmatrix} = \begin{bmatrix} k_{11} & k_{12} & 0 & 0 \\ k_{21} & k_{22} & 0 & 0 \\ 0 & 0 & k_{3,3} & k_{3,4} \\ 0 & 0 & k_{4,3} & k_{4,4} \end{bmatrix} \begin{Bmatrix} \bar{\theta}_j \\ \bar{w}_{j0} \\ \bar{v}_{j0} \\ \bar{u}_j \end{Bmatrix} \quad (\text{B.7a})$$

In global coordinates:

$$\begin{Bmatrix} \bar{M}_{j0} \\ \bar{N}_{\eta j0} \\ \bar{N}_{\xi j0} \\ \bar{S}_{j0} \end{Bmatrix} = \begin{bmatrix} k_{11} & k_{12} & 0 & 0 \\ k_{21} & k_{22} & 0 & 0 \\ 0 & 0 & k_{3,3} & k_{3,4} \\ 0 & 0 & k_{4,3} & k_{4,4} \end{bmatrix} \begin{Bmatrix} \bar{\theta}_j \\ \bar{\eta}_{j0} \\ -\bar{\xi}_{j0} \\ \bar{u}_j \end{Bmatrix} \quad (\text{B.7b})$$

Beam B

$$\begin{Bmatrix} \bar{M}_{n+1,n+2} \\ \bar{V}_{n+1,n+2} \\ \bar{N}_{n+1,n+2} \\ \bar{S}_{n+1,n+2} \end{Bmatrix} = \begin{bmatrix} k_{N-3,N-3} & k_{N-3,N-2} & 0 & 0 \\ k_{N-2,N-3} & k_{N-2,N-2} & 0 & 0 \\ 0 & 0 & k_{N-1,N-1} & k_{N-1,N} \\ 0 & 0 & k_{N,N-1} & k_{N,N} \end{bmatrix} \begin{Bmatrix} \bar{\theta}_{n+1} \\ \bar{w}_{n+1,n+2} \\ \bar{v}_{n+1,n+2} \\ \bar{u}_{n+1} \end{Bmatrix} \quad (\text{B.8a})$$

In global coordinates:

$$\left\{ \begin{array}{l} \bar{M}_{n+1,n+2} \\ -\bar{N}_{n+1,n+2} \\ \bar{N}_{\xi_{n+1,n+2}} \\ \bar{S}_{n+1,n+2} \end{array} \right\} = \left\{ \begin{array}{cccc} k_{N-3,N-3} & k_{N-3,N-2} & 0 & 0 \\ k_{N-2,N-3} & k_{N-2,N-2} & 0 & 0 \\ 0 & 0 & k_{N-1,N-1} & k_{N-1,N} \\ 0 & 0 & k_{N,N-1} & k_{N,N} \end{array} \right\} \left\{ \begin{array}{l} \bar{\theta}_{n+1} \\ -\bar{\eta}_{n+1,n+2} \\ \bar{\xi}_{n+1,n+2} \\ \bar{u}_{n+1} \end{array} \right\} \quad (\text{B.8b})$$

The development of the internal tractions for each edge beam subjected to connection tractions from the appropriate plate is presented in the next pages. This is followed by a description of a computer program with data and results for the model structure. Final results are displayed in graphs.

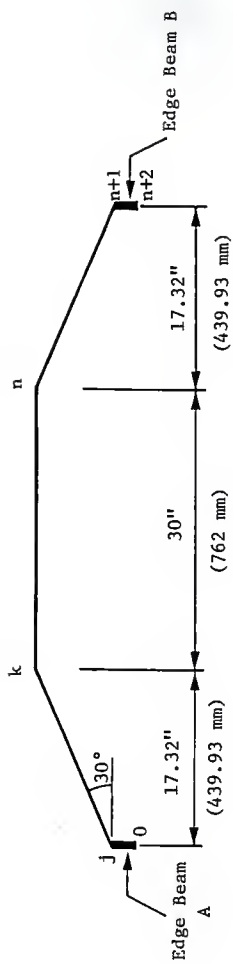


Fig. B.1 Cross-section of the Model with Edge Beams

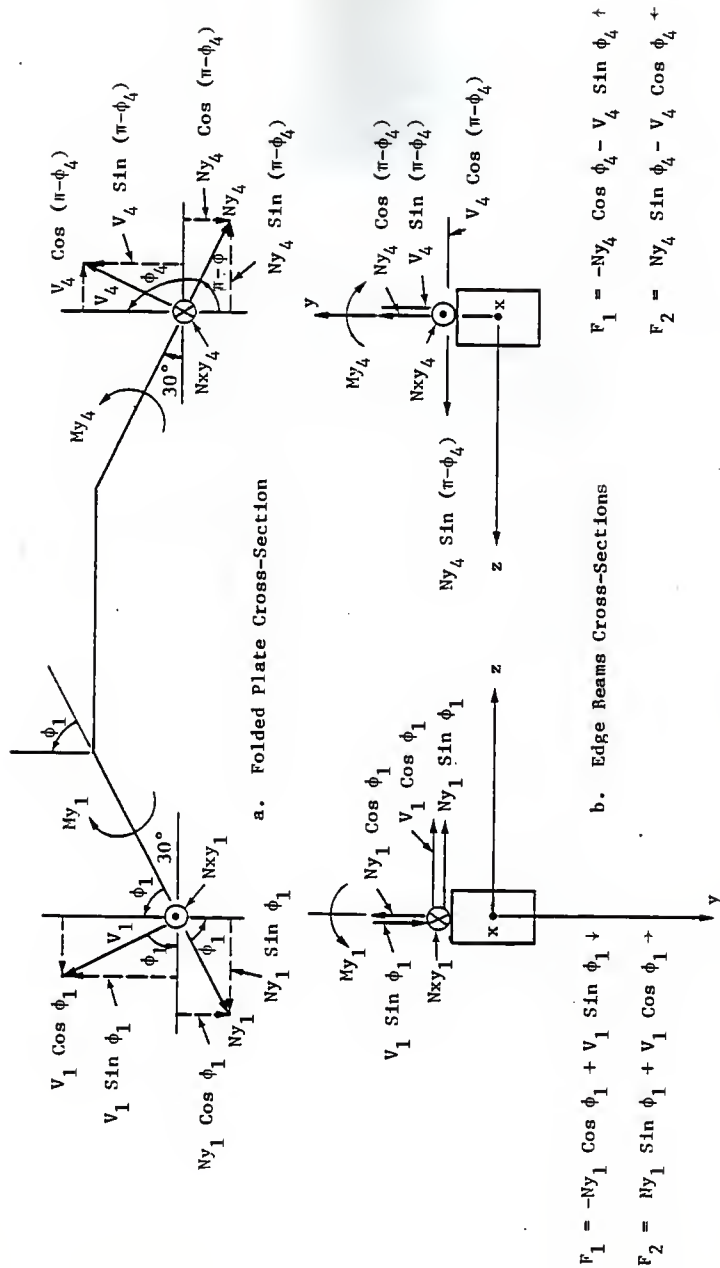
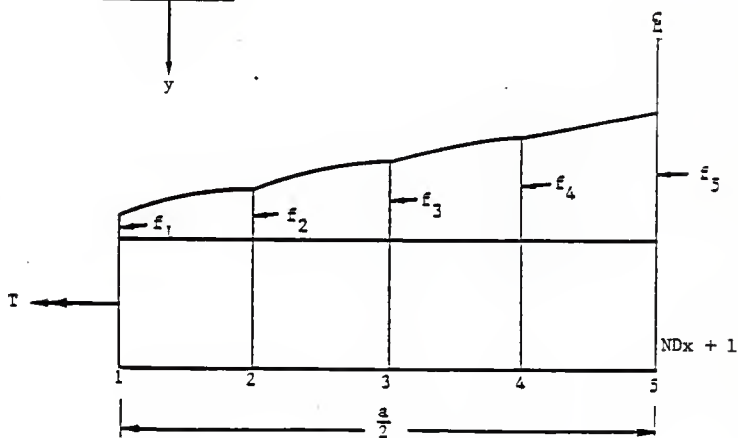
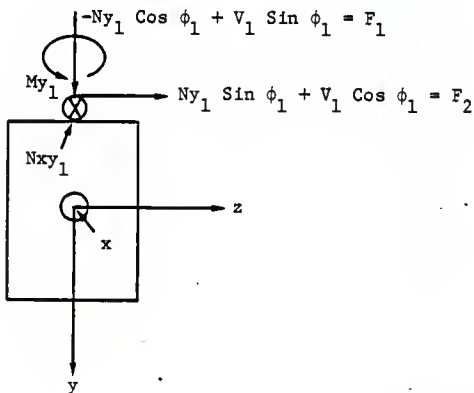
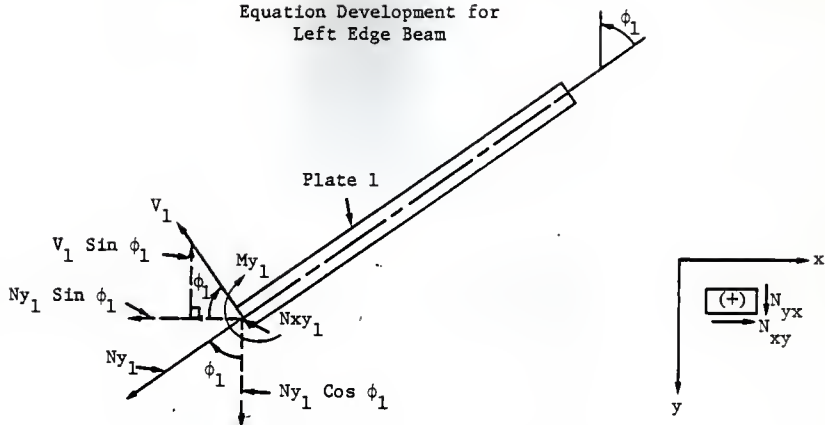
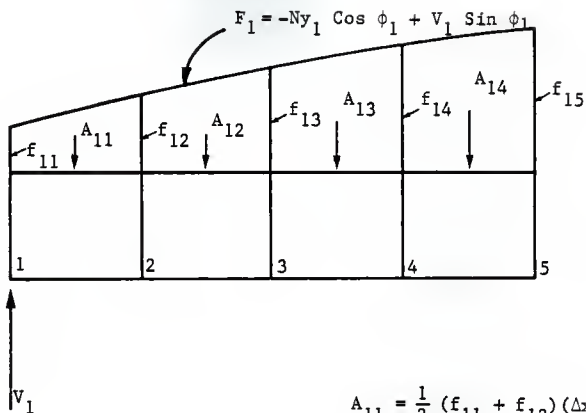


Fig. B.2 Resolution of Forces on Folded Plate and on Edge Beams

Equation Development for
Left Edge Beam



1) Assume $F_1 = -Ny_1 \cos \phi_1 + V_1 \sin \phi_1$



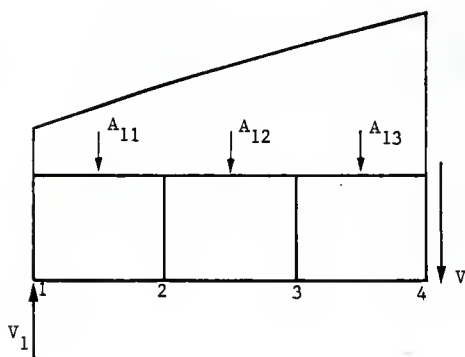
$$V_1 = R = \sum_{j=1}^{NDx} A_{1j};$$

$$A_{11} = \frac{1}{2} (f_{11} + f_{12}) (\Delta x)$$

$$A_{12} = \frac{1}{2} (f_{12} + f_{13}) (\Delta x)$$

$$A_{13} = \frac{1}{2} (f_{13} + f_{14}) (\Delta x)$$

$$A_{14} = \frac{1}{2} (f_{14} + f_{15}) (\Delta x)$$



$$A_{1j} = \frac{1}{2} (f_{1j} + f_{1j+1}) (\Delta x)$$

$$\text{where } \Delta x = \frac{a}{8}$$

$$V_2 = V_1 - A_{11}$$

$$V_3 = V_2 - A_{12}$$

$$V_4 = V_3 - A_{13}$$

$$\therefore V_j = V_{j-1} - A_{j-1}$$

where,

$$V_1 = R$$

$$R = \sum_{j=1}^{NDx} A_{1j}$$

$$A_{V1} = \frac{1}{2} \Delta x (V_1 + V_2)$$

$$A_{V2} = \frac{1}{2} \Delta x (V_2 + V_3)$$

$$A_{V3} = \frac{1}{2} \Delta x (V_3 + V_4)$$

$$\therefore A_{Vj} = \frac{1}{2} \Delta x (V_j + V_{j+1})$$

$$M_2 = M_1 + A_{V1}$$

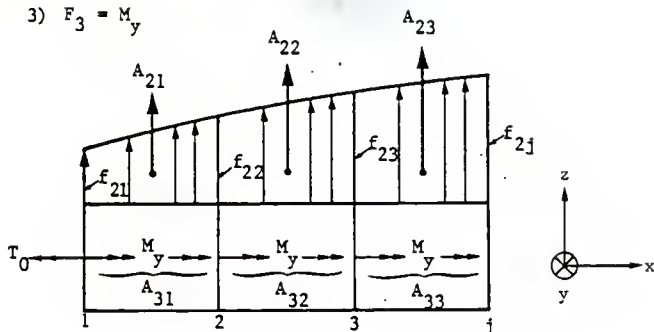
$$M_3 = M_2 + A_{V2}$$

$$M_4 = M_3 + A_{V3}$$

$$\therefore M_j = M_{j-1} + A_{Vj-1}$$

$$2) \text{ Assume } F_2 = N \sin \phi_1 + V_1 \cos \phi_1$$

$$3) F_3 = M_y$$



$$R = \sum_{j=1}^{NDx} A_{2j} = N_1$$

$$A_{2j} = \frac{(f_{2j} + f_{2j+1}) \Delta x}{2}$$

$$A_{3j} = \frac{(f_{3j} + f_{3j+1}) \Delta x}{2}$$

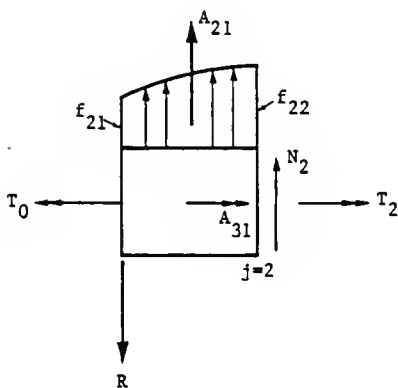
$$N_2 = N_1 - A_{21}$$

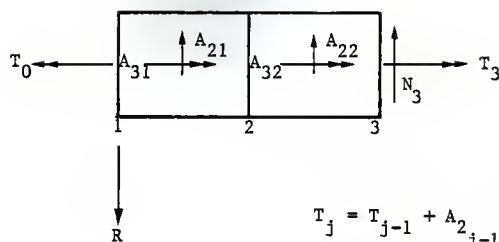
$$N_3 = N_2 - A_{22}$$

$$\therefore N_j = N_{j-1} - A_{2j-1}$$

$$T_0 = - \sum_{j=1}^{NDx} A_{2j} * \frac{d}{2} + \sum_{j=1}^{NDx} A_{3j}$$

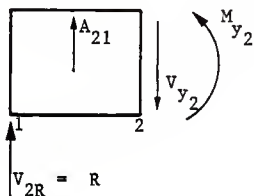
$$T_2 = T_1 + A_{21} * \frac{d}{2} - A_{31}$$





$$T_j = T_{j-1} + A_{2j-1} * \frac{d}{2} - A_{3j-1}$$

Bending about y-axis:



$$R = V_{2R} = - \sum_{j=1}^{N \Delta x} A_{2j}$$

$$V_{y1} = V_{2R}$$

$$V_{y2} = V_{y1} + A_{21}$$

$$V_{y3} = V_{y2} + A_{22}$$

$$V_{yj} = V_{y_{j-1}} + A_{2j-1}$$

$$A_{vy1} = \frac{1}{2} (V_{y1} + V_{y2}) \Delta x$$

⋮

$$A_{vyj} = \frac{1}{2} (V_{yj} + V_{y_{j+1}}) \Delta x$$

$$V_{yj} = -N_j$$

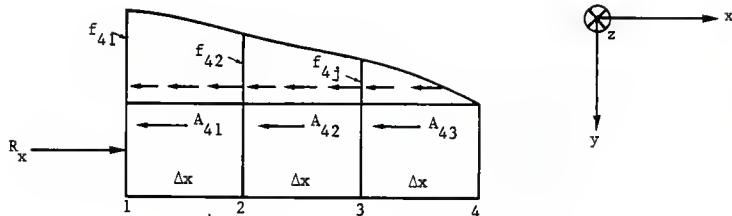
$$M_{y1} = 0$$

$$M_{y2} = M_{y1} + A_{vy1}$$

⋮

$$M_{yj} = M_{y_{j-1}} + A_{vy_{j-1}}$$

$$4) F_4 = N_{xy}$$



$$R_x = 0 \text{ (End diaphragm conditions)}$$

$$A_{4j} = \frac{1}{2} \Delta x (f_{4j} + f_{4j+1})$$

$$M_{Rz} = 0 \text{ (End diaphragm conditions)}$$

$$M_{z1} = M_{Rz}$$

$$M_{z2} = M_{z1} - A_{41} * \frac{d}{2}$$

$$\therefore M_{zj} = M_{zj-1} - \frac{d}{2} * A_{4j-1}$$

$$N_{x2} = -R_x + A_{41}$$

$$N_{x3} = N_{x2} + A_{42}$$

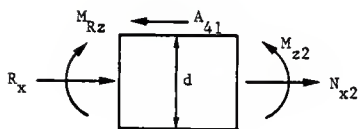
$$\therefore N_{xj} = N_{xj-1} + A_{4j-1}$$

(Due to Case 1)

$$M_{z(\text{total})} = M_j = M_{j-1} + A_{4j-1}$$

$$+ M_{zj-1} - \frac{d}{2} A_{4j-1}$$

(Due to Case 4)



Summary of Equations

Left Edge Beam

$$V_j = V_{j-1} - A_{j-1}$$

$$M_2(\text{total}) = M_{j-1} + A_{vj-1} + M_{zj-1} - \frac{d}{2} * A_{4j-1}$$

$$T_j = T_{j-1} + A_{2j-1} * \frac{d}{2} - A_{3j-1}$$

$$M_{yj} = M_{yj-1} + A_{vyj-1}$$

$$N_{xj} = N_{xj-1} + A_{4j-1}$$

Right Edge Beam

$$V_j = V_{j-1} + A_{j-1}$$

$$M_2(\text{total}) = M_{j-1} + A_{vj-1} + M_{zj-1} + \frac{d}{2} * A_{4j-1}$$

$$T_j = T_{j-1} - A_{2j-1} * \frac{d}{2} + A_{3j}$$

$$M_{yj} = M_{yj-1} + A_{vj-1}$$

$$N_{xj} = N_{xj-1} - A_{4j-1}$$

Computer Program

The program was written to analyze end supported folded plate structures with a maximum number of ten plates. The computer program is based on the exact method of analysis which is presented briefly in Chapter III. Young's modulus and Poisson's ratio and density are assumed to be constant.

Input Data

Card No. 1

```
READ(IR,1)MAXI,IP,IL,NP,NDX,NDY,AL,YM,PR,GAM,IEB
1 FORMAT(6I5,4D10.3,I5)
```

where

- MAXI = maximum mode number in Fourier Series "1,3,5 and normally 7." The number ends in the 5th column of the card.
- IP = 1, if the intermediate output is needed, otherwise IP = 0. The number ends in the 10th column of the card.
- IL = 0, if uniform load in the horizontal projection is to be input and cards 2 and 3 are read, otherwise = 1, if plate loads should be calculated and card 4 is read. The number ends in the 15th column.
- NP = number of plates and ends in the 20th column.
- NDX = (number of output points - 1) in the X direction and ends in the 25th column.
- NDY = (number of output points - 1) in the Y direction and ends in the 30th column.
- AL = length of structure in inches and ends in the 40th column.
- YM = Young's Modulus which is in psi and ends in the 50th column.
- PR = Poisson's ratio and ends in the 60th column.
- GAM = Specific weight of plate materials which is in lb./cu. in. and ends in the 70th column.
- IEB = 1, if there are edge beams, otherwise IEB = 0. The number ends in the 5th column.

If IL = 0, read card two and three.

Card No. 2

```
READ(IR,5)QL
5  FORMAT(5D10.3)
```

where

QL = load on horizontal projection and ends in the 10th column and the units are in psi.

Card No. 3

```
READ(IR,5)B(I),H(I),PH(I)
5  FORMAT(5D10.3)
```

where

B(I) = width of the i^{th} plate in inches, and it ends in the 10th column.

H(I) = thickness of the i^{th} plate in inches, and it ends in the 20th column.

PH(I) = angle in degrees between the i^{th} plate and the vertical. It is measured clockwise and ends in the 30th column.

This completes the data input if IL = 0.

For every plate one card is needed.

Card No. 4

If IL = 1, then this card is read.

```
READ(IR,5)B(I),H(I),PH(I),PN(I),PT(I)
5  FORMAT(5D10.3)
```

where B(I),H(I),PH(I) are as in card 3.

PN(I) = normal load on the i^{th} plate. It ends in the 40th column, and the units are in psi.

PT(I) = tangential load on the i^{th} plate. It ends in the 50th column, and the units are in psi.

This card is read for each plate.

This completes the data input, if there is no edge beam.

If IEB = 1, then this card is read.

```
      READ(IR,200)DB,TB,GB
2000  FORMAT(3D10.3)
```

where

DB = beam depth in inches, and it ends in the 10th column.

TB = beam thickness in inches, and it ends in the 20th column.

GB = modulus of rigidity in psi and it ends in the 30th column.

Output

The forces and deflections for the structure are printed out which are N_x , N_y , N_{xy} , M_x , M_y , v , w and θ in the intervals specified by the input NDX and NDY for every plate. The eight edge displacements in each mode for each plate and the coefficients for edge beam stiffness are printed out.

The units for N_x , N_y , N_{xy} are in lb. per inch, and the units for M_x and M_y are in lb.-in. per inch, while w and v are in inches, and θ in degrees.

Enclosed is a printout of the results for the model using the edge beam modifications.

Left Edge Beam

```

1      $JOB
2      DOUBLE PRECISION F1(51),A,V(51),M(51),T(51),F2(51),D,PH
3      1,F3(51),F4(51),NY(51),NX(51),A1(50),A2(50),A3(50),A4(50)
4      2,AV(50),N1(51),V1(51)
5      DD 50 J=1,51
6      T11=F1(1)=F2(1)=F3(1)=F4(1)=D.
7      50 CONTINUE
8      READ(5,5)A,D,PH,NDX
9      PH=PH*3.14159265359/180.
10     5 FURMAT(30D.3,15)
11     WRITE(6,10)A,D,PH,NDX
12     10 FORMAT(' ',30D.3,15)
13     NDX=NDX+1
14     READ(5,61(NY(1),V1(1),F3(1),F4(1),I=1,NDX1)
15     DD 1D J=1,NDX1
16     11D WRITE(6,11)NY(J),V1(J),F3(J),F4(J)
17     11 FURMAT(' ',40I0.3)
18     6 FURMAT(4(3X,D12.5))
19     CALL EBEAF1A,D,PH,NDX,NY,V1,F3,F4,F1,F2,A1,A2,A3,A4,AV,T)
20     STOP
21     END
22
23     SUDROUTINE EBEAF1A,D,PH,NDX,NY,V1,F3,F4,F1,F2,A1,A2,A3,A4,AV,T)
24     DOUBLE PRECISION NY(51),F3(51),A,D,PH,F4(51),MY(51),F1(51),
25     2F2(51),A1(50),A2(50),A3(50),A4(50),T(51),H(51),V2(51),
26     3AV(50),N1(51),V1(51),AV2(50),V11(51),MZ(51),NX(51),MZT(51),RX(51)
27     NDX1=NDX+1
28     XNDX=NDX
29     DELTAX=A/(2*NDX)
30     DD 100 J=1,NDX1
31     F1(J)={-NY(J)*DCOS(PH)+V1(J)*DSIN(PH)}
32     100 WRITE(6,7) J,F1(J)
33     7 FURMAT1'DF1('I2.0)'=*,012.5)
34     DD 15D J=1,NDX1
35     15D A1(J)=.5*(F1(J)+F1(J+1))*DELTAX
36     C CALCULATION OF VERTICAL FORCE @ JOINT 1
37     V(1)=D.
38     V(8)=D.
39     DD 20D J=1,NDX
40     V(1)=V(1)+A1(J)
41     20D CONTINUE
42     C CALCULATION OF VERTICAL SHEAR FORCE @ OTHER JOINTS
43     NDX1=NDX+1
44     DD 30D J=2,NDX1
45     V(J)=V(J-1)-A1(J-1)
46     30D V(J)=V(J-1)-A1(J-1)
47     C 7D CALCULATE AREAS OF SHEAR
48     DD 40D J=1,NDX1
49     AV(J)=.5*DELTAX*(V(J)+V(J+1))
50     40D CONTINUE
51     C CALCULATE MOMENTS
52     DD 50D J=2,NDX1
53     H(1)=0.
54     H(J)=H(J-1)+AV(J-1)
55     50D CONTINUE
56     YY=D.D
57     DD 60D J=1,NDX1
58     F2(J)=NY(J)*DSIN(PH)+V1(J)*DCOS(PH)
59     60D WRITE(6,8)J,F2(J)
60     8 FURMAT('DF2('I2.0)'=*,012.5)
61     DD 65D J=1,NDX1

```



```

51 A2(J)=.5*(FZLJ)+FZL(J+1))*OELTAX
52 C 650 YY=YY+A2(J)*O/2.
53 C CALCULATION OF N FORCE @ JOINT I
54 N(I)=O.
55 DD 700 J=1,NOX
56 CONTINUE
57 C CALCULATION OF N FORCES @ OTHER JOINTS
58 DD 800 J=2,NOX1
59 C CALCULATION OF VERTICAL SHEAR FORCE @ JOINT I
60 VZ(I)=N(I)
61 C CALCULATION OF VERTICAL SHEAR FORCE @ OTHER JOINTS
62 DD 900 J=2,NOX1
63 VZ(J)=O.
64 C START CALCULATING VZ(J)
65 DD 1000 J=2,NOX1
66 VZ(J)=VZ(J-1)+VZ(J-1)
67 C TO CALCULATE AREAS OF VERTICAL SHEAR FORCE
68 DD 1100 J=1,NOX1
69 AVZ(J)=.5*OELTAX*(VZ(J)+VZ(J+1))
70 C CALCULATION OF MOMENTS
71 DD 1200 J=2,NOX1
72 MY(I)=O.
73 C CALCULATING AREAS OF THE MOMENTS TO GET TORSION AT(I+1).
74 XX=O
75 DD 1300 J=1,NOX1
76 A3(J)=.5*(F3(J)+F3(J+1))*OELTAX
77 C CALCULATION OF TORSION,T(I)
78 XX=XX+A3(J)
79 CONTINUE
80 C CALCULATION OF TORSION,T(I)
81 T(I)=XX-YY
82 STRAT CALCULATING TOTAL TORSION,T(I)
83 T(I)=T(I)+VZ(J-1)*VZ(J-1)*O/2-A3(J-1)
84 C CALCULATION OF NX FORCES
85 DD 1500 J=2,NOX1
86 CONTINUE
87 C START CALCULATING NX(J)
88 DD 1700 J=2,NOX1
89 NX(J)=NX(J-1)+A4(J-1)
90 C CALCULATING MOMENTS,MZ(J)
91 DD 1800 J=2,NOX1
92 MZ(I)=O
93 C CALCULATION OF TOTAL MOMENT,MZT, DUE TO CASE 1 AND CASE 4
94 DD 1900 J=1,NOX1
95 MZT=MZ(J)+MZT(J)
96 WRITE(*,*)
97 FORMAT(1)
98 UU 2000 K=1,NOX1

```

```

97  WRITE(6,12) K,V(K),K,MZ(K),K,PK(K),K,DX(K),K,N(K),K,NY(K)
98  12 FORMAT(3X,'V(',I2,',')=,D12.5,3X,'MZ(',I2,',')=,D12.5,3X,'N(',I2,',')=,
2',D12.5,3X,'DX(',I2,',')=,D12.5,3X,'N(',I2,',')=,D12.5,3X,'NY(',I2,',')=,
6)',',',D12.5)
99
100 13  WRITE(6,13)K,A1(K),K,A2(K),K,AV(K)
101 13  WRITE(6,13)K,A1(',I2,',')=,D12.5,2X,'A2(',I2,',')=,D12.5,3X,'AV(',I2,',')=,
3)',',',D12.5)
102 16  FORMAT(4X,'A1(',I2,',')=,D12.5,2X,'A2(',I2,',')=,D12.5,2X,'AV2(',I2,',')=,D12.5,2X,'AV(',I2,',')=,
8)',',',',',D12.5)
103 17  FORMAT(3X,'A3(',I2,',')=,D12.5)
104 17  FORMAT(3X,'A3(',I2,',')=,D12.5)
105 2000 CONTINUE
106 DO 3000 J=1,NOX1
107 14  WRITE(6,14),J,PZT(J),T(J)
108 14  FORMAT(2X,'MZT(',I2,',')=,D12.5,3X,'T(',I2,',')=,D12.5)
109 3000 CONTINUE
110 RETURN
111 ENO
$ENTRY
0-2160 03 0.3000 01 0.1050 01 6
-C-5000 00 0.0000 00 0.0000 00 0.2310 03
-0-2110 01 0.4360 01-0.7080 00 0.2030 03
-C-1400 01 0.2420 01 0.4010 01 0.1520 03
-0-1850 01 0.3220 01 0.5210 01 0.1150 03
-C-1840 01 0.3190 01 0.5090 01 0.3650 02
-0-1460 01 0.2480 01 0.6320 01-0.1330-10
F1( 1)= 0.000000 00
F1( 2)= 0.497450 01
F1( 3)= 0.432900 01
F1( 4)= 0.279330 01
F1( 5)= 0.371190 01
F1( 6)= 0.368120 01
F1( 7)= 0.287880 01
F2( 1)= 0.000000 00
F2( 2)= 0.101190 00
F2( 3)= 0.600210-01
F2( 4)=-0.235970-02
F2( 5)= 0.493080-02
F2( 6)=-0.229560-03
F2( 7)=-0.199890-01

```

```

VI 11= 0.37673D 03  NZI 11= 0.00000D 00  MI 11= 0.00000D 00  NX( 11)=0.00000D 00  NI 11= 0.27660D 01  MY( 11)= 0.00300D 00
A31 11= 0.44770D 02  AZ1 11= 0.97067D 00  AV1 11= D.63781D 04  AV2( 11)=0.41555D 02  VZ( 11)=0.27643D 01  A4( 11)= 0.39115D 04
VI 21= 0.31960 03  NZI 21=0.58672D 04  MI 21= 0.63781D 04  NX( 21)= 0.39115D 04  NI 21= 0.11853D 01  MY( 21)=0.61550 02
A11 21= 0.83731D 02  AZ1 21= 0.14509D 01  AV1 21= 0.522216D 04  AV2( 21)=0.20302D 02  VZ( 21)=0.18533D 01  A4( 21)= 0.32023D 04
A31 21= 0.29730D 02  MI 31= 0.11600D 05  MI 31= 0.71138D 04  NX( 31)= 0.40243 00  MY( 31)=0.61357D 02
VI 31= 0.24823D 03  NZI 31= 0.182196D 02  AZ1 31= 0.51895D 00  AV1 31= 0.38912D 04  AV2( 31)=0.25732D 01  VZ( 31)=0.42744D 00  A4( 31)= 0.24029D 04
A11 31= 0.82196D 02  MI 41= 0.15491D 05  MI 41= 0.23056D 01  VZ( 41)= 0.11692D 00  A4( 41)= 0.17387D 04
A31 41= 0.12558 03  NZI 41= 0.16275D 05  AZ1 41= 0.23139D 01  AV1 41= 0.15491D 05  NX( 41)= D.95167D 04  NI 41= 0.11652D 00  MY( 41)=0.54430D 07
A11 41= 0.58567D 02  AZ1 41= 0.16083D 05  AV1 41= 0.27873D 04  AV1 51= 0.18278D 05  NI 51= 0.11255D 05  NI 51= 0.13966D 30  MY( 51)= 0.62125D 02
A31 51= 0.66538D 02  AZ1 51= 0.42311D 01  AV1 51= 0.16616D 04  AV1 61= 0.19940D 05  NX( 61)= 0.28946D 01  VZ( 51)= C.133% D 00  A4( 51)= 0.10361D 04
VI 61= 0.59040D 02  NZI 61= 0.12558 03  AZ1 61= 0.18197D 00  AV1 61= 0.53136D 03  NX( 61)= 0.12291D 05  NI 61= 0.18197D 00  A4( 61)= 0.32849D 03
A11 61= 0.10260D 03  NZI 61= 0.18197D 00  AZ1 61= 0.18197D 00  AV1 71= 0.20471D 05  NX( 71)= 0.12620D 05  NI 71= 0.0E000D 30  MY( 71)=0.57592D 02
A31 71= 0.25809D 02  NZI 71= 0.18197D 00  AZ1 71= 0.18197D 00  AV1 71= 0.57554D 12  AV2( 71)= D.00000D 00  VZ( 71)= C.00003D 00  A4( 71)=0.12008D 09
MI 71= 0.16930D 05  NI 71= 0.16930D 05  NI 71= 0.16930D 05  NI 71= 0.16930D 05  NI 71= 0.16930D 05  NI 71= 0.16930D 05
MI 71= 0.48065D 03  NI 71= 0.48065D 03  NI 71= 0.48065D 03  NI 71= 0.48065D 03  NI 71= 0.48065D 03  NI 71= 0.48065D 03
MI 71= 0.51091D 03  NI 71= 0.51091D 03  NI 71= 0.51091D 03  NI 71= 0.51091D 03  NI 71= 0.51091D 03  NI 71= 0.51091D 03
MI 71= 0.46083D 03  NI 71= 0.46083D 03  NI 71= 0.46083D 03  NI 71= 0.46083D 03  NI 71= 0.46083D 03  NI 71= 0.46083D 03
MI 71= 0.12159D 04  NI 71= 0.12159D 04  NI 71= 0.12159D 04  NI 71= 0.12159D 04  NI 71= 0.12159D 04  NI 71= 0.12159D 04
MI 71= 0.13952D 04  NI 71= 0.13952D 04  NI 71= 0.13952D 04  NI 71= 0.13952D 04  NI 71= 0.13952D 04  NI 71= 0.13952D 04
MI 71= 0.15027D 04  NI 71= 0.15027D 04  NI 71= 0.15027D 04  NI 71= 0.15027D 04  NI 71= 0.15027D 04  NI 71= 0.15027D 04
MI 71= 0.15413D 04  NI 71= 0.15413D 04  NI 71= 0.15413D 04  NI 71= 0.15413D 04  NI 71= 0.15413D 04  NI 71= 0.15413D 04

```

STATEMENTS EXECUTED= 438

```

CCRE USAGE      OBJECT CODE=      712D BYTES,ARRAY AREA=      10560 BYTES,TOTAL AREA AVAILABLE=      153696 BYTES
DIAGNOSTICS     NUMBER OF ERRORS=      0, NUMBER OF WARNINGS=      0, NUMBER OF EXTENSICMS=      4
COMPILE TIME=   D.18 SEC.,EXECUTION TIME=      0.08 SEC,      13.12.14      MONDAY      29 APR 85      MATFJV - MAR 1980 V210

```

Right Edge Beam

```

SJOB
1  DOUBLE PRECISION F1(51),A,D,RH,N1(51),T1(51),F2(51),D,RH
  1,F3(51),F4(51),NY(51),NX(51),A1(50),A2(50),A3(50),A4(50)
  2,AV(50),N1(51),V1(51)
2  DO 50 I=1,51
3  T(I)=F1(I)=F2(I)=F3(I)=F4(I)=D.
4  50 CONTINUE
5  REAC(5,5)A,D,RH,NDX
6  PH=PI*.14159265359/180.
7  5  FORMAT(3D10.3,15)
  8  WRITE(6,1)J4,D,RH,NDX
9  10 FORMAT(' ',30D10.3,15)
10  NDX1=NDX+1
11  READ(5,6)(NY(I),V1(I),F3(I),F4(I),)=1,NDX1)
12  DO 110 J=1,NDX1
13  110 WRITE(6,1)(NY(I),V1(I),F3(I),F4(I))
14  11  FORMAT(' ',4D10.3)
15  6  FORMAT(14I3X,D12.5)
16  CALL EBEAF(A,D,RH,NDX,NY,V1,F3,F4,F1,F2,A1,A2,A3,A4,AV,7)
17  STOR
18  END

19  SUBROUTINE EBEAF(A,D,PH,NDX,NY,V1,F3,F4,F1,F2,A1,A2,A3,A4,AV,T)
20  DOUBLE PRECISION NY(51),F3(51),A,D,RH,F4(51),NY(51),F1(51),
  2F2(51),A1(50),A2(50),A3(50),A4(50),T1(51),H1(51),V2(51),
  3AV(50),N1(51),V1(51),AV2(50),V1(51),H2(51),NX(51),H2(51),RX(51)
21  NDX1=NDX+1
22  XNDX=NDX
23  DELTAX=A/(2*NDX)
24  DO 100 J=1,NDX1
25  F1(J)=1-NY(J)*DCOS(PH)-V1(J)*OSIN(PH)
26  100 WRITE(6,7) J,F1(J)
27  7  FORMAT('DF1(',I2,')=',D12.5)
28  DO 150 J=1,NDX1
29  150 A1(J)=.5*(F1(J)+F1(J+1))*DELTAX
  C  CALCULATION OF VERTICAL FORCE @ JOINT 1
30  V1)=D.
31  V1B)=D.
32  DO 200 J=1,NDX
33  V1)=V1)-A1(J)
34  200 CONTINUE
  C  CALCULATION OF VERTICAL SHEAR FORCE @ OTHER JOINTS
35  NDX)=NDX+1
36  DO 300 J=2,NDX1
37  300 V1(J)=V1(J-1)+A1(J-1)
  C  TO CALCULATE AREAS OF SHEAR
38  DO 400 J=1,NDX1
39  AV(J)=.5*DELTAX*(V1(J)+V1(J+1))
40  400 CONTINUE
  C  CALCULATE MOMENTS
41  DO 500 J=2,NDX1
42  H1)=D.
43  H1(J)=H1(J-1)+AV(J-1)
44  500 CONTINUE
45  YY=D.0
46  DO 600 J=1,NDX1
47  F2(J)=NY(J)*OSIN(PH)-V1(J)*DCOS(PH)
48  600 WRITE(6,8)J,F2(J)
49  8  FORMAT('DF2(',I2,')=',D12.5)
50  600 11,NDX1

```

51 AZ1J1=-5*(FZ1J1+F21J1+U1)*DELTA
 52 650 YY=YY+AZ1J1*O/2.
 53 CALCULATION OF N FORCE @ JOINT 1
 54 H111=0.
 55 00 700 J=1,NOX
 56 CONTINUE (-AZ1J)
 57 700 CONTINUE
 58 CALCULATION OF N FORCES @ OTHER JOINTS
 59 00 800 J=2,NOX1
 60 NL1J=NL1J-11+AZ1J-11
 61 CALCULATION OF VERTICAL SHEAR FORCE @ JOINT 1
 62 VZ111=-N111
 63 00 900 J=2,NOX1
 64 VZ11J=0.
 65 STABLOC
 66 CALCULATING VZ1J
 67 00 1000 J=2,NOX1
 68 VZ11J=VZ11J-11
 69 TO CALCULATE AREA OF VERTICAL SHEAR FORCE
 70 00 1100 J=1,NOX1
 71 AV21J1=-5*DELTA*(V21J1+VZ1J1+1)
 72 CALCULATION OF MOMENTS
 73 00 1200 J=2,NOX1
 74 MY111=0.
 75 MY11J=MY11J-11+AV21J1-11
 76 CALCULATING AREAS OF THE MOMENTS TO GET TORSION *T111.
 77 00 1300 J=1,NOX1
 78 A111J=-5*(F31J1+F31J1+1)*DELTA
 79 XX*XX*A31J
 80 CONTINUE
 81 CALCULATION OF TORSION *T101=T111
 82 T111=YY-XX
 83 STRAT CALCULATING TCTAL TORSION *T11J
 84 00 1350 J=2,NOX1
 85 RX111=0.
 86 00 1400 J=1,NOX1
 87 RX111=-RX111
 88 00 1550 J=2,NOX1
 89 A41J1=-5*(F41J1+F41J1+1)*DELTA
 90 RX111=R X111+A41J1
 91 CONTINUE
 92 CALCULATION OF NX FORCES
 93 00 1600 J=2,NOX1
 94 NX1J1=0.
 95 1600 CONTINUE
 96 START CALCULATING NX1J
 97 00 1700 J=2,NOX1
 98 NX11J=NX11J-11+A41J1-11
 99 CALCULATING MOMENTS *MZ1J
 100 00 1800 J=2,NOX1
 101 MZ11J=-MZ11J-11+O/2*4*(L1-11
 102 CALCULATION OF TOTAL MOMENT *MT10UE TO CASE 1 AND CASE 4
 103 00 1900 J=1,NOX1
 104 MZ11J=-MZ11J+MZ1J
 105 WRITE(6,43)
 106 43 FORMAT(1'
 107 00 2000 K=1,NOX1

```

97  MR1E16,12) K,V1K(K,MZIK,K,PIK,K,AKIK),K,K(K),K,K,MV(K)
98  12  FORMAT(3X,'VI',I2,') (=,012.5,3X,'MZI',I2,') (=,012.5,3X,'MI',I2,') =
    6) (=,012.5,3X,'MX',I2,') (=,012.5,3X,'NI',I2,') (=,012.5,3X,'PI',I2,')
99  MR1E16,13)K,A1(K),K,A2(K),K,AV1K(
    3) (=,012.5)
100  13  FORMAT(3X,'A1',I2,') (=,012.5,2X,'A2',I2,') (=,012.5,3X,'AV1',I2,')
101  MR1E16,16)K,AV2(K),K,VZ(K),K,A4(K)
102  16  FORMAT(4,'',68X,'AV2',I2,') (=,012.5,2X,'VZ',I2,') (=,012.5,2X,'A4',
    8,') (=,012.5)
103  MR1E16,17)K,A3(K)
104  17  CONTINUE
105  2000 CONTINUE,'A3',I2,') (=,012.5)
106  DO 3000 (=,NOX)
107  MR1E16,14) K, MZ1(I),I,T(I)
108  14  FORMAT(3X,'MZ1',I2,') (=,012.5,3X,'T',I2,') (=,012.5)
109  3000 CONTINUE
110  RETURN
111  END
$ENTRY
0.2160 03 0.3000 01 0.2090 01 4
0.0000 00 0.0000 00 0.0000 00=0.2310 03
-C.2400 01 0.4360 01=0.7080 00=0.2030 03
-C.2110 01 0.3780 01 0.4010 01=0.1920 03
-C.1400 01 0.2420 01 0.7000 01=0.4150 03
-C.1850 01 0.3220 01 0.5210 01=0.7860 02
-C.1840 01 0.3190 01 0.5090 01=0.3650 02
-0.1460 01 0.2480 01 0.6320 01 0.1330=10
F1( 1) = 0.000000 00
F1( 2) = 0.497450 01
F1( 3) = 0.432900 01
F1( 4) = 0.279330 01
F1( 5) = 0.371190 01
F1( 6) = 0.368120 01
F1( 7) = 0.287880 01
F2( 1) = 0.000000 00
F2( 2) = 0.101150 00
F2( 3) = 0.600210=01
F2( 4) = 0.235970=02
F2( 5) = 0.493080=02
F2( 6) = 0.229560=03
F2( 7) = 0.199890=01

```

VI 11=	0.376733	03	MZI 11=	0.000000	00	KI 11=	0.000000	00	NK 11=	0.000000	00	MY 11=	0.000000	00			
AV 11=	0.447700	02	AZI 11=	0.910610	00	AV 11=	0.637810	04	AVZ1 11=	0.415550	02	VZ 11=	0.216430	01	AA 11=	0.391150	04
VI 21=	0.331960	03	MZI 21=	0.586720	04	MZ 21=	0.637810	04	NK 21=	0.391150	04	MY 21=	0.415550	02			
AV 21=	0.837310	02	AZI 21=	0.145090	01	AV 21=	0.522160	04	AVZ1 21=	0.203020	02	VZ 21=	0.185330	01	AA 21=	0.320230	04
VI 31=	0.297300	02	MZI 31=	0.106710	05	MZ 31=	0.116000	05	NK 31=	0.711380	04	MY 31=	0.402440	00	MY 31=	0.618570	02
AV 31=	0.484300	03	AZI 31=	0.518950	00	AV 31=	0.389120	04	AVZ1 31=	0.257320	01	VZ 31=	0.402440	00	AA 31=	0.240290	04
VI 41=	0.184130	03	MZI 41=	0.142750	05	MZ 41=	0.154910	05	NK 41=	0.951670	04	MY 41=	0.116520	00	MY 41=	0.644300	02
AV 41=	0.595470	02	AZI 41=	0.231370-01		AV 41=	0.278730	04	AVZ1 41=	0.230560	01	VZ 41=	0.116520	00	AA 41=	0.173870	04
VI 51=	0.125580	03	MZI 51=	0.168830	05	MZ 51=	0.182780	05	NK 51=	0.112550	05	MY 51=	0.139660	00	MY 51=	0.621250	02
AV 51=	0.665380	02	AZI 51=	0.423110-01		AV 51=	0.186160	04	AVZ1 51=	0.289460	01	VZ 51=	0.139660	00	AA 51=	0.103610	04
VI 61=	0.926930	02	MZI 61=	0.186370	05	MZ 61=	0.199400	05	NK 61=	0.122910	05	MY 61=	0.181970	00	MY 61=	0.592300	02
AV 61=	0.590400	02	AZI 61=	0.181970	00	AV 61=	0.513360	03	AVZ1 61=	0.163770	01	VZ 61=	0.181970	00	AA 61=	0.328490	03
VI 71=	0.102600	03	MZI 71=	0.189300	05	MZ 71=	0.204710	05	NK 71=	0.126200	05	MY 71=	0.000000	00	MY 71=	0.575920	02
AV 71=	0.216000	13	AZI 71=	0.179900	02	AV 71=	0.703440-12		AVZ1 71=	0.000000	00	VZ 71=	0.000000	00	AA 71=	0.120080-09	
VI 81=	0.568350	02	MZI 81=	0.000000	00	T 11=	0.440650	03	T 11=	0.440650	03	T 21=	0.440650	03			
AV 81=	0.000000	00	MZI 21=	0.510910	03	T 21=	0.440650	03	T 31=	0.440650	03	T 31=	0.440650	03			
VI 91=	0.121590	04	MZI 41=	0.121590	04	T 41=	0.362500	03	T 41=	0.362500	03	T 41=	0.362500	03			
AV 91=	0.139520	04	MZI 51=	0.139520	04	T 51=	0.252610	03	T 51=	0.252610	03	T 51=	0.252610	03			
VI 01=	0.150270	04	MZI 61=	0.150270	04	T 61=	0.159980	03	T 61=	0.159980	03	T 61=	0.159980	03			
AV 01=	0.154130	04	MZI 11=	0.154130	04	T 71=	0.511040	02	T 71=	0.511040	02	T 71=	0.511040	02			

STATEMENTS EXECUTED= 438

CCRE USAGE OBJECT CODE= 71:0 BYTES, ARRAY AREA= 10560 BYTES, TOTAL AREA AVAILABLE= 153696 BYTES

DIAGNOSTICS NUMBER OF ERKURS= 0, NUMBER OF WARNINGS= 0, NUMBER OF EXTENSICNS= 4

COMPILE TIME= 0.17 SEC., EXECUTION TIME= 0.07 SEC., 13.47.15 MONDAY 29 APR 85 WATFIV - MAR 1980 V210

DATA SET NUMBER 1

THE LENGTH OF THE STRUCTURE IS 0.2160+031NCHESES, YOUNGS MODULUS IS 0.3660+07P5.1, POISSONS RATIO IS 0.2000+00DEN5(IV= 0.0
 THE NUMBER OF PLATES IS 3 THE MAXIMUM NUMBER OF FOURIER TERMS IS 7 IP= 0 IL= 0 NJX= 6 NOY= 6 IEB= 1
 THE UNIFORM LIVE LCAO ON THE HORIZONTAL PROJECTION IS OL= 0.1000+01

PH(1)= 0.75000+00 PT(1)= 0.433010+00 PH(2)= 0.10000+01 PT(2)= -0.103070-12 PH(3)= 0.75000+00 PT(3)= -0.433310+00
 TB= 0.2000+01 OB= 0.3000+01 GB= 0.1530+07

EDGE DISPLACEMENTS FOR HOOD NUMBER 1

THB(1)= 0.429536630-02 ETAB(1)= 0.424558010-01 X518(1)= -0.508383650+00 UB(1)= -0.301464950-01
 THB(2)= 0.163163100-02 ETAB(2)= -0.704401610-03 X518(2)= -0.434169170+00 UB(2)= 0.288152290-01
 THB(3)= -0.163163100-02 ETAB(3)= 0.704401610-03 X518(3)= -0.434169170+00 UB(3)= 0.288152290-01
 THB(4)= -0.429536630-02 ETAB(4)= -0.424558010-01 X518(4)= -0.508383650+00 UB(4)= -0.301464950-01
 WBJ(1)= 0.461501050+00 HBK(1)= 0.375649330+00 VBJ(1)= 0.217424020+00 VBK(1)= 0.217694620+00
 WBJ(2)= 0.434169170+00 HBK(2)= 0.434169170+00 VBJ(2)= 0.704401610-03 VBK(2)= -0.704401610-03
 WBJ(3)= 0.375649330+00 HBK(3)= 0.461501050+00 VBJ(3)= -0.217694620+00 VBK(3)= -0.217424020+00

EDGE DISPLACEMENTS FOR HOOD NUMBER 3

THB(1)= 0.370590520-04 ETAB(1)= 0.170676460-02 X518(1)= -0.536467370-02 UB(1)= -0.247416410-03
 THB(2)= -0.409115720-03 ETAB(2)= 0.125419890-03 X518(2)= -0.276827150-02 UB(2)= 0.361562700-03
 THB(3)= 0.409115720-03 ETAB(3)= -0.125419890-03 X518(3)= -0.276827150-02 UB(3)= 0.361562700-03
 THB(4)= -0.370590520-04 ETAB(4)= -0.170676460-02 X518(4)= -0.536467370-02 UB(4)= -0.247416410-03
 WBJ(1)= 0.549932600-02 HBK(1)= 0.246010340-02 VBJ(1)= 0.120042350+00 VBK(1)= 0.127551900-02
 WBJ(2)= 0.276827150-02 HBK(2)= 0.276827150-02 VBJ(2)= -0.125419890-03 VBK(2)= 0.125419890-03
 WBJ(3)= 0.246010340-02 HBK(3)= 0.549932600-02 VBJ(3)= -0.127551900-02 VBK(3)= -0.120042350+00

EDGE DISPLACEMENTS FOR HOOD NUMBER 5

THB(1)= -0.342286520-04 ETAB(1)= 0.239565710-03 X518(1)= -0.701030330-03 UB(1)= -0.128231040-04
 THB(2)= -0.237993490-03 ETAB(2)= 0.806658750-04 X518(2)= -0.514222190-03 UB(2)= 0.593298550-04
 THB(3)= 0.237993490-03 ETAB(3)= -0.806658750-04 X518(3)= -0.514222190-03 UB(3)= 0.593298550-04
 THB(4)= -0.342286520-04 ETAB(4)= -0.239565710-03 X518(4)= -0.701030330-03 UB(4)= -0.128231040-04

WDJ(1)= 0.726892930-03 WDK(1)= 0.485662410-03 VEF(1)= 0.143045170-03 V8K(1)= 0.187252400-03
 WDJ(2)= 0.514222190-03 WDK(2)= 0.514222190-03 VEF(2)= 0.806658750-04 V8K(2)= 0.806658750-04
 WDJ(3)= 0.485662410-03 WDK(3)= 0.726892930-03 VEF(3)= 0.187252400-03 V8K(3)= 0.143045170-03
 EDGE DISPLACEMENTS FOR MODE NUMBER 7
 TH8(1)= 0.231345300-04 ETAB(1)= 0.704259770-04 X518(1)= 0.192096840-03 U8(1)= 0.366308440-05
 TH8(2)= 0.120150090-03 ETAB(2)= 0.502609590-04 X518(2)= 0.219511460-03 U8(2)= 0.228970200-04
 TH8(3)= 0.120150090-03 ETAB(3)= 0.502608590-04 X518(3)= 0.219511460-03 U8(3)= 0.228970200-04
 TH8(4)= 0.231345300-04 ETAB(4)= 0.704259770-04 X518(4)= 0.192096840-03 U8(4)= 0.366308440-05
 WBJ(1)= 0.201573730-03 W8K(1)= 0.215232930-03 V8J(1)= 0.350577330-04 V8K(1)= 0.662285500-04
 WBJ(2)= 0.219511460-03 W8K(2)= 0.219511460-03 V8J(2)= 0.502608590-04 V8K(2)= 0.502608590-04
 WBJ(3)= 0.215232930-03 W8K(3)= 0.201573730-03 V8J(3)= 0.662285500-04 V8K(3)= 0.350577330-04

PRIMARY FORCES AND DEFLECTIONS FOR UNSTIFFENED STRUCTURE

NX	NY	NXZ	MY	V	M	THETA	X	Y	PLH
0.0	0.0	0.23122E+03	0.0	0.0	0.0	0.0	0.0	10.00	1
0.0	0.0	0.283339E+03	0.0	0.0	0.0	0.0	0.0	6.67	1
0.0	0.0	0.31439E+03	0.0	0.0	0.0	0.0	0.0	3.33	1
0.0	0.0	0.32421E+03	0.0	0.0	0.0	0.0	0.0	0.00	1
0.0	0.0	0.31254E+03	0.0	0.0	0.0	0.0	0.0	-3.33	1
0.0	0.0	0.27867E+03	0.0	0.0	0.0	0.0	0.0	-6.67	1
0.0	0.0	0.22145E+03	0.0	0.0	0.0	0.0	0.0	-10.00	1
0.33347E+03	-0.23996E+01	0.20339E+03	0.48002E+01	-0.70792E+00	0.57297E-01	0.12424E+00	0.10826E-02	18.03	10.00
0.22087E+03	-0.10415E+02	0.25296E+03	0.68945E+01	0.93391E+01	0.57372E-01	0.12053E+00	0.11819E-02	18.00	6.67
0.10929E+03	-0.19161E+02	0.28264E+03	0.71410E+01	0.11089E+02	0.57430E-01	0.11821E+00	0.14267E-02	18.00	3.33
-0.26049E+01	-0.28151E+02	0.29263E+03	0.54384E+01	0.48533E+01	0.57472E-01	0.11108E+00	0.16171E-02	18.00	0.00
-0.11626E+03	-0.36824E+02	0.28295E+03	0.18580E+01	-0.96030E+01	0.57497E-01	0.10571E+00	0.15543E-02	18.00	-6.67
-0.23338E+03	-0.44484E+02	0.25352E+03	-0.33562E+01	-0.33078E+02	0.57504E-01	0.10123E+00	0.10254E-02	18.00	-10.00
-0.33604E+03	-0.50227E+02	0.20408E+03	-0.57341E+01	-0.67018E+02	0.57490E-01	0.99655E-01	-0.21290E-03	18.00	-6.67
0.63279E+03	-0.21125E+01	0.15242E+03	0.85441E+01	0.40113E+01	0.10997E+00	0.23654E+00	0.21793E-02	36.00	10.00
0.42054E+03	-0.99925E+01	0.19446E+03	0.99669E+01	0.12534E+02	0.11011E+00	0.22901E+00	0.23641E-02	36.00	6.67
0.21097E+03	-0.19256E+02	0.22100E+03	0.95020E+01	0.28227E+01	0.11020E+00	0.22068E+00	0.26510E-02	36.00	3.33
0.24634E+01	-0.29115E+02	0.22362E+03	0.71530E+01	0.12227E+01	0.11025E+00	0.21145E+00	0.28212E-02	36.00	0.00
-0.20654E+03	-0.38828E+02	0.22962E+03	0.29740E+01	-0.15604E+02	0.11025E+00	0.20225E+00	0.26485E-02	36.00	-3.33
-0.41760E+03	-0.47656E+02	0.20172E+03	-0.29453E+01	-0.43474E+02	0.11025E+00	0.19444E+00	0.19039E-02	36.00	-6.67
-0.63222E+03	-0.54878E+02	0.16532E+03	-0.10466E+02	-0.81019E+02	0.11018E+00	0.19045E+00	0.34785E-03	36.00	-10.00
0.81065E+03	-0.13987E+01	0.11457E+03	0.10696E+02	0.70005E+01	0.15447E+00	0.32940E+00	0.31041E-02	54.00	10.00
0.58138E+03	-0.72595E+01	0.15461E+03	0.11246E+02	0.12153E+02	0.15465E+00	0.31892E+00	0.33105E-02	54.00	6.67
0.29551E+03	-0.14796E+02	0.16570E+03	0.10318E+02	0.98260E+01	0.15477E+00	0.30731E+00	0.35552E-02	54.00	3.33
0.11632E+02	-0.23121E+02	0.17330E+03	0.79704E+01	-0.18970E+00	0.15483E+00	0.29538E+00	0.36498E-02	54.00	0.00
-0.271159E+03	-0.31548E+02	0.16891E+03	0.42164E+01	-0.17901E+02	0.15483E+00	0.23337E+00	0.33987E-02	54.00	-3.33
-0.55530E+03	-0.39440E+02	0.15254E+03	-0.10082E+01	-0.43106E+02	0.15477E+00	0.27332E+00	0.26153E-02	54.00	-6.67
-0.84040E+03	-0.46282E+02	0.12412E+03	-0.7847E+01	-0.75333E+02	0.15466E+00	0.26690E+00	0.11178E-02	54.00	-10.00

0.10309E+04	-0.18517E+01	0.74619E+02	0.11727E+02	0.52141E+01	0.18820E+00	0.39926E+00	0.37296E-02	72.00	10.00	1
0.69631E+03	-0.88626E+01	0.99452E+02	0.12814E+02	0.12097E+02	0.18842E+00	0.38655E+00	0.39081E-02	72.00	6.67	1
0.35675E+03	-0.17405E+02	0.11274E+03	0.12179E+02	0.10353E+02	0.18836E+00	0.37316E+00	0.41521E-02	72.00	3.33	1
0.18636E+02	-0.26773E+02	0.11780E+03	0.97930E+01	0.63057E-01	0.18883E+00	0.35902E+00	0.42478E-02	72.00	0.00	1
-0.31937E+03	-0.36231E+02	0.11473E+03	0.56644E+01	-0.18775E+02	0.18864E+00	0.34524E+00	0.39932E-02	72.00	-3.33	1
-0.65904E+03	-0.45007E+02	0.10335E+03	-0.18834E+00	-0.46253E+02	0.18857E+00	0.33312E+00	0.31447E-02	72.00	-6.67	1
-0.10020E+04	-0.52266E+02	0.83395E+02	-0.76964E+01	-0.82575E+02	0.18842E+00	0.32513E+00	0.15152E-02	72.00	-10.00	1
0.11416E+04	-0.18408E+01	0.36499E+02	0.12397E+02	0.50851E+01	0.20921E+00	0.44218E+00	0.41081E-02	90.00	10.00	1
0.76619E+03	-0.88771E+01	0.47781E+02	0.13461E+02	0.11859E+02	0.20945E+00	0.42821E+00	0.42786E-02	90.00	6.67	1
0.39382E+03	-0.17484E+02	0.54075E+02	0.12795E+02	0.99773E+01	0.20960E+00	0.41362E+00	0.45113E-02	90.00	3.33	1
0.22999E+02	-0.26926E+02	0.56674E+02	0.10376E+02	-0.50604E+00	0.20968E+00	0.39829E+00	0.45918E-02	90.00	0.00	1
-0.34781E+03	-0.36451E+02	0.55289E+02	0.62166E+01	-0.19604E+02	0.20968E+00	0.38341E+00	0.43062E-02	90.00	-3.33	1
-0.72020E+03	-0.45280E+02	0.50083E+02	0.33400E+00	-0.47407E+02	0.20960E+00	0.37024E+00	0.34395E-02	90.00	-6.67	1
-0.10958E+04	-0.52595E+02	0.41310E+02	-0.72068E+01	-0.84091E+02	0.20944E+00	0.36134E+00	0.17728E-02	90.00	-10.00	1
0.11772E+04	-0.14567E+01	-0.13342E-10	0.12705E+02	0.63150E+01	0.21633E+00	0.45658E+00	0.42473E-02	108.00	10.00	1
0.40640E+03	-0.15217E+02	0.13316E+02	0.11445E+02	0.21657E+00	0.21657E+00	0.44212E+00	0.44258E-02	108.00	6.67	1
0.24687E+02	-0.23801E+02	-0.21457E-10	0.12409E+02	0.88303E+01	0.21673E+00	0.42707E+00	0.46380E-02	108.00	3.33	1
-0.35646E+03	-0.22313E+02	-0.19105E-10	0.75444E+00	-0.46137E+02	0.21681E+00	0.41137E+00	0.46892E-02	108.00	0.00	1
-0.73893E+03	-0.40665E+02	-0.19105E-10	0.75444E+00	-0.46137E+02	0.21671E+00	0.39620E+00	0.43825E-02	108.00	-3.33	1
-0.11221E+04	-0.47653E+02	-0.16076E-10	-0.62613E+01	-0.79641E+02	0.21654E+00	0.37591E+00	0.35232E-02	108.00	-6.67	1
0.0	0.0	0.22145E+03	0.0	0.0	0.0	0.0	0.19230E-02	108.00	-10.00	2
0.0	0.0	0.14230E+03	0.0	0.0	0.0	0.0	0.0	0.0	15.00	2
0.0	0.0	0.69681E+02	0.0	0.0	0.0	0.0	0.0	0.0	10.00	2
0.0	0.0	-0.23065E-10	0.0	0.0	0.0	0.0	0.0	0.0	5.00	2
0.0	0.0	-0.69681E+02	0.0	0.0	0.0	0.0	0.0	0.0	0.0	2
0.0	0.0	-0.14230E+03	0.0	0.0	0.0	0.0	0.0	0.0	0.0	2
0.0	0.0	-0.22145E+03	0.0	0.0	0.0	0.0	0.0	0.0	-10.00	2
-0.28663E+03	-0.49165E+02	0.20408E+03	-0.11274E+02	-0.67018E+02	-0.32838E-04	0.11508E+00	-0.21293E-03	18.00	15.00	2
-0.24233E+03	-0.55658E+02	0.13399E+03	0.29798E+01	-0.79623E+01	-0.37218E-04	0.12440E+00	-0.28094E-02	18.00	10.00	2

-0.25964E+03 -0.53752E+02 0.66372E+02 0.12374E+02 0.24439E+02 -0.22721E-04 0.13784E+00 -0.21580E-12 18.00 5.00 2
 -0.24558E+03 -0.59664E+02 -0.20313E-10 0.15627E+02 0.34786E+02 -0.41678E-14 0.14345E+00 0.79379E-15 18.00 0.0 2
 -0.24964E+03 -0.58752E+02 -0.66372E+02 0.12374E+02 0.24439E+02 0.22721E-04 0.13784E+00 0.21580E-12 18.00 -5.00 2
 -0.26253E+03 -0.55658E+02 -0.13399E+03 0.29798E+01 -0.79623E+01 0.37218E-04 0.12440E+00 0.24094E-02 18.00 -10.00 2
 -0.28663E+03 -0.49165E+02 -0.20408E-03 -0.11274E+02 -0.67018E+02 0.32838E-04 0.11508E+00 0.21297E-03 18.00 -15.00 2
 -0.50777E+03 -0.53859E+02 0.16532E+03 -0.12815E+02 -0.81019E+02 0.21159E-03 0.22008E+00 0.34778E-03 36.00 15.00 2
 -0.48552E+03 -0.63424E+02 0.11164E+03 0.13486E+01 -0.13623E+02 0.22886E+00 -0.29805E-02 36.00 10.00 2
 -0.47234E+03 -0.69021E+02 0.11164E+03 0.13486E+01 -0.13623E+02 0.22886E+00 -0.29805E-02 36.00 5.00 2
 -0.46798E+03 -0.70861E+02 0.10786E+02 0.10172E+02 0.25886E+02 -0.53022E-04 0.24985E+00 0.15558E-14 36.00 0.0 2
 -0.47234E+03 -0.69021E+02 -0.15031E-10 0.13164E+02 0.38897E+02 -0.79680E-14 0.24985E+00 0.15558E-14 36.00 0.0 2
 -0.48552E+03 -0.63424E+02 -0.11164E+03 0.10172E+02 0.25886E+02 -0.53022E-04 0.24985E+00 0.15558E-14 36.00 0.0 2
 -0.50777E+03 -0.53859E+02 -0.16532E+03 -0.12815E+02 -0.81019E+02 0.21159E-03 0.22008E+00 0.34778E-03 36.00 -5.00 2
 -0.67407E+03 -0.45564E+02 0.12412E+03 -0.10774E+02 -0.81019E+02 -0.21159E-03 0.30855E+00 0.11177E-02 54.00 15.00 2
 -0.65822E+03 -0.55309E+02 0.82805E+02 0.16717E+02 0.75337E+02 0.50198E-03 0.31294E+00 -0.21652E-02 54.00 10.00 2
 -0.67479E+03 -0.61492E+02 0.82805E+02 0.16717E+02 0.75337E+02 0.50198E-03 0.31294E+00 -0.21652E-02 54.00 5.00 2
 -0.64444E+03 -0.63599E+02 -0.10807E-10 0.84143E+01 0.19387E+02 0.15079E-03 0.32454E+00 -0.19655E-02 54.00 5.00 2
 -0.64797E+03 -0.61492E+02 -0.41441E+02 0.63442E+01 0.19387E+02 0.15079E-03 0.32454E+00 -0.19655E-02 54.00 0.0 2
 -0.65822E+03 -0.55309E+02 -0.82805E+02 0.50822E-01 -0.16717E+02 -0.31425E-03 0.32958E+00 0.22195E-14 54.00 -5.00 2
 -0.67407E+03 -0.45564E+02 -0.12412E+03 -0.10774E+02 -0.81019E+02 -0.21159E-03 0.31294E+00 -0.21652E-02 54.00 -10.00 2
 -0.80355E+03 -0.51424E+02 0.83395E+02 -0.11299E+02 -0.82576E+02 0.63636E-03 0.30855E+00 -0.11177E-02 54.00 -15.00 2
 -0.78319E+03 -0.60876E+02 0.54865E+02 0.16332E+01 -0.18439E+02 0.40404E-03 0.37923E+00 -0.20837E-02 72.00 15.00 2
 -0.77130E+03 -0.66415E+02 0.27262E+02 0.94652E+01 0.19688E+02 0.19604E-03 0.39070E+00 -0.19650E-02 72.00 10.00 2
 -0.76798E+03 -0.68244E+02 -0.71106E-11 0.12077E+02 0.32348E+02 -0.13547E-13 0.39569E+00 0.27235E-14 72.00 5.00 2
 -0.77130E+03 -0.66415E+02 -0.27262E+02 0.94652E+01 0.19688E+02 0.19604E-03 0.39070E+00 -0.19650E-02 72.00 0.0 2
 -0.78319E+03 -0.60876E+02 -0.54865E+02 0.16332E+01 -0.18439E+02 0.40404E-03 0.39070E+00 -0.19650E-02 72.00 0.0 2
 -0.80355E+03 -0.51424E+02 0.83395E+02 -0.11299E+02 -0.82576E+02 0.63636E-03 0.37923E+00 -0.20837E-02 72.00 -5.00 2
 -0.87862E+03 -0.51755E+02 0.41310E+02 -0.11132E+02 -0.84092E+02 0.73520E-03 0.37588E+00 -0.15151E-02 72.00 -10.00 2
 -0.85813E+03 -0.61342E+02 0.28154E+02 0.18825E+01 -0.19597E+02 0.46963E-03 0.41776E+00 0.17726E-02 90.00 15.00 2
 -0.84607E+03 -0.66902E+02 0.14213E+02 0.97737E+01 0.18765E+02 0.22873E-03 0.42009E+00 -0.19303E-02 90.00 10.00 2
 -0.84209E+03 -0.68847E+02 -0.32530E-11 0.12408E+02 0.31501E+02 -0.15031E-13 0.43580E+00 0.30397E-14 90.00 5.00 2
 -0.84209E+03 -0.68847E+02 -0.32530E-11 0.12408E+02 0.31501E+02 -0.15031E-13 0.43580E+00 0.30397E-14 90.00 0.0 2

-0.64607E+03	-0.66282E+02	-0.14213E+02	0.97737E+01	0.18765E+02	-0.22673E-03	0.43103E+00	0.18938E-02	90.00	-5.00	2
-0.85813E+03	-0.61342E+02	-0.28154E+02	0.18825E+01	-0.19597E+02	-0.46963E-03	0.42009E+00	0.19303E-02	90.00	-10.00	2
-0.87862E+03	-0.51755E+02	-0.41310E+02	-0.11132E+02	-0.84092E+02	-0.73520E-03	0.41776E+00	-0.17726E-02	90.00	-15.00	2
-0.89944E+03	-0.46943E+02	-0.16076E-10	-0.10194E+02	-0.79642E+02	0.79942E-03	0.43185E+00	0.19229E-02	108.00	15.00	2
-0.80248E+03	-0.56668E+02	-0.11294E-10	0.10735E+01	-0.20059E+02	0.51251E-03	0.43298E+00	-0.16558E-02	108.00	10.00	2
-0.87181E+03	-0.62719E+02	-0.57779E-11	0.76932E+01	0.16331E+02	0.24999E-03	0.44275E+00	-0.17188E-02	108.00	5.00	2
-0.86819E+03	-0.64765E+02	0.11887E-23	0.98766E+01	0.28551E+02	-0.15531E-13	0.44706E+00	0.31489E-14	108.00	0.0	2
-0.87181E+03	-0.62719E+02	0.57779E-11	0.76932E+01	0.16331E+02	-0.24999E-03	0.44275E+00	0.17188E-02	108.00	-5.00	2
-0.88248E+03	-0.56668E+02	0.11294E-10	0.10735E+01	-0.20059E+02	0.51251E-03	0.43298E+00	0.16558E-02	108.00	-10.00	2
-0.89944E+03	-0.46943E+02	-0.16076E-10	-0.10194E+02	-0.79642E+02	-0.79942E-03	0.43185E+00	-0.19229E-02	108.00	-15.00	2
0.0	0.0	-0.22145E+03	0.0	0.0	0.0	0.0	0.0	0.0	10.00	3
0.0	0.0	-0.2767E+03	0.0	0.0	0.0	0.0	0.0	0.0	6.67	3
0.0	0.0	-0.31254E+03	0.0	0.0	0.0	0.0	0.0	0.0	3.33	3
0.0	0.0	-0.32421E+03	0.0	0.0	0.0	0.0	0.0	0.0	0.00	3
0.0	0.0	-0.31439E+03	0.0	0.0	0.0	0.0	0.0	0.0	-3.33	3
0.0	0.0	-0.28339E+03	0.0	0.0	0.0	0.0	0.0	0.0	-6.67	3
0.0	0.0	-0.23122E+03	0.0	0.0	0.0	0.0	0.0	0.0	-10.00	3
-0.35604E+03	-0.50227E+02	-0.20408E+03	-0.97341E+01	-0.67018E+02	-0.57490E-01	0.99655E-01	0.21290E-03	18.00	10.00	3
-0.23338E+03	-0.44484E+02	-0.25352E+03	-0.33562E+01	-0.33078E+02	-0.57504E-01	0.10123E+00	-0.10254E-02	18.00	6.67	3
-0.11626E+03	-0.36824E+02	-0.28295E+03	0.18580E+01	-0.94030E+01	-0.57497E-01	0.10571E+00	-0.15543E-02	18.00	3.33	3
-0.26099E+01	-0.28151E+02	-0.29263E+03	0.54384E+01	0.48533E+01	-0.57472E-01	0.11108E+00	-0.16171E-02	18.00	0.00	3
0.10929E+03	-0.19161E+02	-0.28264E+03	0.71410E+01	0.11089E+02	-0.57430E-01	0.11621E+00	-0.14267E-02	18.00	-3.33	3
0.22087E+03	-0.10415E+02	-0.25296E+03	0.68965E+01	0.93391E+01	-0.57372E-01	0.12053E+00	-0.11819E-02	18.00	-6.67	3
0.33347E+03	-0.23996E+01	-0.20339E+03	0.48002E+01	-0.70792E+00	-0.57297E-01	0.12424E+00	-0.10826E-02	18.00	-10.00	3
-0.63222E+03	-0.54878E+02	-0.16532E+03	-0.10466E+02	-0.81019E+02	-0.11018E+00	0.19045E+00	-0.34785E-03	36.00	10.00	3
-0.41760E+03	-0.47658E+02	-0.20172E+03	-0.29453E+01	-0.43417E+02	-0.11025E+00	0.19444E+00	-0.19039E-02	36.00	6.67	3
-0.20654E+03	-0.38829E+02	-0.22335E+03	0.29740E+01	-0.15604E+02	-0.11027E+00	0.20225E+00	-0.26485E-02	36.00	3.33	3
0.24634E+01	-0.29115E+02	-0.22962E+03	0.71530E+01	0.28227E+01	-0.11025E+00	0.21145E+00	-0.28212E-02	36.00	0.00	3
0.21097E+03	-0.19256E+02	-0.22010E+03	0.95020E+01	0.12150E+02	-0.11020E+00	0.22068E+00	-0.26518E-02	36.00	-3.33	3
0.42054E+03	-0.99982E+01	-0.19446E+03	0.99669E+01	0.12534E+02	-0.11011E+00	0.22901E+00	-0.23641E-02	36.00	-6.67	3

0.63279E+03 -0.21125E+01 -0.15242E+03 0.85441E+01 0.40113E+01 -0.10997E+00 0.23654E+00 -0.21793E-02 36.00 -10.00 3
 -0.84046E+03 -0.46282E+02 -0.12412E+03 -0.78167E+01 -0.73336E+02 -0.15466E+00 0.26690E+00 -0.111178E-02 54.00 10.00 3
 -0.55530E+03 -0.39440E+02 -0.15254E+03 -0.10082E+01 -0.43106E+02 -0.15477E+00 0.27332E+00 -0.26153E-02 54.00 6.67 3
 -0.27159E+03 -0.31548E+02 -0.16891E+03 0.42164E+01 -0.17901E+02 -0.15483E+00 0.28357E+00 -0.33597E-02 54.00 3.33 3
 0.11632E+02 -0.23121E+02 -0.17330E+03 0.79704E+01 -0.18970E+00 -0.15483E+00 0.29538E+00 -0.36487E-02 54.00 0.00 3
 0.29551E+03 -0.14796E+02 -0.16570E+03 0.10318E+02 0.98260E+01 -0.15477E+00 0.30751E+00 -0.35552E-02 54.00 -3.33 3
 0.58138E+03 -0.72950E+01 -0.14612E+03 0.11246E+02 0.12153E+02 -0.15465E+00 0.31892E+00 -0.33105E-02 54.00 -6.67 3
 0.87065E+03 -0.13987E+01 -0.11457E+03 0.10696E+02 0.70005E+01 -0.15447E+00 0.32960E+00 -0.31041E-02 54.00 -10.00 3
 -0.10020E+04 -0.52266E+02 -0.83395E+02 -0.76964E+01 -0.82375E+02 -0.18842E+00 0.32513E+00 -0.15152E-02 72.00 10.00 3
 -0.65902E+03 -0.45007E+02 -0.10335E+03 -0.18834E+00 -0.46253E+02 -0.18857E+00 0.33312E+00 -0.31447E-02 72.00 6.67 3
 -0.31937E+03 -0.36231E-02 -0.11473E+03 0.56644E+01 -0.18775E+02 -0.18864E+00 0.34524E+00 -0.39832E-02 72.00 3.33 3
 0.18696E+02 -0.26773E+02 -0.11780E+03 0.97930E+01 0.63057E-01 -0.18863E+00 0.35902E+00 -0.42478E-02 72.00 0.00 3
 0.35675E+03 -0.17405E+02 -0.11274E+03 0.12179E+02 0.10353E+02 -0.18856E+00 0.37316E+00 -0.41521E-02 72.00 -3.33 3
 -0.69631E+03 -0.88626E+01 -0.99652E+02 0.12814E+02 0.12097E+02 -0.18842E+00 0.38655E+00 -0.39083E-02 72.00 -6.67 3
 0.10389E+04 -0.18517E+01 -0.78619E+02 0.11727E+02 0.52141E+01 -0.18820E+00 0.39926E+00 -0.37296E-02 72.00 -10.00 3
 -0.10958E+04 -0.52595E+02 -0.41310E+02 -0.72068E+01 -0.84091E+02 -0.20944E+00 0.36134E+00 -0.17728E-02 90.00 10.00 3
 -0.72020E+03 -0.45280E+02 -0.50083E+02 0.33440E+00 -0.47407E+02 -0.20960E+00 0.37024E+00 -0.34395E-02 90.00 6.67 3
 -0.34781E+03 -0.36451E+02 -0.55289E+02 0.62164E+01 -0.19604E+02 -0.20968E+00 0.38341E+00 -0.43062E-02 90.00 3.33 3
 0.22999E+02 -0.26926E+02 -0.56674E+02 0.10374E+02 -0.50604E+00 -0.20968E+00 0.39829E+00 -0.45918E-02 90.00 0.00 3
 0.9382E+03 -0.17484E+02 -0.54075E+02 0.12795E+02 0.99773E+01 -0.20960E+00 0.41362E+00 -0.45113E-02 90.00 -3.33 3
 0.7619E+03 -0.88771E+01 -0.47381E+02 0.13461E+02 0.11859E+02 -0.20945E+00 0.42821E+00 -0.42786E-02 90.00 -6.67 3
 0.11416E+04 -0.19408E+01 -0.36499E+02 0.12397E+02 0.50851E+01 -0.20921E+00 0.44218E+00 -0.41081E-02 90.00 -10.00 3
 -0.11221E+04 -0.47653E+02 0.16076E-10 -0.62613E+01 -0.79641E+02 -0.21654E+00 0.37351E+00 -0.19230E-02 108.00 10.00 3
 -0.73831E+03 -0.40665E+02 0.20975E-10 0.75444E+00 -0.46137E+02 -0.21671E+00 0.38278E+00 -0.35232E-02 108.00 6.67 3
 -0.35646E+03 -0.32513E+02 0.21457E-10 0.61492E+01 -0.20034E+02 -0.21680E+00 0.39620E+00 -0.43825E-02 108.00 3.33 3
 0.24687E+02 -0.23801E+02 0.20407E-10 0.10017E+02 -0.16656E+01 -0.21681E+00 0.41137E+00 -0.46892E-02 108.00 0.00 3
 0.40640E+03 -0.15217E+02 0.20407E-10 0.12409E+02 0.88303E+01 -0.21673E+00 0.42707E+00 -0.46380E-02 108.00 -3.33 3
 0.79010E+03 -0.75073E+01 0.17729E-10 0.13316E+02 0.11445E+02 -0.21657E+00 0.44212E+00 -0.44258E-02 108.00 -6.67 3
 0.11772E+04 -0.14567E+01 0.13342E-10 0.12705E+02 0.63150E+01 -0.21633E+00 0.45658E+00 -0.42473E-02 108.00 -10.00 3

Table B.1 Model Output Data

Type of Analysis	N_x (lb/in)	N_y (lb/in)	N_{xy} (lb/in)	M_x (lb-in/in)	M_y (lb-in/in)	v (in)	w (in)	x (in)	y (in)	Plate No.
W/O Edge Beam	0.0	0.0	230.9	0.0	0.0	0.0	0.0	0.0	10	2
Edge Beam	0.0	0.0	231.2	0.0	0.0	0.0	0.0	0.0	10	1
W/O Edge Beam	0.0	0.0	221.7	0.0	0.0	0.0	0.0	0.0	-10	2
Edge Beam	0.0	0.0	221.4	0.0	0.0	0.0	0.0	0.0	-10	1
W/O Edge Beam	335	-2.4	203.0	4.8	-0.335	0.057	0.121	18	10	2
Edge Beam	333	-2.4	203.4	4.8	-0.707	0.057	0.124	18	10	1
W/O Edge Beam	-356	-50.2	204.3	-9.6	-66.5	-0.058	0.099	18	-10	2
Edge Beam	-356	-50.2	204.1	-9.7	-67.0	0.057	0.099	18	-10	1
W/O Edge Beam	636	-2.1	152.1	8.7	5.5	0.110	0.231	36	10	2
Edge Beam	633	-2.1	152.4	8.5	4.0	0.110	0.236	36	10	1
W/O Edge Beam	-633	-54.9	165.5	-10.2	-80.0	0.110	0.191	36	-10	2
Edge Beam	-632	-54.9	165.3	-10.5	-81.0	0.110	0.190	36	-10	1
W/O Edge Beam	875	-1.4	114.4	10.9	9.3	0.155	0.322	54	10	2
Edge Beam	871	-1.4	114.6	10.7	7.0	0.154	0.329	54	10	1
W/O Edge Beam	-841	-46.3	124.2	-7.5	-73.9	0.155	0.267	54	-10	2
Edge Beam	-840	-46.3	124.1	-7.8	-75.3	0.155	0.267	54	-10	1

Table B.1 (continued)

Type of Analysis	N_x (lb/in)	N_y (lb/in)	N_{xy} (lb/in)	M_x (lb-in/in)	M_y (lb-in/in)	v (in)	w (in)	x (in)	y (in)	Plate No.
W/O Edge Beam	1043	-1.8	78.5	11.9	7.6	0.188	0.390	72	10	2
Edge Beam	1038	-1.8	78.6	11.7	5.2	0.188	0.399	72	10	1
W/O Edge Beam	-1003	-52.3	83.4	-7.3	-80.9	0.188	0.325	72	-10	2
Edge Beam	-1002	-52.3	83.4	-7.7	-82.6	0.188	0.325	72	-10	1
W/O Edge Beam	1146	-1.8	36.5	12.6	7.5	0.210	0.432	90	10	2
Edge Beam	1142	-1.8	36.5	12.4	5.1	0.210	0.442	90	10	1
W/O Edge Beam	-1096	-52.6	41.3	-6.8	-82.2	0.210	0.362	90	-10	2
Edge Beam	-1096	-52.6	41.3	-7.2	-84.1	0.210	0.361	90	-10	1
W/O Edge Beam	1182	-1.4	0.0	12.9	8.9	0.217	0.446	108	10	2
Edge Beam	1177	-1.4	0.0	12.7	6.3	0.216	0.456	108	10	1
W/O Edge Beam	-1123	-47.7	0.0	-5.8	-77.7	0.217	0.374	108	-10	2
Edge Beam	-1122	-47.6	0.0	-6.3	-79.6	0.216	0.373	108	-10	1
W/O Edge Beam	0.0	0.0	221.6	0.0	0.0	0.0	0.0	0.0	15	3
Edge Beam	0.0	0.0	221.4	0.0	0.0	0.0	0.0	0.0	15	2
W/O Edge Beam	0.0	0.0	-221.6	0.0	0.0	0.0	0.0	0.0	-15	3
Edge Beam	0.0	0.0	-221.4	0.0	0.0	0.0	0.0	0.0	-15	2

Table B.1 (continued)

Type of Analysis	N_x (lb/in)	N_y (lb/in)	N_{xy} (lb/in)	M_x (lb-in/in)	M_y (lb-in/in)	v (in)	w (in)	x (in)	y (in)	Plate No.
W/O Edge Beam	-287	-49.1	204.3	-11.2	-66.5	-0.00003	0.115	18	15	3
Edge Beam	-287	-49.2	204.1	-11.3	-67.0	-0.00003	0.115	18	15	2
W/O Edge Beam	-287	-49.1	-204.3	-11.2	-66.5	0.00003	0.115	18	-15	3
Edge Beam	-287	-49.2	-204.1	-11.3	-67.0	0.00003	0.115	18	-15	2
W/O Edge Beam	508	-53.9	165.5	-12.6	-80.1	0.0002	0.221	36	15	3
Edge Beam	-508	-53.8	165.3	-12.8	-81.0	0.0002	0.220	36	15	2
W/O Edge Beam	-508	-53.9	-165.5	-12.6	-80.1	-0.0002	0.221	36	-15	3
Edge Beam	-508	-53.8	-165.3	-12.8	-81.0	0.0002	0.220	36	-15	2
W/O Edge Beam	-675	-45.6	124.3	-105.0	-74.0	0.0005	0.309	54	15	3
Edge Beam	-674	-45.6	124.1	-107.7	-75.3	0.0005	0.308	54	15	2
W/O Edge Beam	-675	-45.6	-124.3	-105.0	-74.0	-0.0005	0.309	54	-15	3
Edge Beam	-674	-45.6	-124.1	-107.7	-75.3	0.0005	0.308	54	-15	2
W/O Edge Beam	-804	-51.4	83.4	-10.9	-80.9	0.0006	0.377	72	15	3
Edge Beam	-803	-51.4	83.4	-11.3	-82.6	0.0006	0.376	72	15	2
W/O Edge Beam	-804	-51.4	-83.4	-10.9	-80.9	-0.0006	0.377	72	-15	3
Edge Beam	-803	-51.4	-83.4	-11.3	-82.6	-0.0006	0.376	72	-15	2

Table B.1 (continued)

Type of Analysis	N_x (lb/in)	N_y (lb/in)	N_{xy} (lb/in)	M_x (lb-in/in)	M_y (lb-in/in)	v (in)	w (in)	x (in)	y (in)	Plate No.
W/O Edge Beam	-879	-51.7	41.3	-10.7	-82.2	0.0007	0.419	90	15	3
Edge Beam	-879	-51.7	41.3	-11.1	-84.1	0.0007	0.418	90	15	2
W/O Edge Beam	-879	-51.7	-41.3	-10.7	-82.2	-0.0007	0.419	90	-15	3
Edge Beam	-879	-51.7	-41.3	-11.1	-84.1	-0.0007	0.418	90	-15	2
W/O Edge Beam	-900	-46.9	0.0	-9.8	-77.7	0.0008	0.433	108	15	3
Edge Beam	-899	-46.9	0.0	-10.2	-79.6	0.0008	0.432	108	15	2
W/O Edge Beam	-900	-46.9	0.0	-9.8	-77.7	-0.0008	0.433	108	-15	3
Edge Beam	-899	-46.9	0.0	-10.2	-79.6	-0.0008	0.432	108	-15	2
W/O Edge Beam	0.0	0.0	-221.6	0.0	0.0	0.0	0.0	0.0	10.	4
Edge Beam	0.0	0.0	-221.4	0.0	0.0	0.0	0.0	0.0	10	3
W/O Edge Beam	0.0	0.0	-230.9	0.0	0.0	0.0	0.0	0.0	-10	4
Edge Beam	0.0	0.0	-231.2	0.0	0.0	0.0	0.0	0.0	-10	3
W/O Edge Beam	-356	-50.2	-204.3	-9.6	-66.5	-0.058	0.099	18	10	4
Edge Beam	-356	-50.2	-204.1	-9.7	-67.0	-0.057	0.099	18	10	3
W/O Edge Beam	335	-2.4	-203.0	4.8	-0.335	-0.057	0.121	18	-10	4
Edge Beam	333	-2.4	-203.4	4.8	-0.707	-0.057	0.124	18	-10	3

Table B.1 (continued)

Type of Analysis	N_x (lb/in)	N_y (lb/in)	N_{xy} (lb/in)	M_x (1b-in/in)	M_y (1b-in/in)	v (in)	w (in)	x (in)	y (in)	Plate No.
W/O Edge Beam	-633	-54.9	-165.5	-10.2	-80.0	-0.110	0.191	36	10	4
Edge Beam	-632	-54.9	-165.3	-10.5	-81.0	-0.110	0.190	36	10	3
W/O Edge Beam	636	-2.1	-152.1	8.7	5.5	-0.110	0.231	36	-10	4
Edge Beam	633	-2.1	-152.4	8.5	4.0	-0.110	0.236	36	-10	3
W/O Edge Beam	-841	-46.3	-124.2	-7.5	-73.9	-0.155	0.267	54	10	4
Edge Beam	-840	-46.3	-124.1	-7.8	-75.3	-0.155	0.267	54	10	3
W/O Edge Beam	875	-1.4	-114.4	10.9	9.3	-0.155	0.322	54	-10	4
Edge Beam	871	-1.4	-114.6	10.7	7.0	-0.154	0.329	54	-10	3
W/O Edge Beam	-1003	-52.3	-83.4	-7.3	-80.9	-0.188	0.325	72	10	4
Edge Beam	-1002	-52.3	-83.4	-7.7	-82.6	-0.188	0.325	72	10	3
W/O Edge Beam	1043	-1.8	-78.5	11.9	7.6	-0.188	0.390	72	-10	4
Edge Beam	1038	-1.8	-78.6	11.7	5.2	-0.188	0.399	72	-10	3
W/O Edge Beam	-1096	-52.6	-41.3	-6.8	-82.2	-0.210	0.362	90	10	4
Edge Beam	-1096	-52.6	-41.3	-7.2	-84.1	-0.210	0.361	90	10	3
W/O Edge Beam	1146	-1.8	-36.5	12.6	7.5	-0.210	0.432	90	-10	4
Edge Beam	1142	-1.8	-36.5	12.4	5.1	-0.210	0.442	90	-10	3

Table B.1 (continued)

Type of Analysis	N_x (lb/in)	N_y (lb/in)	N_{xy} (lb/in)	M_x (lb-in/in)	M_y (lb-in/in)	v (in)	w (in)	x (in)	y (in)	Plate No.
W/O Edge Beam	-1123	-47.7	0.0	-5.8	-77.7	-0.217	0.374	108	10	4
Edge Beam	-1122	-47.6	0.0	-6.3	-79.6	-0.216	0.373	108	10	3
W/O Edge Beam	1182	-1.4	0.0	12.9	8.9	-0.217	0.446	108	-10	4
Edge Beam	1177	-1.4	0.0	12.7	6.3	-0.216	0.456	108	-10	3

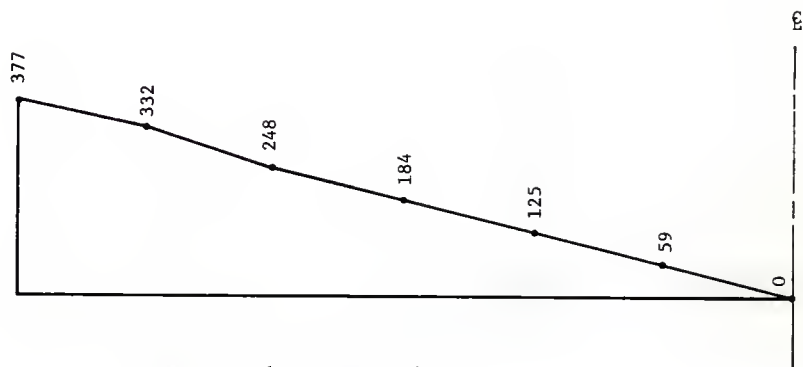
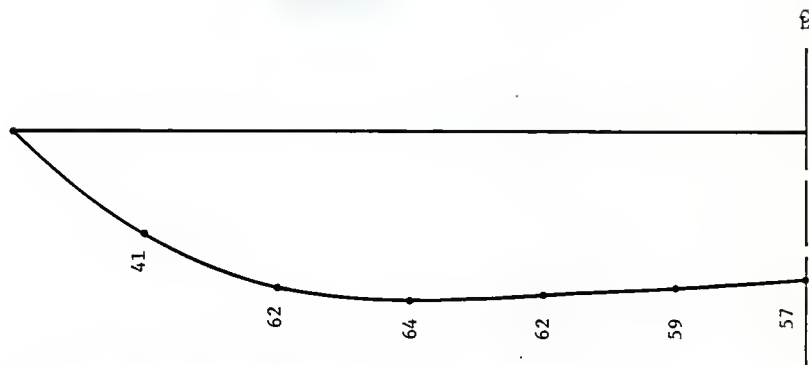
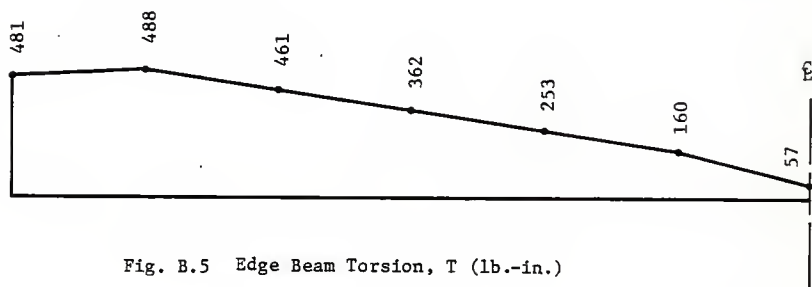
Left Edge Beam

Fig. B.3 Shear Diagram (lb.)

Left Edge BeamFig. B.4 Edge Beam Bending Moment About y-axis, M_y (lb.-in.)Fig. B.5 Edge Beam Torsion, T (lb.-in.)

Left Edge Beam

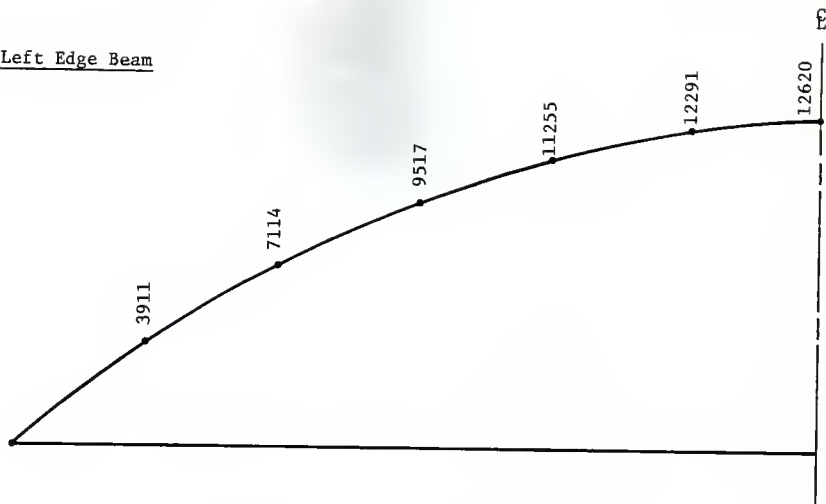


Fig. B.6 Edge Beam Axial Force, N_x (lb.)

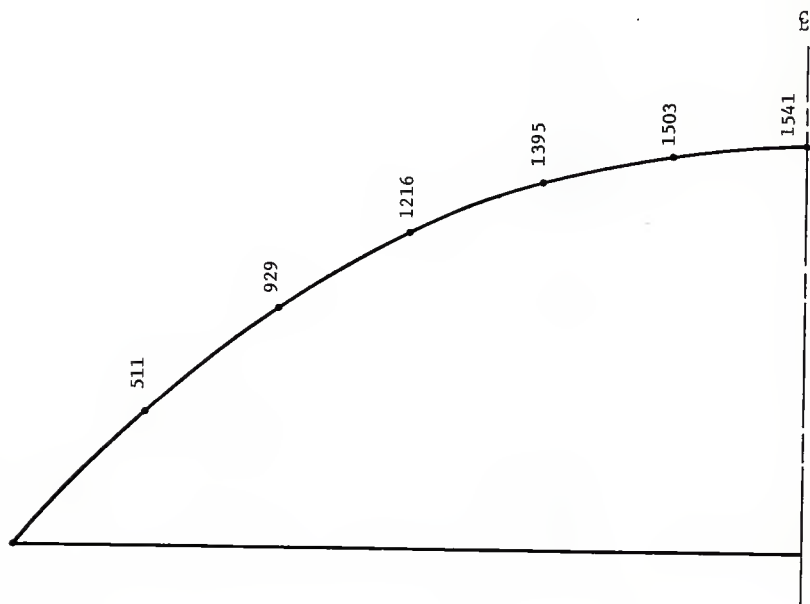


Fig. B.7 Edge Beam Bending Moment About z-axis, M_z (lb.-in.)

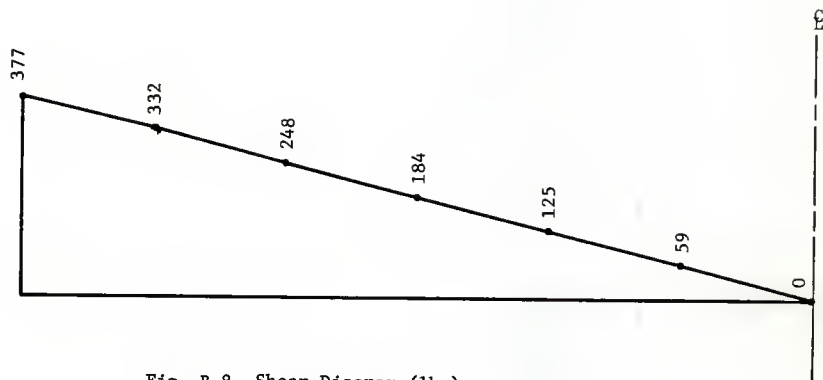
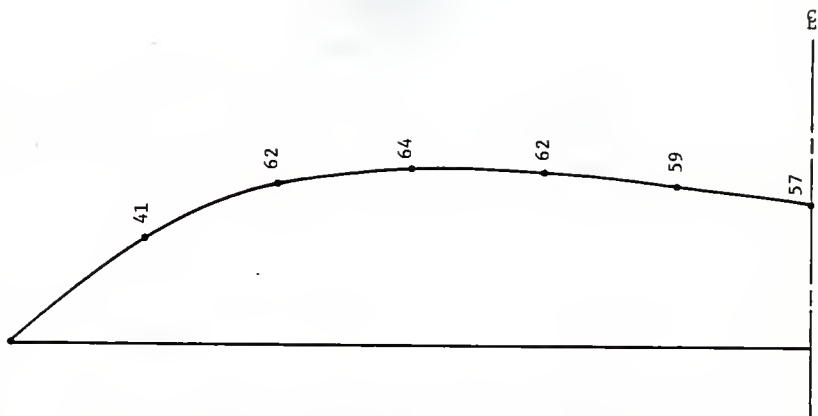
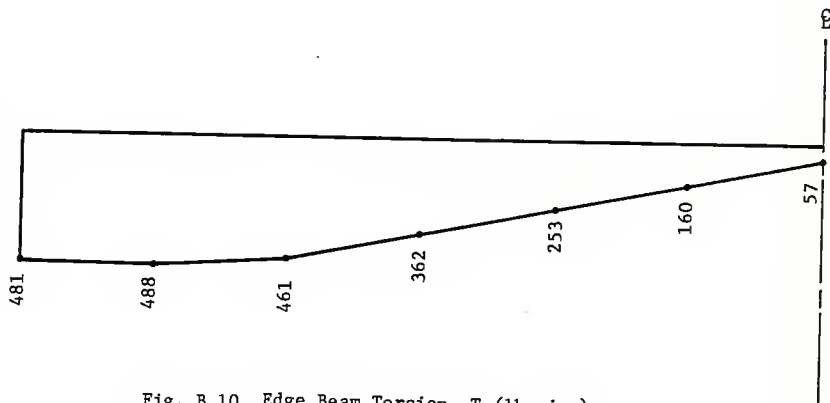
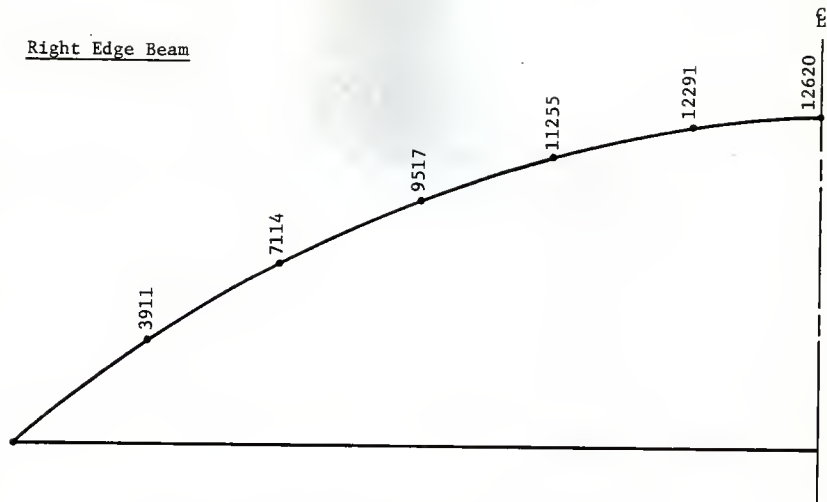
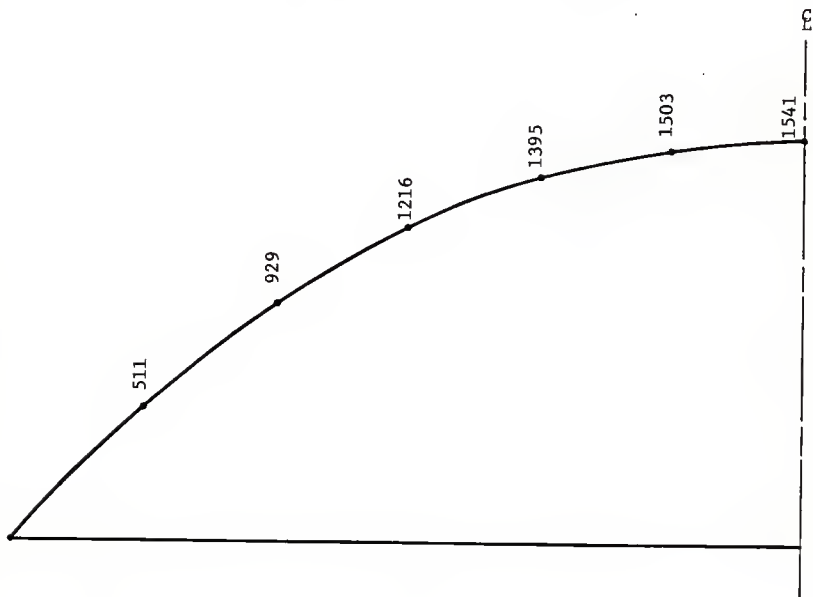
Right Edge Beam

Fig. B.8 Shear Diagram (lb.)

Right Edge BeamFig. B.9 Edge Beam Bending Moment About y-axis, M_y (lb.-in.)Fig. B.10 Edge Beam Torsion, T (lb.-in.)

Right Edge BeamFig. B.11 Edge Beam Axial Force, N_x (lb.)Fig. B.12 Edge Beam Bending Moment About z-axis, M_z (lb.-in.)

APPENDIX C

Experimental and Theoretical Load
Calculations and Strain Data

Example calculation of P_{theor} :

The whiffle tree layout is shown in Fig. C.1.

Assume a 1000 lb. delivered to point 9 as shown in Fig. C.2. The load will be distributed as indicated on the figure. The R_1 and R_2 values were calculated taking the average readings of the ram calibration (Table 6.1) for each load level, from which P_{theor} was calculated.

Figure C.2 shows the load distribution on whiffle tree.

$$R_1 = \frac{250 \text{ lb} \times 7.5 \text{ in}}{16.166 \text{ in}} = 116 \text{ lb}$$

$$\frac{R_1}{2} = \frac{116}{2} = 58 \text{ lb}$$

$$R_2 = 250 \times \frac{8.66}{16.166} = 134 \text{ lb}$$

$$\frac{R_2}{4} = \frac{134}{4} = 34 \text{ lb}$$

For gage nos. 31 through 46:

$$P_{\text{theor}} = \frac{625 \text{ lb}}{1000 \text{ lb}} \times \frac{R_2}{4}$$

$$= .625 * 33.504 = 21 \text{ lb}$$

$$P_{\text{theor}} = 21 \text{ lb @ 100 psi}$$

For gage nos. 47 through 50:

$$P_{\text{theor}} = \frac{625 \text{ lb}}{1000 \text{ lb}} * R_2 = .625 * 134.016 = 84 \text{ lb}$$

$$P_{\text{theor}} = 84 \text{ lb @ 100 psi}$$

For gage nos. 51 through 54:

$$P_{\text{theor}} = .625 * R_1 = .625 * 116$$

$$= 72 \text{ lb @ 100 psi}$$

For gage nos. 55 through 60:

$$P_{\text{theor}} = .625 * \frac{R_1}{2} = .625 * 58.0 = 36 \text{ lb}$$

$$P_{\text{theor}} = 36 \text{ lb @ 100 psi}$$

Example calculation of P_{exp} :

Stress is expressed as

$$\sigma = \frac{P}{A}$$

where σ is the stress, or force per unit area,

P is the applied load, and A is the cross-sectional area.

From the above relation

$$P = \sigma A$$

but $\sigma = E\epsilon$

$$P = AE\epsilon$$

The value of E was found experimentally to be:

$$E = 29.4 \times 10^6 \text{ psi}$$

$$A = 0.25 \text{ in}^2$$

For gage nos. 31 and 32:

$$\epsilon = 14.1 \times 10^{-6} \text{ in/in}$$

$$P_{exp} = 29.4 \times 10^6 \text{ psi} \times 14.1 \times 10^{-6} \text{ in/in} \times .25 \text{ in}^2$$

$$P_{exp} = 104 \text{ lb. @ 100 psi}$$

$$P_{exp} = 96 \text{ lb. @ 200 psi}$$

$$P_{exp} = 143 \text{ lb. @ 300 psi}$$

$$P_{exp} = 193 \text{ lb. @ 600 psi}$$

In the same way P_{exp} was calculated for other gages for each load increment.

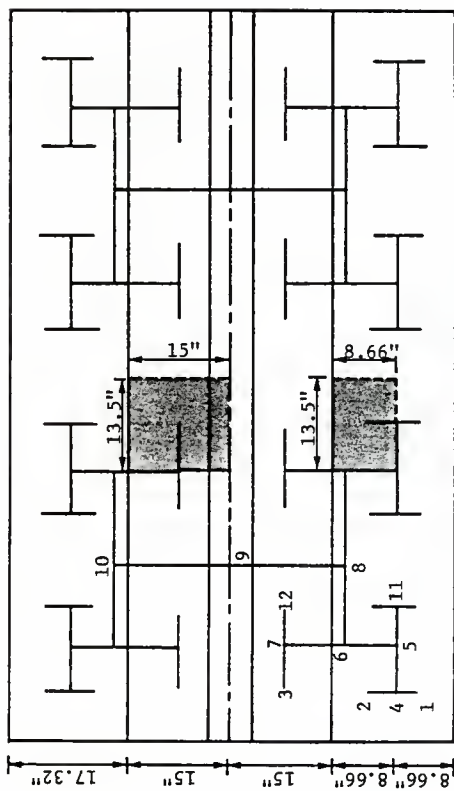


Fig. C.1 Layout of Whiffle Tree Load Points,
1 inch = 25.4 mm

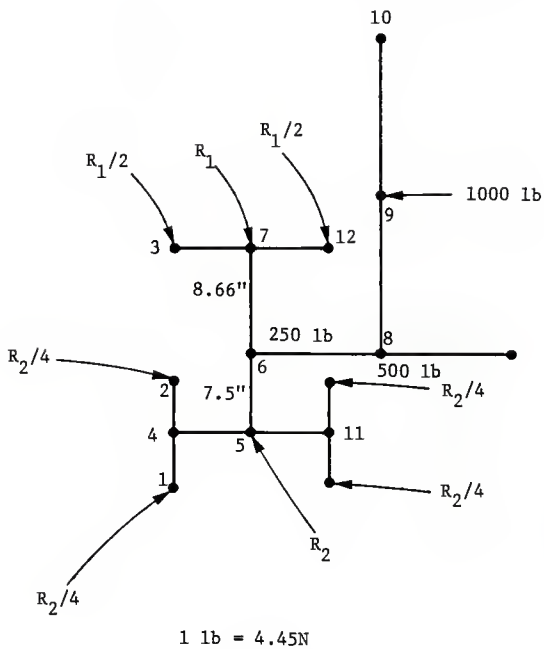


Fig. C.2 Load Distribution on Whiffle Tree

Table C.1 Calculated Experimental vs. Theoretical Loads
(Gages 31 and 32)

Load, psi	P_{exp} , lb.	P_{theor} , lb.
0	0	0
100	104	21
200	96	47
300	143	69
400	132	90
500	150	110
600	193	141

Table C.2 Calculated Experimental vs. Theoretical Loads
(Gages 35 and 36)

Load, psi	P_{exp} , lb.	P_{theor} , lb.
100	110	21
200	90	47
300	136	69
400	129	90
500	161	110
600	179	141

Table C.3 Calculated Experimental vs. Theoretical Loads
(Gages 37 and 38)

Load, psi	P _{exp} , lb.	P _{theor} , lb.
100	75	21
200	68	47
300	107	69
400	100	90
500	125	110
600	161	141

Table C.4 Calculated Experimental vs. Theoretical Loads
(Gages 41 and 42)

Load, psi	P _{exp} , lb.	P _{theor} , lb.
100	47	21
200	50	47
300	76	69
400	79	90
500	97	110
600	115	141

Table C.5 Calculated Experimental vs. Theoretical Loads
(Gages 43 and 44)

Load, psi	P _{exp} , lb.	P _{theor} , lb.
100	54	21
200	68	47
300	97	69
400	104	90
500	133	110
600	154	141

Table C.6 Calculated Experimental vs. Theoretical Loads
(Gages 45 and 46)

Load, psi	P _{exp} , lb.	P _{theor} , lb.
100	79	21
200	75	47
300	111	69
400	122	90
500	136	110
600	143	141

Table C.7 Calculated Experimental vs. Theoretical Loads
(Gages 47 and 48)

Load, psi	P _{exp} , lb.	P _{theor} , lb.
100	93	84
200	164	188
300	254	275
400	311	358
500	419	439
600	512	563

Table C.8 Calculated Experimental vs. Theoretical Loads
(Gages 49 and 50)

Load, psi	P _{exp} , lb.	P _{theor} , lb.
100	75	84
200	82	188
300	142	275
400	171	358
500	228	439
600	282	563

Table C.9 Calculated Experimental vs. Theoretical Loads
(Gages 57 and 58)

Load, psi	P _{exp} , lb.	P _{theor} , lb.
100	75	36
200	89	81
300	139	119
400	161	155
500	204	190
600	222	243

Table C.10 Calculated Experimental vs. Theoretical Loads
(Gages 59 and 60)

Load, psi	P _{exp} , lb.	P _{theor} , lb.
100	86	36
200	86	81
300	143	119
400	165	155
500	193	190
600	229	243

Zero Load Values

CHAN.031	CHAN.032	CHAN.033	CHAN.034	CHAN.035	CHAN.036	CHAN.037	CHAN.038
STRAIN	STRAIN	STRAIN	STRAIN	STRAIN	STRAIN	STRAIN	STRAIN
14.6	0	6.8	-47.7	2.9	5.8	1.9	2.9

CHAN.039	CHAN.040	CHAN.041	CHAN.042	CHAN.043	CHAN.044	CHAN.045	CHAN.046
STRAIN	STRAIN	STRAIN	STRAIN	STRAIN	STRAIN	STRAIN	STRAIN
-134.5	5.8	3.8	3.8	3.8	.9	7.7	6.8

CHAN.047	CHAN.048	CHAN.049	CHAN.050	CHAN.051	CHAN.052	CHAN.053	CHAN.054
STRAIN	STRAIN	STRAIN	STRAIN	STRAIN	STRAIN	STRAIN	STRAIN
-.9	.9	0	-16.5	0	-2650.5	3.8	-2.9

CHAN.055	CHAN.056	CHAN.057	CHAN.058	CHAN.059	CHAN.060
STRAIN	STRAIN	STRAIN	STRAIN	STRAIN	STRAIN
1.9	1.9	-2.9	.9	0	.9

CHAN.000

STRAIN

.9

MEASUREMENT NO.: 2 FOLDED PLATE BUCKLING RUN NO. SHELL NO. 1

Ram Pressure = 100 psi

CHAN.031	CHAN.032	CHAN.033	CHAN.034	CHAN.035	CHAN.036	CHAN.037	CHAN.038
STRAIN	STRAIN	STRAIN	STRAIN	STRAIN	STRAIN	STRAIN	STRAIN
-12.6	-25.3	-17.5	-70.1	-22.4	-17.5	-12.6	-25.3

CHAN.039	CHAN.040	CHAN.041	CHAN.042	CHAN.043	CHAN.044	CHAN.045	CHAN.046
STRAIN	STRAIN	STRAIN	STRAIN	STRAIN	STRAIN	STRAIN	STRAIN
-175.4	-6.8	-23.3	0	10.7	-31.1	-21.4	-44.8

CHAN.047	CHAN.048	CHAN.049	CHAN.050	CHAN.051	CHAN.052	CHAN.053	CHAN.054
STRAIN	STRAIN	STRAIN	STRAIN	STRAIN	STRAIN	STRAIN	STRAIN
80.9	33.1	12.6	-47.7	155.9	-2497.4	76	-48.7

CHAN.055	CHAN.056	CHAN.057	CHAN.058	CHAN.059	CHAN.060
STRAIN	STRAIN	STRAIN	STRAIN	STRAIN	STRAIN
-32.1	63.3	-12.6	8.7	-38	-2.9

CHAN.000

STRAIN
=====

-5002.9

Ram Pressure = 200 psi

CHAN.031	CHAN.032	CHAN.033	CHAN.034	CHAN.035	CHAN.036	CHAN.037	CHAN.038
STRAIN	STRAIN	STRAIN	STRAIN	STRAIN	STRAIN	STRAIN	STRAIN
29.2	13.6	18.5	-25.3	17.5	21.4	10.7	14.6
CHAN.039	CHAN.040	CHAN.041	CHAN.042	CHAN.043	CHAN.044	CHAN.045	CHAN.046
STRAIN	STRAIN	STRAIN	STRAIN	STRAIN	STRAIN	STRAIN	STRAIN
-112.1	16.5	7.7	12.6	17.5	1.9	23.3	12.6
CHAN.047	CHAN.048	CHAN.049	CHAN.050	CHAN.051	CHAN.052	CHAN.053	CHAN.054
STRAIN	STRAIN	STRAIN	STRAIN	STRAIN	STRAIN	STRAIN	STRAIN
17.5	7.7	2.9	.9	32.1	-2656.3	37	-3.8
CHAN.055	CHAN.056	CHAN.057	CHAN.058	CHAN.059	CHAN.060		
STRAIN	STRAIN	STRAIN	STRAIN	STRAIN	STRAIN		
3.8	32.1	7.7	10.7	9.7	14.6		

CHAN.000

STRAIN

0

Ram Pressure = 300 psi

CHAN.031	CHAN.032	CHAN.033	CHAN.034	CHAN.035	CHAN.036	CHAN.037	CHAN.038
STRAIN	STRAIN	STRAIN	STRAIN	STRAIN	STRAIN	STRAIN	STRAIN
28.2	12.6	19.4	-20.4	14.6	18.5	11.6	11.6

CHAN.039	CHAN.040	CHAN.041	CHAN.042	CHAN.043	CHAN.044	CHAN.045	CHAN.046
STRAIN	STRAIN	STRAIN	STRAIN	STRAIN	STRAIN	STRAIN	STRAIN
-126.7	17.5	7.7	13.6	21.4	1.9	25.3	9.7

CHAN.047	CHAN.048	CHAN.049	CHAN.050	CHAN.051	CHAN.052	CHAN.053	CHAN.054
STRAIN	STRAIN	STRAIN	STRAIN	STRAIN	STRAIN	STRAIN	STRAIN
32.1	12.6	0	5.8	58.4	-2680.7	55.5	-11.6

CHAN.055	CHAN.056	CHAN.057	CHAN.058	CHAN.059	CHAN.060
STRAIN	STRAIN	STRAIN	STRAIN	STRAIN	STRAIN
2.9	47.7	9.7	12.6	7.7	16.5

CHAN.000

STRAIN
=====

-5001.9

Ram Pressure = 400 psi

CHAN.031	CHAN.032	CHAN.033	CHAN.034	CHAN.035	CHAN.036	CHAN.037	CHAN.038
STRAIN	STRAIN	STRAIN	STRAIN	STRAIN	STRAIN	STRAIN	STRAIN
34.1	19.4	25.3	-51.6	22.4	23.3	16.5	17.5

CHAN.039	CHAN.040	CHAN.041	CHAN.042	CHAN.043	CHAN.044	CHAN.045	CHAN.046
STRAIN	STRAIN	STRAIN	STRAIN	STRAIN	STRAIN	STRAIN	STRAIN
-153	21.4	9.7	18.5	28.2	2.9	33.1	11.6

CHAN.047	CHAN.048	CHAN.049	CHAN.050	CHAN.051	CHAN.052	CHAN.053	CHAN.054
STRAIN	STRAIN	STRAIN	STRAIN	STRAIN	STRAIN	STRAIN	STRAIN
51.6	17.5	7.7	14.6	87.7	-2591	76	-4.8

CHAN.055	CHAN.056	CHAN.057	CHAN.058	CHAN.059	CHAN.060
STRAIN	STRAIN	STRAIN	STRAIN	STRAIN	STRAIN
4.8	65.3	12.6	23.3	14.6	25.3

CHAN.000

STRAIN

-5001.9

Ram Pressure = 500 psi

CHAN.031	CHAN.032	CHAN.033	CHAN.034	CHAN.035	CHAN.036	CHAN.037	CHAN.038
STRAIN	STRAIN	STRAIN	STRAIN	STRAIN	STRAIN	STRAIN	STRAIN
34.1	16.5	25.3	-71.1	20.4	23.3	16.5	15.5

CHAN.039	CHAN.040	CHAN.041	CHAN.042	CHAN.043	CHAN.044	CHAN.045	CHAN.046
STRAIN	STRAIN	STRAIN	STRAIN	STRAIN	STRAIN	STRAIN	STRAIN
-187.1	21.4	7.7	21.4	30.2	2.9	35	12.6

CHAN.047	CHAN.048	CHAN.049	CHAN.050	CHAN.051	CHAN.052	CHAN.053	CHAN.054
STRAIN	STRAIN	STRAIN	STRAIN	STRAIN	STRAIN	STRAIN	STRAIN
62.3	22.4	13.6	16.5	102.3	-2934.2	85.7	0

CHAN.055	CHAN.056	CHAN.057	CHAN.058	CHAN.059	CHAN.060
STRAIN	STRAIN	STRAIN	STRAIN	STRAIN	STRAIN
8.7	73.1	14.6	27.2	16.5	29.2

CHAN.000

STRAIN

-5002.9

Ram Pressure = 600 psi

CHAN.031	CHAN.032	CHAN.033	CHAN.034	CHAN.035	CHAN.036	CHAN.037	CHAN.038
STRAIN	STRAIN	STRAIN	STRAIN	STRAIN	STRAIN	STRAIN	STRAIN
36	19.4	32.1	-78.9	23.3	29.2	21.4	17.5

CHAN.039	CHAN.040	CHAN.041	CHAN.042	CHAN.043	CHAN.044	CHAN.045	CHAN.046
STRAIN	STRAIN	STRAIN	STRAIN	STRAIN	STRAIN	STRAIN	STRAIN
-180.3	24.3	9.7	24.3	35	5.8	37	14.6

CHAN.047	CHAN.048	CHAN.049	CHAN.050	CHAN.051	CHAN.052	CHAN.053	CHAN.054
STRAIN	STRAIN	STRAIN	STRAIN	STRAIN	STRAIN	STRAIN	STRAIN
77	37	29.2	16.5	130.6	-2553	103.3	3.8

CHAN.055	CHAN.056	CHAN.057	CHAN.058	CHAN.059	CHAN.060
STRAIN	STRAIN	STRAIN	STRAIN	STRAIN	STRAIN
14.6	88.7	18.5	33.1	19.4	34.1

CHAN.000
STRAIN
-5002.9

Ram Pressure = 700 psi

CHAN.031	CHAN.032	CHAN.033	CHAN.034	CHAN.035	CHAN.036	CHAN.037	CHAN.038
STRAIN	STRAIN	STRAIN	STRAIN	STRAIN	STRAIN	STRAIN	STRAIN
41.9	25.3	37	-83.8	26.3	31.1	27.2	21.4

CHAN.039	CHAN.040	CHAN.041	CHAN.042	CHAN.043	CHAN.044	CHAN.045	CHAN.046
STRAIN	STRAIN	STRAIN	STRAIN	STRAIN	STRAIN	STRAIN	STRAIN
-196.9	27.2	9.7	29.2	42.8	4.8	37	16.5

CHAN.047	CHAN.048	CHAN.049	CHAN.050	CHAN.051	CHAN.052	CHAN.053	CHAN.054
STRAIN	STRAIN	STRAIN	STRAIN	STRAIN	STRAIN	STRAIN	STRAIN
90.6	48.7	37	23.3	160.8	-290.1	116	8.7

CHAN.055	CHAN.056	CHAN.057	CHAN.058	CHAN.059	CHAN.060
STRAIN	STRAIN	STRAIN	STRAIN	STRAIN	STRAIN
13.6	110.1	19.4	38.9	21.4	41.9

CHAN.000

STRAIN

ACKNOWLEDGMENTS

The author wishes to express his deep appreciation to Dr. S. E. Swartz for his advice, valuable guidance and encouragement which led to the completion of this work. His untiring help and patience during the period of graduate study and preparation of this manuscript are very much appreciated.

The author wishes to extend his gratitude and appreciation to the members of his graduate advisory committee: Dr. K. K. Hu and Dr. T. O. Hodges, for their assistance and review of this thesis.

The author wishes to recognize Sana'a University for their financial assistance.

A debt of gratitude is owed to Mr. Russell Gillespie and to those close friends who were always available for help.

Appreciation is extended to Mrs. Peggy Selvidge for her excellent job in typing the manuscript.

The author wishes to acknowledge his deepest appreciation to his wife, Suad, for an immeasurable contribution of encouragement, patience and support. Thanks to his daughters, Ghidah and Roweidah, for enduring much less attention during the course of this study.

TESTS ON A MICRO-CONCRETE MODEL
OF A LONG-SPAN FOLDED PLATE SHELL

by

YOUSEF NAGI AHMAD (Assalimy)
Diploma in Civil Engineering, Kiev Civil
Engineering Institute, Kiev, USSR, 1974
M.S., Kansas State University, 1981

AN ABSTRACT OF A MASTER'S THESIS
Submitted in partial fulfillment of the
requirements for the degree

MASTER OF SCIENCE

Department of Civil Engineering

KANSAS STATE UNIVERSITY
Manhattan, Kansas

1985

ABSTRACT

The objective of this thesis is to report analytical and experimental results of tests on a prismatic folded plate model shell. In this research, a long span reinforced concrete model was built and was tested three times. The loading system was constructed. The performance of the model under the working service load was as predicted by the analysis. The performance of the whiffle tree was determined, where measured load versus theoretical load is given for different rods. It was shown that the average readings of experimental values agree well with theory. A computer program was developed to carry out the computations involved in the analytical solution of the "exact" elastic method of analysis. Two subroutines were added to the main program to account for analysis of edge beams. The coefficients for edge beams stiffness and stresses on edge beams were calculated. Results from the model which analyzed the structure as edge beams are compared with results of analysis which treated edge beams as end plates are shown. It is believed that considering edge beams in the analysis as edge beams gives more reliable results than treating them as end plates in the analysis.